The transcription factor FOXO1 orchestrates growth and maturation of lymphatics

Inauguraldissertation

zur Erlangung des Grades eines Doktors der Medizin

des Fachbereichs Medizin

der Justus-Liebig-Universität Gießen

vorgelegt von Fasse, Jannik Werner Dieter

aus Göttingen

Gießen 2025

Aus dem Fachbereich Medizin der Justus-Liebig-Universität Gießen, Max-Planck-Institut für Herz- und Lungenforschung Bad Nauheim, Campus Kerckhoff

Gutachter: Prof. Dr. Klaus T. Preissner

Gutachter: Prof. Dr. Saverio Bellusci

Tag der Disputation: 10. Februar 2026

To my family

Erklärung zur Dissertation

Hiermit erkläre ich, dass ich die vorliegende Arbeit selbstständig und ohne unzulässige Hilfe oder Benutzung anderer als der angegebenen Hilfsmittel angefertigt habe. Alle Textstellen, die wörtlich oder sinngemäß aus veröffentlichten oder nichtveröffentlichten Schriften entnommen sind, und alle Angaben, die auf mündlichen Auskünften beruhen, sind als solche kenntlich gemacht. Bei den von mir durchgeführten und in der Dissertation erwähnten Untersuchungen habe ich die Grundsätze guter wissenschaftlicher Praxis, wie sie in der „Satzung der Justus-Liebig-Universität Gießen zur Sicherung guter wissenschaftlicher Praxis“ niedergelegt sind, eingehalten sowie ethische, datenschutzrechtliche und tierschutzrechtliche Grundsätze befolgt. Ich versichere, dass Dritte von mir weder unmittelbar noch mittelbar geldwerte Leistungen für Arbeiten erhalten haben, die im Zusammenhang mit dem Inhalt der vorgelegten Dissertation stehen, oder habe diese nachstehend spezifiziert. Die vorgelegte Arbeit wurde weder im Inland noch im Ausland in gleicher oder ähnlicher Form einer anderen Prüfungsbehörde zum Zweck einer Promotion oder eines anderen Prüfungsverfahrens vorgelegt. Alles aus anderen Quellen und von anderen Personen übernommene Material, das in der Arbeit verwendet wurde oder auf das direkt Bezug genommen wird, wurde als solches kenntlich gemacht. Insbesondere wurden alle Personen genannt, die direkt und indirekt an der Entstehung der vorliegenden Arbeit beteiligt waren. Mit der Überprüfung meiner Arbeit durch eine Plagiatserkennungssoftware bzw. ein internetbasiertes Softwareprogramm erkläre ich mich einverstanden.

_____ _____

Ort, Datum Unterschrift

Table of content

1 Introduction

1.1 The circulatory system

The circulatory system of the human body comprises two vascular networks: the blood and the lymphatic vasculature. Both tubular networks are lined by endothelial cells. These specialized cells execute diverse functions depending on the environment they reside in. The blood vasculature, consisting of arteries, capillaries and veins, is one of the first organs formed in vertebrate development and a prerequisite for normal development[1]. It transports oxygen- and nutrient-rich blood from the heart to peripheral organs (e.g., brain, liver, muscle) and collects metabolic waste products from these tissues. The lymphatic system, on the other hand, returns extravasated tissue fluids to the blood circulation and is indispensable for organ homeostasis, immune surveillance, and dietary fat absorption[2].

1.2 The lymphatic system

For many years, the lymphatic vasculature has been neglected because specific markers to visualize these vessels were lacking. During the late 1990s first lymphatic markers were identified, opening a new field of biomedical research[3–6].

In contrast to the cardiovascular system, the lymphatic system is a blind ended, unidirectional network, consisting of lymphatic vessels, lymph nodes and associated lymphoid tissue[2]. Lymphatic vessels follow a hierarchical organization of capillaries and collecting vessels, both exhibiting specialized morphologic features. It forms a connection from the extracellular space to the venous blood circulation, enabling one-way transportation of lymph. Lymph stems from extracellular fluid generated by the tissue parenchyma. This lymph fluid is then taken up by lymphatic vessels and transported through a series of lymph nodes into the right lymphatic duct (in case of the upper right quadrant of the body) or into the thoracic duct (for the lower half and the upper left quadrant of the body), before it is released into the larger veins of the body circulation[7]. This process is controlled by four lymphovenous valves (LVVs), which prevent backflow[8].

The lymphatic system has three main tasks: (1) It is actively involved in regulation of tissue homeostasis, (2) it represents an important part of the “hardware” of the immune system, and (3) it is responsible for the absorption and transportation of gastrointestinal lipids to the blood circulation[9]. In addition, it also secretes paracrine factors, so-called lymphangiocrines, that are important for tissue regeneration and repair[10]. These tasks will be discussed in due course.

1.2.1 Development of the lymphatic system

1.2.1.1 Origin of lymphatics in the mammalian embryo

The lymphatic system develops after the blood circulation has been established. Already in 1902, Florence Sabin postulated a venous origin of the lymphatic vasculature, when she was studying lymphangiogenesis in pig and mouse embyros[11]. More than 100 years later, several investigators confirmed this model in lineage tracing studies in developing mouse embryo and zebrafish embryos[12]. According to this model, lymphatic endothelial cell (LEC) progenitors originate from the cardinal veins (CVs), but also from the intersomitic veins and the superficial venous plexus[11,13,14]. However, these original experiments did not exclude additional sources of LECs. Nonvenous sources of LEC progenitors have been proposed in the chick[15], as well as in the skin, heart, and mesentery of mice[16–18]. Overall, the notion emerges that the origin of lymphatic endothelium is heterogenous and thereby might contribute to tissue specific function[2]. Nevertheless, the following overview will focus on the venous origin of lymphatics, which is a major source of lymphatic endothelium.

1.2.1.2 LEC fate specification

The transdifferentiation of blood endothelial cells (BECs) into LECs is achieved by tight spatiotemporal coordination of gene expression[19]. In the last years, several key regulators of this process have been identified, unraveling the complexity of this process[20]. The initial step involves the upregulation of the transcription factor Prospero-related homeobox gene 1 (PROX1) in a subset of venous endothelial cells (VECs) in the dorsolateral CV at embryonic day (E) 9.5, leading to the formation of LEC progenitor cells[4,12,13]. Knockout of *Prox1* in mice leads to the complete absence of lymphatic sacs and vessels, suggesting that the lymphatic fate cannot be aquired[4]. Also, *Prox1*-heterozygous embryos show fewer LEC progenitors and develop edema, indicating lymphatic malfunction[21]. PROX1 induces the transcription of many lymphatic-specific genes and represses blood-vessel markers. Moreover, PROX1 overexpression directs ECs towards a lymphatic fate *in vitro* and *in vivo*[22–24]. Taken together, PROX1 plays a crucial role in induction and maintenance of LEC fate.

PROX1 itself is mainly regulated by two transcription factors, SOX18 and COUP-TFII (also known as NR2F2). COUP-TFII is expressed in the CV at E8.5, promoting venous identity by suppression of arterial gene expression before inducing PROX1[25]. SOX18 belongs to the SRY-related HMG domain family of transcription factors, whose

dysfunction has been identified as a causative factor for lymphatic diseases such as the human syndrome hypotrichosis-lymphoedema-telangiectasia syndrome[26,27]. Both proteins are indispensable for activation of PROX1 transactivation by directly binding to regulatory DNA domains in the *Prox1* gene[28,29]. Additionally, COUP-TFII represses Notch activity, and Notch signaling seems to be an inhibitor of LEC differentiation and sprouting *in vitro* and *in vivo*, suggesting a partnership between COUP-TFII and Notch pathways during EC fate decisions[20,28,30–32]. Loss of COUP-TFII or SOX18 leads to the absence of LEC progenitors, highlighting their requirement for lymphatic vascular development[28,29]. Furthermore, it was shown that a direct interaction of COUP-TFII and PROX1 is necessary for the maintenance of PROX1 expression[28].

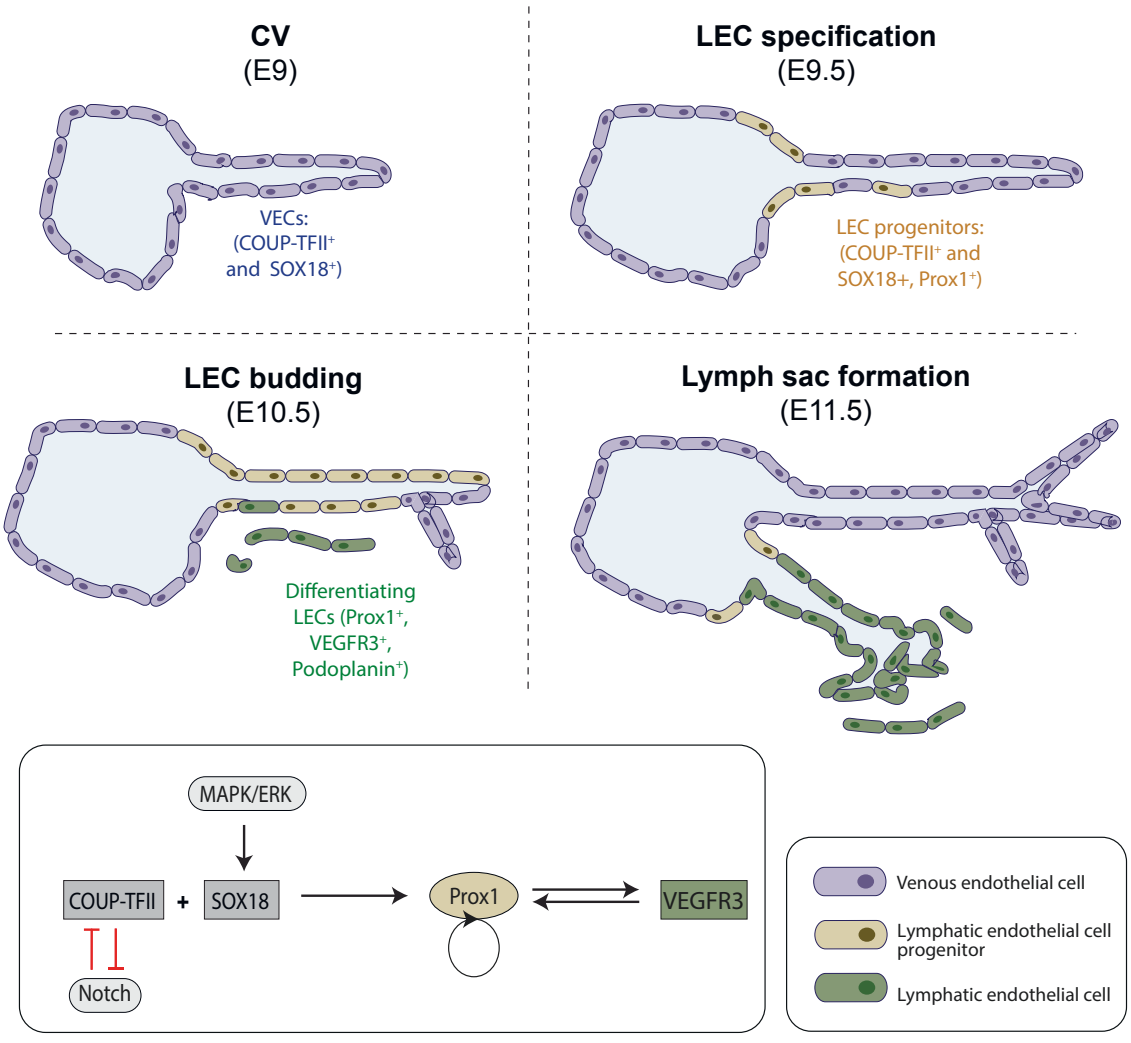

Figure 1: Development of the mammalian lymphatic vasculature. Murine development from the venous originated lymphatic system. Initially, venous ECs in the CV express the transcription factors COUP-TFII and SOX18. These transcription factors induce PROX1 expression in a subpopulation of venous endothelial cells. PROX1 expressing ECs are referred to as lymphatic progenitors hereafter. At E10.5, these progenitors start to bud from the CV. This process requires a VEGF-C gradient in the surrounding mesenchyme, and the expression of VEGFR-3 on the lymphatic progenitors. At approximately E11.5 formation of different lymph

sacs starts, source of most LECs from the developing lymphatic system. Adapted from Yang et al., 2014[20]

1.2.1.3 Budding of LECs from the veins and formation of lymph sacs

After transdifferentiation, LEC progenitors start to migrate into the surrounding mesenchyme at around E10.5 towards a gradient of vascular endothelial growth factor C (VEGF-C)[4,33]. This process is associated with changes in cell and nuclear shape and requires dynamic regulation of intercellular connections to sustain vascular integrity [13,14,34]. While VEGF-A is the essential factor in angiogenesis, VEGF-C is essential for the orchestration of lymphangiogenesis. In VEGF-C deficient mice, ECs commit to LEC fate but do not sprout into the surrounding tissue. Moreover, VEGF-C overexpression induces hyperplasia of lymphatic vasculature[33,35]. VEGF-Cs receptor, VEGFR-3, is a direct target of PROX1 - and its signaling regulates PROX1, constituting a feedback loop required for maintenance of LEC identity[36]. Interestingly, not all PROX1 expressing LEC progenitors leave the CV towards the VEGF-C gradient[22,37,38]. A subpopulation persists and contributes to the formation of lymphovenous valves in cooperation with VECs[38]. The migrating LECs form streams that merge lateral of the CV, forming intermediately luminal structures, the primordial thoracic duct, the peripheral longitudinal lymphatic vessel and four additional lymphsacs[14]. LECs from these initial structures contribute to the development of the entire lymphatic system by lymphangiogenic sprouting[13]. It has been shown that a number of other genes regulate these processes Examples include NRP2[39,40], CCBE1[14,41,42], NFATc1[43] or GATA2[44,45], whose deficiency contributes to lymphatic diseases. This aspect will be discussed in more detail in the later part of this thesis.

1.2.1.4 Maturation of lymphatic vessels

During lymphatic expansion, the primitive lymphatic plexus remodels into a mature lymphatic system with hierarchical structure[20]. It is composed of lymphatic capillaries and collecting vessels, both specialized to fulfill different functions. Precollectors have also been proposed as a third lymphatic vessel type; however - their differentiation is ambiguous and their existence as a distinct lymph vessel type has not been generally implemented.

Lymphatic capillaries (LCs) are thin, blind ended vessels responsible for the uptake of fluids, lipids, macromolecules and immune cells. LCs only have a rudimentary basement membrane and lack mural cell support, facilitating tissue drainage[9]. This process is supported by button-like intercellular junctions, forming endothelial microvalves with the oak-leaf-shaped LECs[46,47]. Anchoring filaments connect LECs to

the ECM, preventing collapse under high interstitial pressure conditions[48]. Additionally, more recent studies suggest that transcellular transport mechanisms contribute to lymphproduction[49].

The transportation of lymph from the drained tissue to lymph nodes and subsequently to the venous circulation is conducted by collecting vessels. Zipper-like junctions and a continuous basement membrane prevent leakage into surrounding tissue[47,50]. Collecting vessels do not constitute static conduits, but rather an active transit system that overcomes flow-opposing pressure gradients[9]. To this end, collecting vessels possess smooth muscle cell (SMC) coverage and lymphatic valves. SMCs contract periodically to enable lymph flow, while intraluminal lymphatic valves prevent backflow[7,50]. The valves subdivide the collecting vessels in functional units, termed lymphangions, which facilitate lymph transport towards the venous circulation[7].

Several signaling pathways have been identified as essential regulators of lymphatic maturation, a process that forms specialized collecting vessels from immature lymphatic capillaries[20].

The best characterized pathway is the FOXC2-calcineurin-NFATC1 cascade. This signaling axis is indispensable for maturation of collecting vessels, as well as the assembly and maintenance of lymphatic valves. Maturation into collecting vessels is accompanied by downregulation of lymphatic capillary markers such as lymphatic vessel endothelial hyaluron receptor 1 (LYVE1), VEGFR-3 and PROX1[51]. The downregulation of these markers is preceded by a decrease in the levels of FOXC2 and PROX1, which remain highly expressed in lymphatic valve-forming cells, indicating a crucial function of FOXC2 in collecting vessel patterning and valve assembly[51,52]. *Foxc2*-knockout mice are characterized by sustained high expression of lymphatic capillary markers, valve defects and increased pericyte coverage[53]. Moreover, point mutations in the human *FOXC2* gene are linked to lymphedema-distichiasis syndrome, exhibiting similar phenotypes[54,55]. Genome wide Chip-on-Chip-analyses revealed that FOXC2 interacts with NFATC1 in LECs[51], a protein essential for cardiac valve morphogenesis[56], and pharmacological inhibition of calcineurin, an upstream regulator of NFAT, affects lymphatic valve formation[51]. Further studies revealed that FOXC2 and PROX1 regulate the expression of the gap junction protein Connexin 37 together with flow and depletion of Cx37 leads to reduced calcineurin-NFATC1 signaling and lack of lymphatic valve-forming cells[52,57]. Together, these results suggest an essential role of this pathway in the process of collecting vessel assembly, maturation and maintenance, including the formation of lymphatic valves of lymphatic valves.

Another important molecule in this process is Reelin. Even though all LECs produce Reelin, only collecting vessel LECs secrete it into the extracellular environment, while

capillary LECs store it intracellularly[58]. Secretion and processing of Reelin seems to be stimulated by SMCs, leading to an autocrine upregulation of MCP1, thereby further stimulating SMC recruitment[58]. In agreement with this, Reelin-deficient mice exhibit normal capillaries, while the collecting vessels are dilated, lack proper SMC coverage and are dysfunctional[58].

As the basement membrane is an important feature of collecting vessels, it seems logical that ECM proteins also modulate lymphatic vessel maturation. Integrins are major receptors for cell adhesion to the ECM and execute tissue specific functions by activating intracellular signaling pathways[59]. The integrin family consists of eight α and 18 β subunits, which are able to assemble into 24 integrin heterodimers with nonredundant functions[59]. In lymphangiogenesis they are involved in processes such as proliferation, migration, and survival[60–65]. For instance, the interaction of Integrin-α9 with its ligand Fibronectin and the ECM protein EMILIN1 is required for lymphatic valve morphogenesis, and Itga9-knockout mice suffer from leakage and backflow of lymph[66]. Together these findings illustrate the complex regulation of developmental lymphangiogenesis. However, additional signaling pathways are involved in lymphangiogenesis and the interested reader is referred to literature cited here [20,67].

1.2.2 Functions of the lymphatic system

1.2.2.1 Tissue fluid homeostasis

The lymphatic system is indispensable in the process of microvascular fluid exchange (MFE). MFE describes the considerable fluid movements between blood capillaries, the interstitium and lymphatic capillaries, enabling the exchange of nutrients, oxygen, hormones and waste products between blood capillaries and cells of an organism[50]. Under physiological conditions, blood plasma is constantly filtered through the semipermeable capillaries into the interstitium, which are permeable for plasma but not for proteins, mainly albumin. This process depends on four variables: the colloid osmotic pressure in the capillary (π_{Ka}) created by plasma proteins, the hydrostatic pressure in the capillaries (P_{Ka}) caused by the heartbeat, the colloid osmotic (π_{Is}) and the hydrostatic pressure (P_{Is}) in the interstitium[68]. Since the interstitial fluid has a substantial concentration of proteins, Ernest H. Starling recognized that the endothelial barrier is leaky and, depending on the vascular bed, a certain percentage of intravascular proteins reaches the interstitium[69]. The ‘leakiness’ of the membrane is represented in the osmotic reflection coefficient σ and differs substantially between different vascular beds[68]. Q represents the filtration volume per second. This process is represented in the Starling equation:

$$Q = K_f[(P_{Ka} - P_{Is}) - \sigma(\pi_{Ka} - \pi_{Is})]$$

Consequently, π_{Ka} decreases the further the blood flows through the microvascular bed, and only a certain part of the interstitial fluid can be reabsorbed by blood capillaries or venules. A relevant portion remains in the interstitium and is drained by lymphatic capillaries. It has been estimated that the total plasma volume of the body (in humans ≈ 3L) extravasates from the blood circulation every 9 hours and is transported back to the venous blood circulation[70]. This substantial fluid turnover illustrates the relevance of lymphatics for maintaining fluid homeostasis under physiological conditions and suggests how vulnerable MFE is under disease conditions.

1.2.2.2 Intestinal lipid absorption

A highly specialized lymphatic vessel type, called lacteals, has been identified in the intestine, where it is critical for dietary fat adsorption and immune responses[71]. The luminal surface of the small intestine is strongly enlarged by so called *Plicae circulares* and *Villi intestinalis*, creating a capacious absorptive area. An intestinal villus is an enterocyte-covered bulge filled with connective tissue, highly vascularized by a blood capillary network and one central lacteal[9]. While water-soluble components of nutrition, such as carbohydrates, proteins and hydrophile vitamins and drugs, are absorbed by blood vessels, the diffusion of long-chain fatty acids and fat-soluble vitamins across BECs is limited. Instead, these components are transported by lacteals via paracellular and active transcellular mechanisms[72], and drained by contraction of smooth muscle cells in the intestinal villus[73]. The lymph is transported through the mesenteric lymphatic vessels and the thoracic duct into the venous circulation bypassing the liver, thereby depicting an appealing drug delivery route[9]. Drugs particularly designed for lacteal uptake represent an elegant strategy to circumvent the hepatic first pass-effect, increase oral bioavailability and may decrease undesirable side effects[74].

1.2.2.3 Immune response

The lymphatic system plays crucial roles in the adaptive immunity[75]. Dendritic cells (DCs) and leukocytes in the periphery are directed into lymphatic vessels by upregulation of several adhesion molecules and chemokine secretion[75,76]. Extensively studied are the lymphoid homing chemokines CCL21 and CCL19, ligands for the receptor CCR7 expressed by DCs and other leucocytes[76]. Ccr7 knockout mice exhibit

decreased T-cell and DC homing and delayed immune responses, highlighting the function of guiding DCs and leukocytes into the LN[76]. Another example is the semaphorin-3A-Plexin-A1/neuropilin-1-interaction, enabling DCs to transmigrate into lymphatic vessels. Consistent with this, lack of dermal lymphatics leads to decreased antibody titers after dermal immunization in mice, underlining that lymphatic vessels are indispensable player for mounting a humoral immune response[77]. Although the mice were able to establish a T-cell response, it was delayed and occurred in the spleen instead of the LNs[77]. Beyond that, one-year old mice lacking dermal lymphatic vasculature show signs of autoimmunity, suggesting that the constant rinsing of LNs with self-antigens is mandatory for deletion of autoreactive T-cells and thereby maintenance of immunetolerance[77]. Although LECs only make up a small part of the cells of a lymph node, recent studies revealed astonishing heterogeneity of LN LECs[78] with diverse, indispensable functions in antigen sorting, antigen presentation and orchestration of LN organogenesis[79]. Subcapsular LECs control antigen distribution within the LN through fenestrations and Plasmalemma vesicle-associated protein deficient (PLVAP) positive transendothelial channels[80]. PLVAP deficient mice lack diaphragms and molecules of up to 500kD, instead of 70KDa, started to enter the conduit system[80]. Electron microscopy revealed that sinusoidal LECs possess numerous surface invaginations, cytoplasmic vesicles, transfer tubules and multivesicular bodies, indicating manifold transcellular processes[79,81]. In addition, LN LEC present peripheral tissue antigens (PTA) to $CD8^+$ T-cells, supporting tissue-resident DCs to eliminate auto-reactive T-cells that escaped thymic negative selection[82]. Mechanistically, LN LECs present PTAs on MHC I molecules and mediate deletion of recognizing $CD8^+$ T-cells via the programmed death ligand 1 (PD-L1)[82]. Blocking of this receptor resulted in increased number of autoreactive T-cells and autoimmune vitiligo in mice, underlining the impact of LN LECs in maintenance of peripheral immune tolerance[83]. Although LN LEC also express MHCII, they lack H2-M, which is required for the loading of endogenous antigens onto MHCII[84]. Instead, they transfer the PTAs to DCs, which then subsequently present it to $CD4^+$ T-cells[84]. In summary, the lymphatic system is a fundamental part of the adaptive immune system, crucial for the effective response to pathogens as well as promotion of tolerance towards self-antigens.

1.2.3 Lymphatic system in disease

1.2.3.1 Lymphedema

The cardinal manifestation of lymphatic malfunction is lymphedema[9]. Due to inefficient drainage and reduced flow, interstitial fluid accumulates in the affected tissue, typically in the extremities[85]. Malfunction of lacteals leads to the aggregation of milky fluid in the peritoneum, named chylous ascites. This manifestation was observed in mutant *Vegfc*, *Prox1*, *Angpt2* mice as well as in Chy mice[86–88]. Chy mice possess a point mutation in the *Flt4* gene, encoding for the VEGFR3 protein. This resultant mutant protein lacks tyrosine kinase activity of the receptor, resulting in blunted VEGFC-VEGFR3-signaling[86].

A distinction is made between primary and secondary lymphedema. Primary lymphedema is the result of defective lymphatic vessel development and/or function, caused by gene mutations. Depending on the occurrence, primary lymphedemas are further divided in congenital, peripubertal and late-onset. Secondary or acquired lymphedema develops following physical obstruction or injury of LVs or LNs.

Mutations in 19 genes have been identified in primary lymphedema, the majority of which affect the VEGFC/VEGFR3-axis[89]. Some of them lead isolated lymphatic malfunction, others occur as part of a syndrome. The adequate differential diagnosis of primary lymphedema requires a complex algorithm[90].

The most common form is Milroy's disease (OMIM 153100), caused by heterozygous mutations in the FLT4 gene, leading to decreased downstream signaling and thus defective lymphatic development. The mutation is inherited in an autosomal dominant manner with reduced penetrance and *de novo* mutations are also observed[86, 91–94]. Typically, affected patients have bilateral lower limb edema and may also suffer from hydrocele or in utero hydrops[95,96]. However, only 70% of patients with Milroy's disease-like phenotype have mutations in VEGFR3, suggesting genetic heterogeneity. In 2013, a family with mutations in VEGFC were identified, suffering from a phenotype indistinguishable from Milroy's lymphedema. The suspected mutant protein was expressed in zebrafish but did not show detectable activity[97].

Homozygous or compound heterozygous mutations of the collagen and calcium-binding EGF domain-containing protein1 (CCBE1) lead to lymphedema as well as visceral lymphangiectasia, accompanied with typical facial features and mental retardation. This complex of symptoms was recently associated with Hennekam lymphagiectasia-lymphedema syndrome (OMIM 235510)[98,99]. CCBE1 interacts with extracellular matrix and VEGF-C, thereby modulating the development of lymphatic

vessels[41,42]. The impact on the development and function of other organs suggests additional functions outside the lymphatic system.

PTPN14 has been associated to the lymphedema-choanal atresia syndrome (OMIM 608911). Upon stimulation with VEGFC, PTPN14 is recruited to VEGFR3, inhibiting downstream signaling[100]. Audrey et al. reported a family with a homozygous deletion of PTPN14, suffering of peripubertal lymphedema. The consequence of PTPN14 malfunction was confirmed using a murine PTPN14 gene trap model, leading to a hyperplastic lymphatic phenotype and lymphedema. This rare disease thereby demonstrates that not only decreased, but also increased VEGFR3 signaling can lead to lymphatic malfunction and lymphedema[100].

Several other genes have been identified as candidates for primary lymphedema, for example the junctional proteins GJC2 (CX47)[101,102] and GJA1(CX43)[103], the mechanically activated ion channel PIEZO1[104,105], transcription factors involved in lymphatic development like FOXC2[54,55] and SOX-18[27,29,106], and many more. The interested reader is referred to reference [85] for a more detailed discussion.

Over 99% of lymphedema cases are secondary, i.e. due to damage of lymphatic vessels[107]. The subtype distribution of acquired lymphedema differs considerably between southern and northern hemisphere.

Predominantly in low- and middle-income countries in the southern hemisphere, about 120 million people are infected with the mosquito-transmitted filarial nematodes *Wuchereria bancrofti*, *Brugia malayi* and *Brugia timori*, causing lymphatic filariasis (LF). Only a part of the infected people develops LF, but they are clustered in families, indicating a genetic predisposition for this disease[108]. The adult parasites reside and reproduce in lymphatic vessels, leading to dilation and destruction of the lymphatic system[109]. The final stage is known as elephantiasis due to the massive swelling of external genitalia and lower limbs, predisposing the affected individually for bacterial infections and social stigmatization[110]. It is the most common cause for acquired lymphedema worldwide[108].

In the industrialized world, the leading cause for secondary lymphedema is breast cancer surgery. In 6 to 30%, the surgery or irradiation of the breast and associated axillary LN, leads to edema of the upper ipsilateral limb, caused by decreased afferent lymph flow[111]. More recent studies suggest that beside the surgical injury also genetics can predispose a patient to develop post-surgical edema[112].

Podoconiosis (endemic nonfilarial elephantiasis) is a geochemical disease, caused by the long-term absorption of volcanic minerals in red-clay soils through chronic exposure of barefoot feeds[113]. A study in Ethiopia revealed high association between

HLA variants and disease outbreak, suggesting that the inflammation of lymphatic vessels leads to obstruction, presumably through a T-cell response[113].

Although lymphedema is a prevalent disease reducing quality of life significantly, treatment options are limited and require further research. Possible strategies include classical conservative approaches such as physiotherapy and controlled compression stockings, as well as surgical strategies like liposuction or even microsurgical lymph node transplantation [114]. Preclinical studies further indicate that reconstitution of damaged lymphatic vessels using VEGFC as a lymph specific growth factor could represent a promising treatment option. In Chy mice as well as in a mouse model of postmastectomy lymphedema, adenoviral VEGFC overexpression leads to the functional restauration of lymphatic network in damaged areas[86,115].

1.2.3.2 Inflammation

Inflammation is a complex biological response to potential harmful stimuli, such as pathogens, damaged cells or irritants[116]. The spectrum of inflammation is diverse, ranging from highly acute inflammatory responses, like sepsis, to chronic, low-level inflammatory states such as atherosclerosis or obesity[116,117]. Furthermore, inflammation is regularly associated with lymphangiogenesis (also called inflammation-associated lymphangiogenesis, IAL), increasing lymphatic drainage of inflammatory cells, cytokines, debris and edema, supporting resolution of inflammation[118]. Several cell types start to express VEGF-C, induced by NFκB signaling triggered by bacterial lipopolysaccharide and proinflammatory cytokines[119,120]. Blocking of VEGFR3 signaling aggravates the inflammation and increases duration of inflammation and edema in several disease models[121–124], indicating that IAL is crucial for physiological inflammatory response. On the other hand, IAL can catalyze immune. In transplant surgery, rejection of a transplanted organ is associated with a broad lymphangiogenic response[125], and blocking of VEGFR3 signaling increases graft survival[126,127].

1.2.3.3 Cancer and tumor metastasis

The World health organization defines cancer as a large group of diseases characterized by the division of abnormal cells, which can invade adjoining parts of the body and spread to other organs. It is the second leading cause of death globally. Most patients do not die from the primary tumor, but rather from its metastatic spread[128]. The lymphatic system is centrally involved in the pathogenesis of cancer. First, as origin of solid tumors (so called lymphovascular tumors), and secondly as route for tumor cells

to metastazise[129]. Most epithelial tumors metastasize by spreading via lymphatic vessels, not blood vessels[130].

There is evidence that intratumoral LVs are non-functional due to high intratumoral pressure, whereas peritumoral vessels are functional and may constitute a favorable environment for metastasis[131]. Some cancer cells express CCR7, using the CCL21 gradient sustained by LVs to hijack the lymphatic system[132,133]. Another mechanism is the expression of CXCR4, binding to CXCL12 produced by LECs, favoring a microenvironment supporting tumor growth[134]. Clinically, LV density can be correlated with probability of LN metastasis in several cancer types[135,136], and in primary melanomas tumor lymphangiogenesis was a more accurate predictor for LN metastasis then tumor thickness[136]. The first LN to which a tumor will likely metastasize is called sentinel LN (SLN) and detection of cancer cells in it has profound impact on therapy and prognosis of patients[137].

Cancer research is an enormous field of research with thousands of laboratories around the world working on different aspects of it, and it is not possible to expose all facets in the framework of this thesis. The interested reader is referred to one of the excellent reviews about this topic[129,130].

1.2.3.4 Cardiovascular system

Prox1$^{+/-}$ mice develop adult on-set obesity and lymph promotes adipogenesis *in vitro*, tempting to conclude that leakage of lymph leads to development of obesity in mice. Furthermore, human and mouse lymphedema are characterized by the accumulation of fat in the connective tissue[138]. However, PROX1 is also expressed in the skeletal muscle and liver, known key players in energy metabolism, making it difficult to interpret this phenotype[21].

It is well known that high-salt-diets lead to hypertension[139]. Furthermore, high-salt-diet increases lymphangiogenesis, and VEGF-C can lower blood pressure over a VEGFR-2/eNOS-mediated mechanism[140]. Vice versa, blocking of lymphangiogenesis elevates blood pressure of mice under salt diet[140]. This leads to the conclusion, that the lymphatic system is an extrarenal regulator of blood pressure by regulating fluid and electrolyte homeostasis, although the relevance for blood pressure physiology in humans is not elucidated yet.

It is well established that atherosclerosis is driven by a chronic inflammation due to cholesterol accumulation in the arterial wall[141]. Cholesterol removal from the arterial wall, also called reverse cholesterol transport (RCT), constitutes a step towards resolution[142]. Cholesterol, mainly transported in high-density lipoproteins (HDL), uses

the lymphatic system to exit the interstitium towards blood circulation[49,143], and obstruction of collecting vessels in the popliteal area reduce RCT of the footpad to 20%[49], suggesting that postcapillary venous circulation is not sufficient to sustain RCT. Entry of HDL into the lymphatic system succeeds through passive and active mechanisms[49]. These data indicate that the lymphatic system is tightly involved in the pathogenesis of atherosclerosis and could represent an appealing target for future therapy strategies. Atherosclerosis can cumulate in myocardial infarction, followed by a robust inflammatory response, also resulting in reinforced lymphangiogenesis. It has been shown that VEGF-C stimulation enhances lymphatic sprouting in the heart, leading to improved cardiac function post-myocardial infarction[144].

1.3 FOXO-transcription factors

1.3.1 What are FOXOs?

FOXOs are a subclass of the forkhead box family of transcription factors, involved in the regulation of fundamental cellular processes such as cell proliferation, differentiation, apoptosis and metabolism[145]. Due to their complex upstream regulation and their impact on cellular responses to environmental changes they are often referred to as homeostasis regulators, or rheostats of the cell[145,146]. Members of this family are characterized by a highly conserved DNA-binding domain, the so-called forkhead domain. The name rests on the helix-turn-helix-motif, consisting of three α-helices and two large loops, enabling binding to the core consensus DNA sequence 5'-TTGTTTAC-3'[147]. Differences in gene regulation between different family members are achieved by differences in N- and C-terminal parts of the proteins.

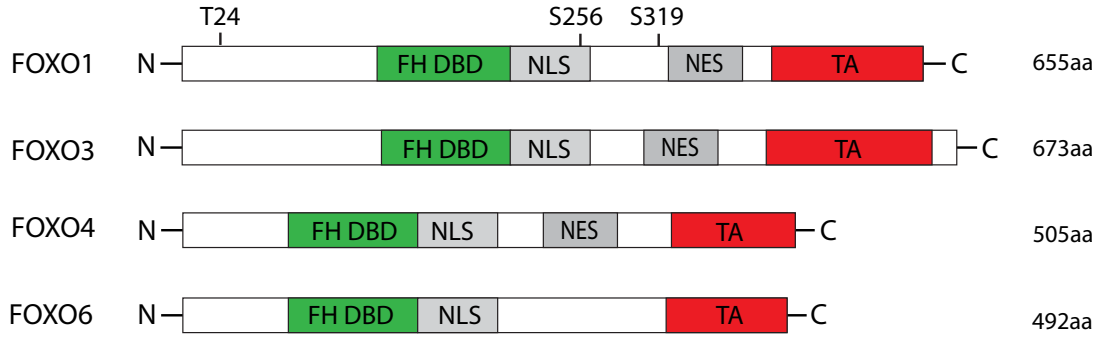

Figure 2: Structure of FOXOs. Schematic diagram showing the different domains that characterize the FOXO subclass. Besides the forkhead DNA-binding domain (FH DBD), shared by all Fox proteins, FOXOs also possess a nuclear localization sequence (NLS) as well as a nuclear export sequence (NES), enabling nucleo-cytoplasmic shuttling. The transactivation domain (TA) contains binding sites for other proteins. The AKT-binding sites for FOXO1 are shown. Adapted from Lam et al., 2013[148]

In 2000, a standardized nomenclature for genes and transcripts of forkhead transcription factors has been proposed. *FOX* was introduced as a unifying symbol, followed by the letter *A-S* (19 subgroups). All uppercase letters indicate human origin (e.g., *FOXO1*), only the first letter capitalized mouse (e.g., *Foxo1*), and the first and subclass letter capitalized all other chordate origin (e.g. *FoxO1*)[149]. All proteins, irrespective of their species, are written in capital letters. This nomenclature will be used in this thesis.

The FOXO subgroup consists of four members: FOXO1, FOXO3, FOXO4 and FOXO6. FOXO2 is homologous to FOXO3, FOXO5 is only expressed in *Danio rerio*. While the expression of FOXO6 seems to be restricted to the brain, FOXO1, 3 and 4 are ubiquitously expressed, even though expression levels can differ between tissues[150]. The overlapping but divergent expression patterns of FOXOs indicates that FOXO family members have distinct but also redundant functions[151]. Indeed, *Foxo1*-deficient mice die aroung E10.5 due to impaired vascular development[152,153], while *Foxo3*-null mice are viable and show an abnormal ovarian phenotype leading to secondary infertility[154]. *Foxo4*-null mice do not show obvious phenotypes[153]. Induced compound knockouts of *Foxo1*, *Foxo3* and *Foxo4* knockouts develop a cancerous phenotype characterized by lymphomas and hemangiomas[155].

1.3.2 Functions of FOXO1

1.3.2.1 Control of proliferation

Proliferation requires cell division, achieved by entering the cell cycle from a quiescent state, consisting of G1 (gap phase 1), S (synthesis of DNA phase), G2 (gap phase 2) and Mitosis. The cell cycle is stringently supervised and controlled to ensure proper organismal growth, development and function. The control of the cell cycle is primarily executed by cyclin dependent kinases (CDKs) and their regulatory subunits, the Cyclins, which are expressed periodically throughout the cell cycle[156]. FOXOs regulate cellular proliferation by interfering with cell cycle progression at different levels.

1.3.2.1.1 G1/S phase transition

Upregulation of D-type cyclins activate CDK 4 and 6, leading to the hyperphosphorylation of retinoblastoma protein and subsequent activation of E2F transcription factors, mediating the expression of gene subsets transacting the G1/S transition[157]. The regulation of this point is especially important, because once the restriction point is passed, the cells become independent of growth factors and are committed to the next round of cell cycle[158]. FOXOs interfere at multiple levels to

prevent transition into S-phase. Several Cyclin-dependent kinase inhibitors (CKIs), of the Cip/Kip family as well as the INK4-family are induced by FOXO. CKIs inhibit the assembly as well as the activity of CDK-Cyclin-complexes. There is evidence for a FOXO-dependent upregulation of Cip/Kip-family-members $p21^{Cip1}$ and $p27^{Kip1}$, leading to decreased activity of cyclin A, E and D[159–162].

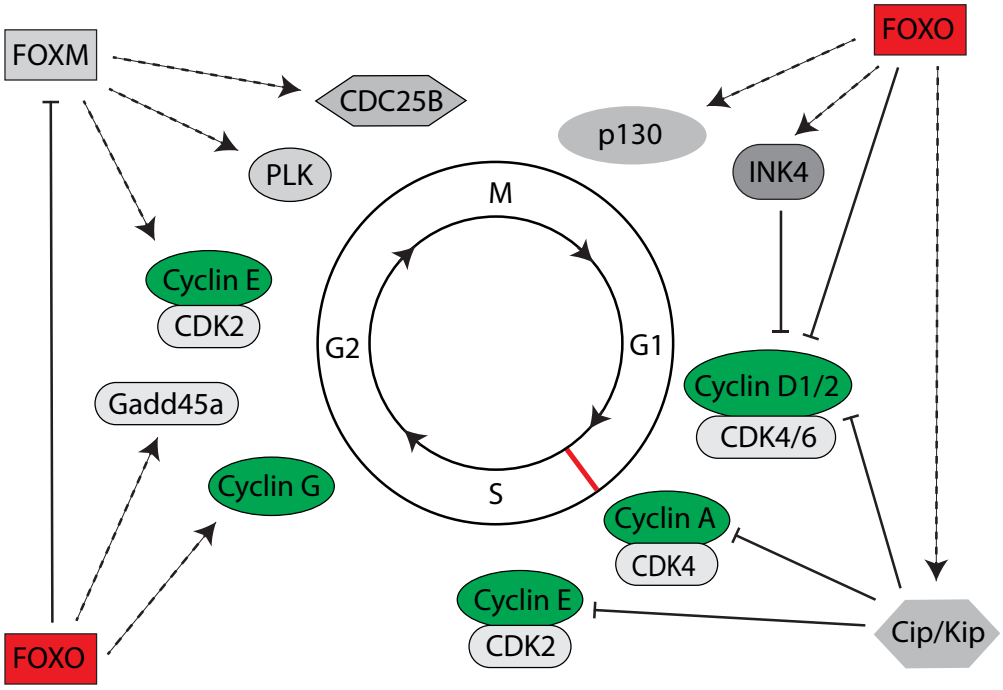

Figure 3: FOXOs participate in cell cycle regulation by a variety of cell cycle regulatory proteins (CCRP). G1 and G2/M checkpoints are holded by the activation (dotted lines) of a number of CCRPs, including p130, members of the Cip/Kip and INK4 CKI families, cyclin G and Gadd45a. Furthermore, FOXOs can simplify cell cycle arrest through the inhibition (solid lines) of the D-type cyclins and FoxM, a subgroup of Fox transcription factors which is known to promote G2/M phase transition. Adapted from Ho et al., 2008[156]

In vivo, the entry into the cell cycle of FOXO isoform-deficient hematopoietic stem cells can be prevented by expression of $p21^{Cip1}$ and $p27^{Kip1}$. Sustained upregulation of $p21^{Cip1}$ can induce senescence, a state of permanent cell cycle arrest[163]. The CDK-4/5-specific CKIs of the INK4-family $P15^{Ink4b}$ and $p19^{Ink4d}$ are also regulated by FOXOs, leading to G1 arrest of the cell.

Additionally, FOXOs interfere with cell cycling by downregulating Cyclin D1 and D2 indirectly via Bcl-6[164], and might also target directly the pRB proteins p107 and p130[165]. In conclusion, FOXOs are able to influence many proteins involved in G1/S phase transition, leading to decreased transcriptional activity of E2F.

1.3.2.1.2 G2/M phase transition

This checkpoint allows DNA damage repair, preventing transmission of mutant DNA to the next generation of cells, thereby representing an important component of the cell's

stress response[156]. *In vivo*, defects in G2/M phase transition cause genomic instability and subsequently cancer development[166]. The role of FOXOs in this context is not fully elucidated yet and, in some points, controversial. Alvarez et al. reported the FOXO-dependent induction of genes responsible for G2/M progression, such as cyclin B and polo-like kinase[158]. On the other hand, there is evidence that FOXO acts as an inhibitor of the G2/M transition. Microarray analysis revealed that FOXO1 upregulation leads to the downregulation of genes indispensable for G2/M transition, such as CDK2, Cyclin B1/B2 or CDK1[167]. This results partly oppose those of reference [158], and might be the result of tissue-specific differences in FOXO regulation and function. Additionally, the cyclin G2 seems to be a direct target of FOXOs. By inhibiting the Cyclin B/CDK1 complex, this unconventional Cyclin leads to G2/M arrest[168]. Furthermore, FOXO-dependent regulation of the DNA damage response gene GADD45a[169] and the Bcl-2 family member Bcl-XL[170] support this hypothesis. More recent studies suggest that FoxM, a transcription factor promoting G2/M progression is repressed by FOXO, underlining the complex regulation of the cell cycle by a transcriptional network[171,172].

1.3.2.1.3 Metabolic adjustments in proliferation

Proliferation is metabolically demanding, requiring an adjustment of metabolism. To adjust cell metabolism to the current proliferative status of the cell, FOXO1 regulates c-Myc[146] and the mammalian target of rapamycin (mTOR)[173], among others. The role of c-Myc in endothelial cells has been studied, characterizing a quiescent state in endothelial cells caused by FOXO1 dependent inhibition of c-Myc. This quiescent state goes along with reduced glycolysis and mitochondrial oxidative metabolism[146].

The serine/threonine kinase mTOR has been characterized by intensive research over the last decades as one of the fundamental regulators of cell growth[174]. mTOR assembles with different proteins to form two complexes, called mTORC1 (complex with RAPTOR and mLST8) and mTORC2 (complex with RICTOR and mLST8). Integrating multiple upstream pathways, mTORC1 regulates protein synthesis, lipid and nucleotide synthesis and autophagy, depending on the current growth state of the cell[174,175]. Most upstream pathways converge on Ras-related GTPase Rheb, an important inductor of mTORC1. Rheb is tightly controlled by the GTPase-activating proteins TSC1 and TSC2[175].

Although FOXO1 and mTORC1 are both targets of AKT[176], Chen et al. describe a FOXO1-dependent regulation of mTORC1 in an TSC2-dependent and independent manner[173]. On one hand, FOXO1 is identified as a direct inducer of Sestrin 3 (SESN3) in mouse embryonic fibroblasts (MEFs)[173]. SESN3 inhibits TSC2 regulating Rheb, thereby inhibiting mTORC1 by inactivating Rheb[177,178]. Independent of TSC2, FOXO1

induces RICTOR, thereby diverting mTOR signaling towards mTORC2 at the expense of mTORC1[173,178].

In conclusion, FOXO activation promotes cell cycle arrest, an important cellular event preceding differentiation, thereby playing a key role in cell fate decisions. A well-studied example is chronic myeloid leukemia, related to Bcr-Abl-induced PI3K-AKT-overexpression and thereby FOXO inhibition. FOXO overexpression in these cells can induce erythroid differentiation, suggesting that a FOXO-induced cell cycle arrest is a crucial event for proper differentiation of the myeloid cell lineage[179].

1.3.2.2 Stress resistance

For survival, organisms must cope with diverse stress conditions to protect the integrity of their DNA and the functionality of the cell. FOXOs are activated upon oxidative stress by phosphorylation through c-Jun N-terminal kinase (JNK), translocate into the nucleus and induce protective genes[180]. Well-studied is the direct regulation of superoxide dismutase 2 (SOD2) by FOXOs[181]. This enzyme converts superoxide to oxygen and hydrogen peroxide, thereby scavenging an important byproduct of the mitochondrial electron transport chain[181]. There is evidence that at least in erythroblasts FOXO3 also regulates SOD-1, promoting the protective function of these transcription factors[182]. Hydrogen peroxide is a strong oxidizing agent with cytotoxic effects, for which reason it must get reduced rapidly. The reaction of hydrogen peroxide to water and oxygen can be catalyzed by the enzyme catalase, a peroxisomal heme peroxidase under the regulation of FOXO3[183]. Additionally, hydrogen peroxide can be reduced by antioxidants such as thioredoxin and glutathione. Several enzymes that catalyze this reaction, such as Peroxiredoxin-3, Prx3 and 5, glutathione peroxidase-1 and GPx-1, are downstream of FOXO[182,184,185]. It has also been proposed that FOXOs and p53 cooperate, to find the fitting response to the stress amount the cell is exposed to[145,186]. Under acute metabolic stress, FOXO-mediated gene regulation aims to restore metabolic homeostasis. If this stress starts to cause substantial harm, additional activation of p53 induces DNA damage repair. If the harm is not manageable, senescence or apoptosis is induced[145].

1.3.2.3 Apoptosis

FOXOs are actively involved in the regulation of apoptosis, and thereby indirectly in the process of differentiation, immune tolerance and cell number homeostasis. FOXOs induce the transcription of proteins inducing apoptosis in a mitochondrial-dependent

and -independent manner[151]. Mechanistically, FOXOs induce death receptor ligands by direct binding to their promotors. These ligands activate death receptors, subsequently leading to the activation of caspase subsets and execution of apoptosis in an mitochondrial-independent manner. Namely, FOXOs induce FasL, leading to the translation of a protein activating the death receptor Fas/CD95/APO-1[151]. The promotor of FasL contains three DNA binding elements, suggesting a direct regulation by FOXO[187,188]. *In vivo*, constitutive FOXO3 expression induces apoptosis in cerebellar granule neurons by the Fas signaling cascade[187]. Overexpression of FOXO1 and 3 in prostate cancer cells leads to apoptosis and an increase in the expression of tumor necrosis factor-related apoptosis-inducing ligand (TRAIL). The promotor of TRAIL contains DNA binding elements for FOXO, indicating that also this death receptor ligand seems to be regulated directly by FOXO[189]. By regulating the expression of FasL and TRAIL, FOXOs can influence cell survival in an autocrine and paracrine manner.

Besides the regulation of death receptor ligands, FOXOs also control the transactivation of the BCL-2 family and thereby the mitochondria-dependent pathway of apoptosis[151]. The BCL-2 family consists of both anti- and proapoptotic proteins and plays a critical role in regulating cell death. The BCL-2 family member Bim is directly controlled by FOXO by two DNA binding elements and exerts its function in the mitochondrial apoptotic pathway via a BH3 domain[190]. *In vivo*, FOXO3 induces Bim in hematopoietic stem cells under conditions of growth factor deprivation[191,192]. In a clinical context, paclitaxel responsive breast cancer cells showed paclitaxel-dependent FOXO3a upregulation and subsequent elevation of Bim, explaining at least in part the antitumoral effects of paclitaxel[193]. Other proapoptotic BCL2 members regulated by FOXOs are bNIP3 and Bcl-X_L.

In summary, FOXOs can promote apoptosis intrinsically by changing the ratio of proapoptotic to antiapoptotic BCL-2 members, and on the other hand by inducing the expression of death receptor ligands (death cytokine mechanism). However, it is not well understood which factors are responsible for cell-type specific responses to certain stress stimuli and how the decision to enter quiescence, senescence or apoptosis is processed.

1.3.3 Regulation of FOXOs

The most conserved FOXO regulatory pathway is the PI3K-AKT/PKB signaling cascade, linking extracellular growth signals with proliferation, metabolism and stress resistence[194]. Growth factors, for example VEGF-C, bind to the VEGFR3 on LECs, leading to receptor autophosphorylation and thereby to the recruitment of SH2-domain-containing proteins, such as the Phosphatidylinositol-3-Kinase (PI3K), among others.

Activated PI3K phosphorylates the membrane-bound lipid phosphatidylinositol-4,5-bisphosphate [PI(4,5)P_2] to phosphatidylinositol-3,4,5-triphosphate [PI(3,4,5)P_3], which is recognized by a broad spectrum of proteins possessing a Pleckstrin homology (PH) domain, including protein serine-threonine kinases, protein tyrosine kinases and exchange factors regulating G-proteins[194–196].

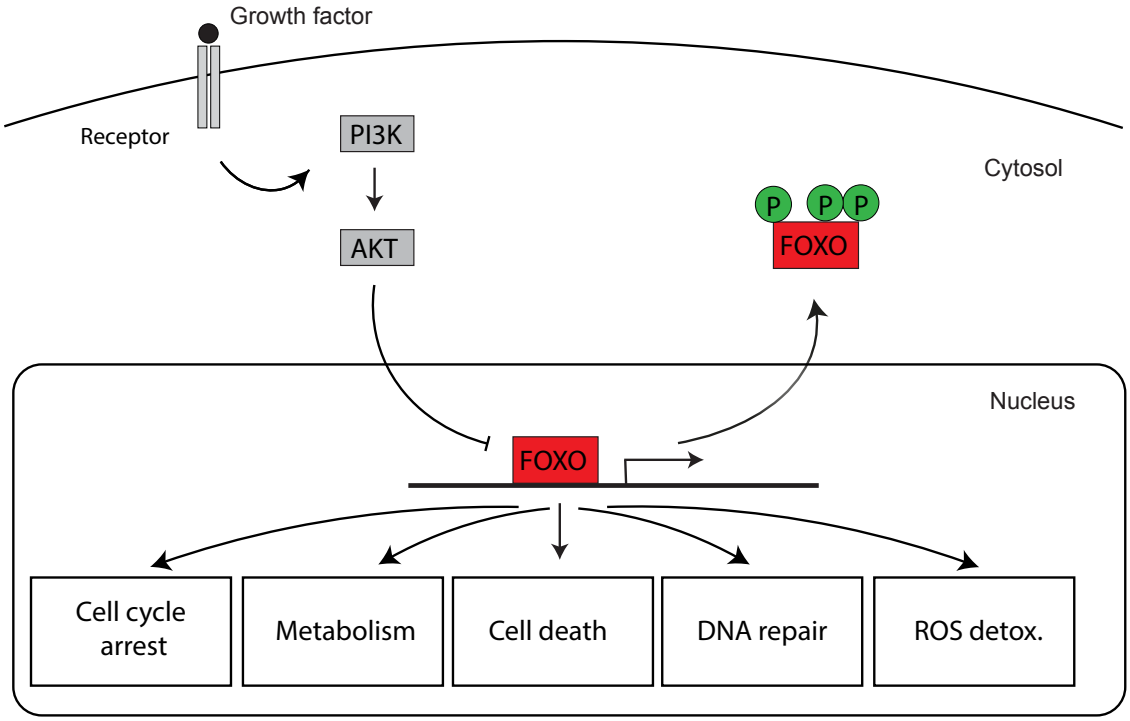

Figure 4: Regulation of FOXO by the PI3K-AKT pathway. FOXOs control various cellular responses, ranging from proliferation and metabolism to DNA repair, ROS detoxification and apoptosis. On stimulation of PI3K/AKT signaling by growth factors, AKT phohphorylates FOXOs on 3 conserved residues, which leads to their cytoplasmic sequestration and inactivation. Adapted from Oellerich and Potente, 2012[197].

Of particular interest are the phosphoinositide-dependent kinase-1 (PDK1) and AKT (PKB), both recruited to the plasma membrane and thereby brought into proximity, leading to increased phosphorylation and subsequent activation of AKT by PDK1[194,198,199]. AKT phosphorylates proteins possessing the canonical AKT consensus sequence (Arg-Xaa-Arg-Xaa-Xaa-(Ser-Thr))[200]. FOXOs are *bone fide* AKT targets and are phosphorylated at three consensus sites: Thr-24, Ser-256 and Ser-319[201–204]. Phosphorylation at these sites enables binding of so called 14-3-3 proteins - regulatory proteins recognizing phosphorylated serine or threonine[205–207]. This protein-protein-interaction leads to the disruption of FOXO binding to the DNA and export into the cytoplasm, resulting in an inhibition of target gene transcription[187,202,208–210]. In the cytoplasm, FOXO is prevented from reentering the nucleus by 14-3-3 interfering with

the Nuclear Localization Sequence (NLS). Subsequently, it gets rapidly ubiquitinated by the E3-ubiquitin ligase SKP2 leading to proteasomal degradation[211–213].

PI3K-AKT-signaling can be terminated by two different phosphatases: While the phosphatase PTEN dephosphorylates $PI(3,4,5)P_3$ at the D3-position, leading to an almost complete switch-off, the phosphatases SHIP1 and SHIP2 dephosphorylate at the D5-position, resulting in reduced PI3K-AKT-signaling. Loss of SHIP2 increases insulin sensitivity[214] and Loss of PTEN has been found to be relevant in several human cancers[215], suggesting that tightly controlled PI3K-AKT, and thereby also FOXO-signaling, is a prerequisite for proper cell metabolism, cell growth and survival[194].

Several studies showed that PI3K-AKT-signaling is indispensable for blood vascular development[216,217]. Specific for lymphangiogenesis, it has been shown that knockout of AKT1 leads to reduction of LV diameter, cell number and valves, and the SMC coverage was sparser compared with wild type mice[218]. Additionally, it has been shown that several venous and lymphatic malformations are caused activating mutations in the PI3K-AKT-signalling pathway[85,219].

Oxidative stress leads to the activation of c-Jun N-terminal kinase (JNK), resulting in inactivation of PI3K-AKT-signaling and subsequent activation of FOXO. JNK phosphorylates FOXOs at Thr447 and Thr451, leading to shuttling of FOXO into the nucleus[180]. This is supported by phosphorylation of IRS and 14-3-3, overriding PI3K-AKT-signaling and favoring nuclear re-localization of FOXOs[220,221]. JNK signaling thereby enables FOXO target gene transcription (e.g. MnSOD) counteracting cellular stress[180].

AMPK is a protein kinase whose activation indicates low energy levels within the cell. This energy-sensing kinase leads to the induction of metabolic pathways providing ATP and turn off of ATP-consuming pathways[222]. FOXO3 is phosphorylated by AMPK at 6 phosphorylation sites, leading to the activation of the transcription factor without affecting its subcellular localization[223]. Microarray data suggests that phosphorylation at AMPK-specific sites induces a specific set of FOXO target genes, maybe by recruitment of specific coactivator complexes[223].

Besides theses kinases[224], FOXOs are regulated by a wide range of other posttranslational modifications (PTMs), including acetylation and ubiquitylation, reviewed in more detail elsewhere[225].

Anne Brunet proposed a model called ‘The FOXO code’, ‘written’ by different enzymes with different PTMs depending on the cellular environment and intracellular state[225]. This code would be ‘read’ by different interacting proteins and modulate the diverse gene programs controlled by FOXO, leading to specification of an appropriate cellular

response[225]. In summary, FOXOs integrate a wide range of signals, thereby positioning this transcription factor as an upstream regulator of cell fate, growth and development.

1.3.4 FOXO1 in endothelial cells

The germline knockout of *Foxo1* in mice, published in 2004, highlighted the importance of FOXOs for the blood vasculature[152,153]. Mouse embryos lacking *Foxo1* die around E10.5 due to defective angiogenesis, pointing towards an indispensable function of FOXOs in blood vessel development. A study by Sengupta et al. illustrated that the conditional knockout of *Foxo1* in ECs phenocopies the global knockout, emphasizing its importance in the endothelium[226]. Paik et al. published the first inducible somatic *Foxo1* knockout in 2007, which allowed to bypass the embryonic lethal phenotype[155]. FOXO1 deficiency led to liver hemangiomas and premature death, and broad knockout of *Foxo1*, *Foxo3* and *Foxo4* lead to cancers, such as angiosarcomas, hemangiomas and thymic lymphomas. Wilhelm et al. were the first researchers studying the role of FOXO1 in the blood endothelium using inducible conditional gene knockout and overexpression techniques[146]. The study identified FOXO1 as a key regulator of endothelial quiescence, coupling metabolic activity and cell cycle state[227]. Nevertheless, this study focused on the mouse retina, leaving other vascular beds and endothelial subtypes unaddressed.

The first study about FOXO1 in lymphatic vessels was published in 2020[228]. Niimi et al. studied the effect of postnatally induced, conditional *Foxo1*-Knockout in the murine tail skin, describing the phenotype as disconnected and dilated. As a mechanism they postulate impaired migration to the C-X-C chemokine ligand 12 (CXCL12), due to strong reduction of the complementary receptor CXCR4, a target of FOXO1 in LECs. Additionally, they reported higher proliferation and lower apoptosis in FOXO1-deficient lymphatic vessels. However, the effects of FOXO1 overexpression were not reported. In 2021, two studies were published studying the role of FOXO1 in lymphatic valve formation and maintainance[229,230]. Scallan et al. suggested a model in mesentery lymphatics, where FOXO1 suppresses valve-specific genes, thereby acting as a negative regulator of valve formation[229]. Niimi et al. support this data, mechanistically adding PRDM1 as the downstream repressor of FOXO1 for lymphatic valve specific genes[230]. In 2024, Du et al. reports of the mechanosensitive channel PIEZO1 as a an upstream inducer of the angiopoietin/TIE/FOXO signaling pathway, linking mechanosensitive channels and lympho-vascular signaling[105].

1.3.5 FOXO transcription factors in disease

The discussed roles of FOXOs merge in a broad spectrum of diseases related to FOXO deregulation or malfunction. This thesis will focus on the development of cancer as a proliferative disease, although FOXOs play important roles in many other diseases such as diabetes. For further information the interested reader is referred to one of the excellent reviews about the pathophysiological roles of FOXOs in diseases[186].

The first causal link between FOXO1 and cancer was found in alveolar rhabdomyosarcomas (ARMS)[231]. A chromosomal translocation leads to a chimeric protein of PAX3 or PAX7 with FOXO1, consisting of the DNA-binding domain of Pax3/7 and the transactivation domain of FOXO1. This protein is no longer under the control of AKT[231], leading to subsequent increase in Pax target gene transcription able to induce oncogenic transformation *in vitro*[232]. However, overexpression of the PAX3-FOXO1 chimeric protein is not able to induce tumors *in vivo*, refuting this hypothesis[233]. Instead, the expression of the chimeric protein seems to significantly decrease the levels of FOXO1 protein as an important tumor suppressor[234], probably by upregulating SKP2[235]. It seems likely that the induction of tumor promoting genes as well as the downregulation of a tumor suppressor genes contribute to tumorigenesis of ARMS.

Activated PI3K-AKT-signalling and subsequent inhibition of FOXOs seems to be an obligate event in cancer development. Reintroduction of FOXO in PTEN-deficient tumors leads to cell cycle arrest and apoptosis, revealing the intimate connection between cell cycle control and FOXO signaling[236]. Additionally, tumorigenesis in PTEN-deficient mice can be prevented by introduction of a constitutive active FOXO1[237].

The data presented above argue that FOXO1 acts as a classical tumor suppressor. Indeed, FOXO1 reduces stress levels in cells and can clear damaged cells by induction of senescence or apoptosis or induce repair mechanisms, preventing the development of cancer. On the other hand, it is well known that's FOXOs maintain leukemia-initiating cells[238,239]. Tumor development generates stress within the cell, and oxidative stress signaling can override PI3K-AKT-signaling and thereby activate FOXO signaling[180]. FOXO might stabilize these cells by acting as a homeostatic regulator and become part of the problem by supporting survival of these cells[145]. In summary, the role of FOXOs in tumors is heterogenous and highly context-dependent.

2 Aim of the study

In this thesis I will explore the role of the forkhead transcription factor FOXO1 in lymphatic growth and maturation. The effect of increased FOXO1 signaling in LECs will be analyzed *in vivo* and *in vitro* using mostly gain-of-function approaches. With transcriptome analysis at different time points, I explore mechanisms of how FOXO1 exerts its function at a molecular level, and how this transcription factor is involved in the coordination of proliferation and maturation of lymphatic vessels.

3 Materials

3.1 Laboratoy equipment

Equipment	**Company**
Agarose gel electrophoresis equipment	Peqlab, GE
Agilent 2100 Bioanalyzer	Agilent Technologies, USA
Biofuge pico Heraceus	Heraceus, GE
Centro XS^3 LB 960 Microplate Luminometer	Berthold Technologies, GE
Coombs and chambers for electrophoresis	Peqlab, GE
ChemiDoc™ MP System	BioRad, GE
Eppendorf centrifuge 5417	Eppendorf, GE
Eppendorf centrifuge 5810R	Eppendorf, GE
Gel Doc Analyzer system	BioRad, GE
StepOnePlus qPCR instrument	Applied biosystems, USA
Thermo Cycler	BioRad, GE
Innova 4300 incubator shaker	New Brunswick Scientific, USA
Leica SP8 confocal microscope	Leica, GE
Luna Automated cell counter	Logos biosystems, GE
Magnetic Mini-Stirrer	HANNA, GE
Magnetic mixer	Variomag, GE
Microwave heater	Panasonic, GE
NanoDrop ND2000 Spectrophotometer	Biozym, GE
pH 211 Microprocessor pH meter	HANNA, GE
Photospectrometer	Thermo Fisher Scientific, USA
Refrigerators, 4 °C, -20 °C, -80°C	Liebherr Premium, GE
Stereomicroscope	Leica, GE
Thermomixer compact Eppendorf	Eppendorf, GE
Vortexer	A.Hartenstein, GE
Water bath	Eppendorf, GE
Western blot equipment	BioRad, GE

Table 1: Laboratory equipment

3.2 Laboratory supplies

Laboratory supplies	**Company**

Beakers	Brand, GE
Cell culture dishes	Greiner Bio One, GE
Cell culture pipettes	BD Bioscience, GE
Cell culture plates	Greiner BioONe, GE
Eppendorf tubes 0.5ml, 1.5ml, 2ml	Eppendorf, GE
Falcon tubes 15, 50ml	BD Bioscience, GE
Filter paper	Neolab, GE
Gilson pipettes	Gilson, USA
Flass bottom culture dishes	Mattek, USA
Glass bottles, Kolen	Brand, GE
Glass cylinders	Brand, GE
Microscop coverslip	Hartenstein, GE
Microscope slides	Hartenstein, GE
Needle, 27G, 24G	BD Bioscience, GE
Pateur pipette Greiner	BioOne, GE
PCR wells	Roche, GE
Pipette tips (10μl, 200μl, 1000μl)	Brand, GE
Plastic pipette 5ml	Greiner BioOne, GE
Precast Gradient Gels	BioRad, GE
Scalpel	Dahle, Rödental, GE
Surgical tools	Megro/Ratiomed, GE
Syringe 1ml	BD Bioscience, GE
Syringe filter, 0.22μm	Roth, GE

Table 2: Laboratory supplies

3.3 Chemicals

Chemicals	**Company**
Agarose	Invitrogen
BSA	Biomol
Chloroquine	Sigma Aldrich
Complete Protease Inhibitor cocktail tablets	Roche
Cycloheximide	Sigma Aldrich
Direct PCR Tail lysis buffer	Peqlab
DNA loading dye 6x	Fermentas
EDTA	Roth
Ethanol absolute	Roth

Ethidium bromide	Merck
Glucose D(+)	Merck
Glycerol 99%	Merck
Goat serum	Vector labs
Hydrogen peroxide	Sigma
Isopropanol 99% (2-propanol)	Roth
Nonfat dried milk powder	AplliChem
Paraformaldehyde	Sigma
Peanut oil	Sigma
Phenol	Roth
Phenol/Chloroform	Roth
Phenylmethylsulfonylfluorid	Sigma
Prolong Gold Antifade Mounting Medium	Invitrogen
RedSafe Nucleic Acid Staining solution	Intron Biotechnology
Smart ladder marker 100bp	Eurogentec
Sodium chloride	AppliChem
Sodium hydroxide	Roth
Sodium hydrogencarbonate-monohydrate	Sigma
Sodium-di-hydrogenphosphate-monohydrate	Neolab
Sodiumdeoxycholate	Sigma
4-Hydroxy-Tamoxifen	Sigma
TaqMan Gene Exxpression Master Mix	Applied Biosystems
Trishydroxymethylaminomethan	AplliChem, GE
Triton-X 100	Sigma
Tween-20	Sigma
Vecta Shield Mounting Medium	Vectorlabs

Table 3: Chemicals

3.4 Buffers and solutions

Buffer	**Composition; Company**
HBSS	8.0 g/l NaCl, 0.4g/l KCl, 0.14g/l $CaCl_2$, 0.1g/l $MgSO_4$-$7H_2O$, 0.1g/l $MgCl_2$-$6H_2O$, 0.06g/l Na_2HPO_4-H_2O, 0.06 g/l KH_2PO_4, 1g/l Glucose, 0,35g/l $NaHCO_3$, pH 7,4; ThermoFisher
PBS	8.0g/l NaCl, 0.2g/l KCL, 1.44g/l Na_2HPO_4, 0,24g/l KH_2PO_4, pH 7,4; ThermoFisher
RIPA	150 mM NaCl, 1.0% IGEPAL CA-630, 0.5% sodium

	deoxycholate, 0.1% SDS, and 50 mM Tris, pH 8.0; ThermoFisher
TAE	40mM Tris acetate, 1mM EDTA, pH 8.0

Table 4: Buffers and solutions

3.5 Cell culture

	Company
Human Dermal Lymphatic endothelial cells	Lonza, CH
EBM2-Media + Supplements	Lonza, CH
Human umbilical vein endothelial cells	Lonza, CH
EBM-Media + Supplements	Lonza, CH
BSA	Invitrogen, USA
VEGF-C	Promocell, GE
FBS	Invitrogen, USA
Trypsin EDTA	Invitrogen, USA
PBS	Invitrogen, USA
HBSS	Invitrogen, USA
Lipofectamine	Invitrogen, USA
OptiMEM	Invitrogen, USA
Gelatin	Sigma Aldrich, USA
Fibronektin	Corning, USA

Table 5: Cell culture

3.6 Enzymes

Enzymes	**Company**
Proteinase K	Sigma, GE
Taq Polymerase	Invitrogen, USA
DNAse	Qjagen, USA

Table 6: Enzymes

3.7 Kits

Kit	**Company**	**Reference**
Click-it EdU Alexa Fluor 555 Imaging Kit	ThermoFisher Scientific	C10338
Clarity Western ECL Substrate	BioRad	#1705060
RNeasy Mini Kit	Qiagen	#74104
miRNeasy Micro Kit	Qiagen	#217084

QIAshredder	Qiagen	#79656

Table 7: Kits

3.8 Viruses

Virus	**Company**	**Catalog No.**
AdFlag-FOXO1-A3	Vector Biolabs	Custom made construct
Ad-CMV-GFP	Vector Biolabs	#1060
Ad-CMV-Null	Vector Biolabs	#1300

Table 8: Viruses

3.9 qRT-PCR probes

Gene	**Reporter**	**Reference number**	**Company**
ACTIN	VIC-MGB	Hs99999903_m1	Applied biosystems
CITED2	FAM-MGB	Hs01897804_s1	Applied biosystems
CCND1	FAM-MGB	Hs00765553_m1	Applied biosystems
FOXO1	FAM-MGB	Hs00231106_m1	Applied biosystems
MXI1	FAM-MGB	Hs00365651_m1	Applied biosystems
MYC	FAM-MGB	Hs00153408_m1	Applied biosystems
NFTAC1	FAM-MGB	Hs00542675_m1	Applied biosystems
PROX1	FAM-MGB	Hs00896293_m1	Applied biosystems
RELN	FAM-MGB	Hs01022646_m1	Applied biosystems
SOD2	FAM-MGB	Hs00167309_m1	Applied biosystems
SPROUTY2	FAM-MGB	Hs01921749_s1	Applied biosystems

Table 9: qRT-PCR probes

3.10 Antibodies used in Western Blot

3.10.1 Primary Antibodies

Antigen, source	**Concentration**	**Company**	**Reference number**
c-Myc, rabbit	1:1000	Cell Signaling Technology	#9402
Caspase-3, rabbit	1:1000	Cell Signaling Technology	#9662
Cleaved Caspase-3, rabbit	1:1000	Cell Signaling Technology	#9664
Cleaved PARP, rabbit	1:1000	Cell Signaling Technology	#5625
Cyclin D1, rabbit	1:1000	Cell Signaling Technology	#2922

Flag M2, mouse	1:1000	Sigma Aldrich	#F3165
FOXO1, rabbit	1:1000	Cell Signaling Technology	#2880
GFP, rabbit	1:1000	Cell Signaling Technology	#2555
Mxi1, mouse	1:500	Santa Cruz	#sc-130627
PARP, rabbit	1:1000	Cell Signaling Technology	#9532
Phospho-FOXO1	1:1000	Cell Signaling Technology	#9464
Prox1, goat	1:500	R&D Systems	#AF2727
Sestrin 3, rabbit	1:1000	Abcam	#ab97792
Tubulin, rabbit	1:1000	Cell Signaling Technology	#2148

Table 10: Primary Antibodies Western Blot

3.10.2 Secondary Antibodies

Antigen, source	Concen-tration	Company	Reference number
Peroxidase AffiniPure Goat Anti-Rabbit IgG	1:5000	Jackson Immuno Research	111-035-008
Peroxidase AffiniPure Rabbit Anti-Mouse IgG (H+L)	1:5000	Jackson Immuno Research	315-005-003
Peroxidase AffiniPure Rabbit Anti-Goat IgG, Fc fragment specific	1:5000	Jackson Immuno Research	305-036-008

Table 11: Secondary Antibodies Western Blot

3.11 Antibodies used in Immunohistochemistry

3.11.1 Primary Antibodies

Antigen	Concentration	Company	Reference number
Connexin 43, rabbit	1:100	Sigma Aldrich	C6219
ERG, goat	1:200	Abcam	Ab77258
ERG, rabbit	1:200	Abcam	Ab92513
FoxC2, sheep	1:100	R&D Systems	AF6989
FOXO1, rabbit	1:100	Cell Signaling Technology	#2880
Integrin a9, goat	1:200	R&D Systems	AF3827
Collagen IV, rabbit	1:400	BioRad	2150-1470

LYVE1, rat	1:200	R&D Systems	MAB2125-500
LYVE1, rabbit	1:200	AngioBio Co.	11-034
MYC, rabbit	1:100	Sigma Aldrich	#06-340
Neuropilin 2, goat	1:200	R&D Systems	AF567
PECAM, goat	1:200	R&D Systems	A3628
PECAM, rat	1:200	BD Pharmingen	550274
Podocalyxin, goat	1:100	R&D Systems	AF1556
Podoplanin, hamster	1:200	BD Pharmingen	566390
PROX1, goat	1:200	R&D Systems	AF2727
PROX1, rabbit	1:200	AngioBio Co.	11-002P
Reelin, goat	1:100	R&D Systems	AF3820
TER-119, rat	1:200	BD Pharmingen	553670
VE-Cadherin, rat	1:200	BD Pharmingen	555289
VE-Cadherin, goat	1:200	R&D Systems	AF1002
VEGFR3, goat	1:200	R&D Systems	AF743

Table 12: Primary Antibodies Immunohistochemistry

3.11.2 Secondary Antibodies

Antigen	Concentration	Company	Reference number
Chicken anti-rat Alexa Fluor 594	1:500	Invitrogen	A21471
Chicken anti-rat Alexa Fluor 647	1:500	Invitrogen	A21472
Donkey anti-goat Alexa Fluor 488	1:500	Invitrogen	A11055
Donkey anti-goat Alexa Fluor 555	1:500	Invitrogen	A21432
Donkey anti-goat Alexa Fluor 647	1:500	Invitrogen	A21447
Donkey anti-mouse Alexa Fluor 488	1:500	Invitrogen	A21202
Donkey anti-rabbit Alexa Fluor 488	1:500	Invitrogen	A21206
Donkey anti-rabbit Alexa Fluor 555	1:500	Invitrogen	A31572
Donkey anti-rabbit Alexa Fluor 594	1:500	Invitrogen	A21207
Donkey anti-rabbit Alexa Fluor 647	1:500	Invitrogen	A31573
Donkey anti-rat Alexa Fluor 488	1:500	Invitrogen	A21208
Donkey anti-sheep Alexa Fluor 555	1:500	Invitrogen	A21436
Goat anti-hamster Alexa Fluor 647	1:500	Invitrogen	A21451
Goat anti-rat Alexa Fluor 555	1:500	Invitrogen	A21434
Goat anti-rat Alexa Fluor 647	1:500	Invitrogen	A21247
Rabbit anti-hamster IgG; FITC	1:500	Invitrogen	#31587

Rabbit anti-mouse Alexa Fluor 647	1:500	Invitrogen	A21239

Table 13: Secondary Antibodies Immunohistochemistry

3.11.3 Directly conjugated antibodies & other staining dyes

Antigen	Concentration	Company	Reference number
Anti rabbit-GFP Alexa Fluor 488	1:100	Invitrogen	A21311
DAPI (4',6-diamidino-2-phenylindole)	1:1000	Sigma Aldrich	#D9542
Phalloidin-TRITC	1:200	Sigma Aldrich	#P1951
α-Smooth Muscle-Cy3	1:200	Sigma Aldrich	#C6198

Table 14: Directly conjugated antibodies & other staining dyes

3.12 Mouse strains

Lab nomenclature	Official strain name	Collaborator
F1dfl	Foxo1^{tm1Rdp}	Ronald A. DePinho
Prox1-CreERT2	Tg(Prox1-cre/ERT2)$^{\#aTmak}$	Taija Mäkinen
RF1fl	R26-Foxo1-ADA-IRES-GFP	Jens Brüning

Table 15: Mouse strains

3.13 Software

Software	Company
Adobe Design Suite CS6	Adobe Systems Incorporated, USA
FIJI	NIH, USA
Microsoft Office 2011	Microsoft, USA
Gene Set Enrichment Analysis	Broad Institute, USA
GraphPadPrism 5	Graphpad Software, USA
Image Lab	BioRad, GE
Volocity	PerkinElmer, USA
StepOne^{TM}	Thermo Fisher Scientific, USA

Table 16: Software

4 Methods

4.1 Animals

4.1.1 Maintenance

All animal experiments were performed in accordance with institutional guidelines and the animal welfare application, approved by the governmental Commission of Animal Care Darmstadt, permit number B2/1124. The mice were maintained under specific pathogen-free conditions with water and food *ad libitum*. All mutant mice had a C57BL/6 genetic background and got regularly health checked by animal care takers.

4.1.2 The Cre-LoxP-system

The Cre-LoxP system is a frequently used experimental tool in molecular biology, which allows the investigation of a gene of interest under spatial as well as temporal control[240].

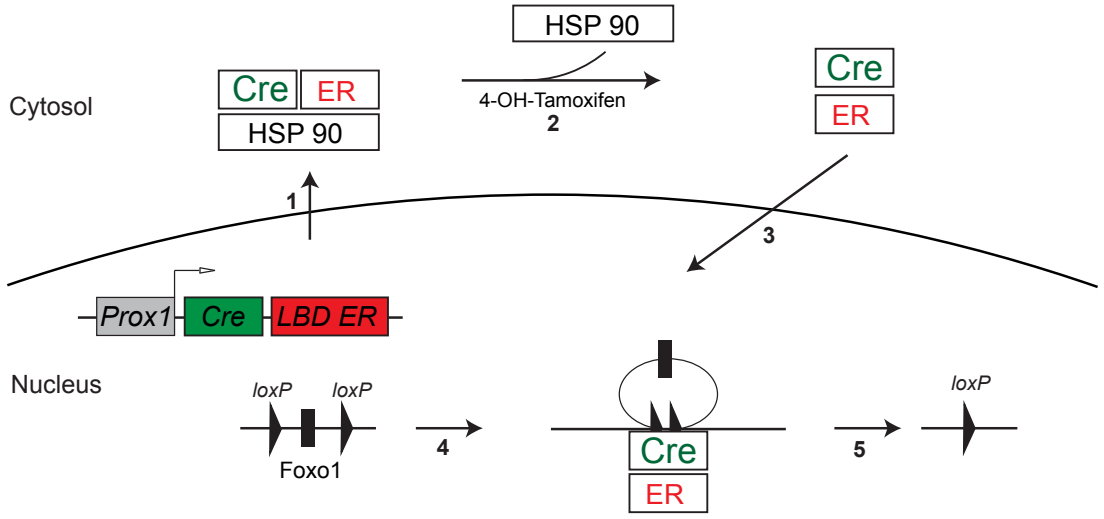

Figure 5: Mechanism of the inducible Cre-loxP system. 1, Cre is fused to an estrogen receptor (CreER) and transcribed under control of a tissue specific promotor, in this example the promotor of Prox1. In the absence of 4-OHT, CreER interacts with Heat shock protein 90 (HSP90), preventing translocation in the nucleus. **2,** Administration of 4-OHT disrupts the interaction and leads to shuttling of Cre into the nucleus **(3)**, where Cre recognizes the loxP sites **(4)** and inactivates the floxed gene, here *Foxo1* **(5).** Adapted from Kim et al., 2018[240]

To generate mice exhibiting inducible (temporal) and conditional (spatial) mutation, Cre-driver strain, expressing the Cre-recombinase under the control of a tissue-specific promotor, are bred with mice, in which the gene of interest is flanked by the recognition sites of Cre (LoxP sites). By fusing Cre to an estrogen receptor with a mutated ligand

binding domain, Cre is excluded from the nucleus in the absence of 4-OH-Tamoxifen (CreER) by binding to heat shock protein 90 (HSP90). In the presence of 4-OH-Tamoxifen, CreER can translocate to the nucleus, recognize the loxP sites and excise the floxed gene. Nowadays a new version, called CreERT2 with an about teen-folds higher sensitivity to 4-OH-Tamoxifen is generally used[241].

4.1.3 Mouse strains

4.1.3.1 Prox1-CreERT2-deleter

This mouse line expresses a Tamoxifen inducible CreER under the control of the promoter of the gene Prox1, which is highly enriched in lymphatic but not blood endothelial cells[242]. To avoid Off-target effects, Cre is only expressed on one allele (heterozygous). The mouse line was generated in the lab of Taija Mäkinen (Uppsala, Sweden) and kindly provided by her.

4.1.3.2 Floxed Foxo1 mice

This mouse possesses two loxP sites flanking the Exon 2 and 3 of *Foxo1* and was kindly provided by Ronald A. DePinho (Boston, USA). For generation, a targeting vector containing the floxed *Foxo1* gene and a Neomycin resistance cassette were introduced via electroporation in mouse embryonic stem cells (ES)[243]. After ES selection with successful integration via Neomycin incubation the ES were used to generate chimeras, and the neomycin resistance cassette was outcrossed by crossing the mouse with Flpe expressing mouse.

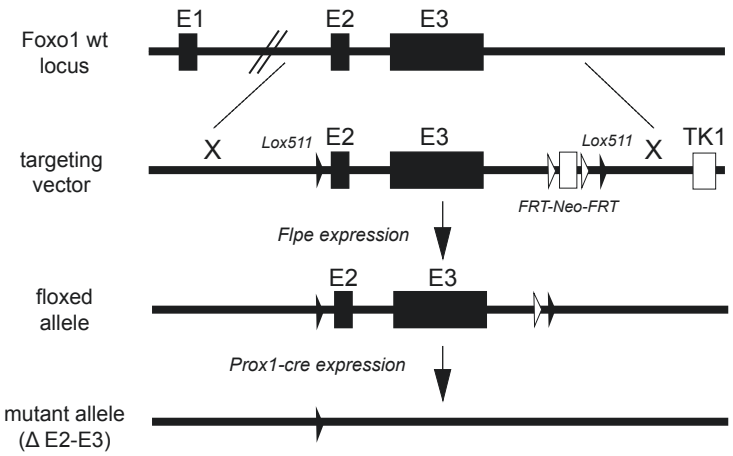

Figure 6: Strategy to generate conditional *Foxo1* mutant allele. Exons 2 and 3 are flanked by lox sites. The structures of the genomic locus, the targeting vector, and the targeted allele are shown. FRT-Neo-FRT, neomycin resistance cassette flanked by FRT-sites. TK1, thymidine kinase. Adapted from Keller et al., 2004[243]

4.1.3.3 Rosa26-Foxo1-ADA-IRES-GFP mice

This mouse line is characterized by a *Foxo1*-mutant with mutated AKT-phosphorylation sites (*Foxo1*-ADA), preventing phosphorylation and following exclusion of Foxo1 from the nucleus[244]. This mutant is introduced into the Rosa26 locus. IRES-GFP is cloned behind this mutant, allowing monitoring of successful recombination. The expression of these CAGS promotor driven genes is inhibited by a loxP-flanked stop cassette[244]. 4-OH-Tamoxifen administration leads to excision of the stop cassette and consequently transcription of FOXO1-ADA and GFP. This mouse was kindly provided by Jens Brüning (Cologne, Germany).

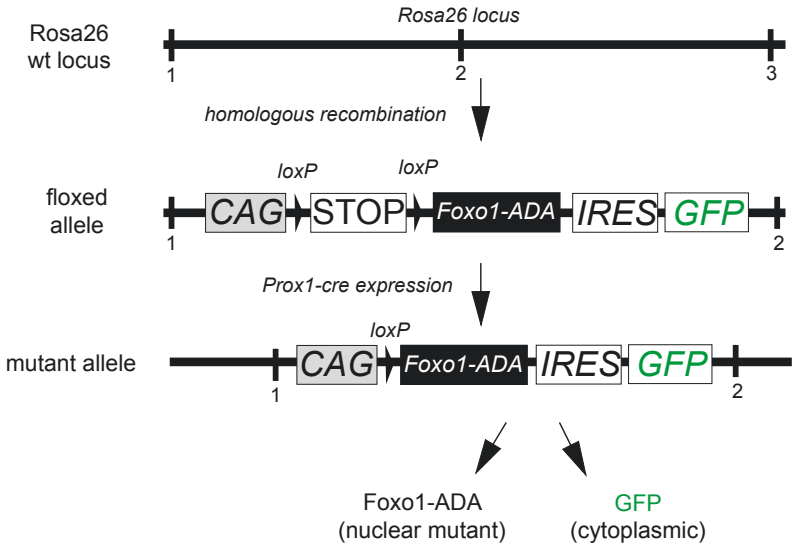

Figure 7: Strategy to generate conditional Foxo1 gain-of-function allele. A cassette containing the CAG promotor, a floxed STOP sequence, a cDNA encoding for Foxo1-ADA, and IRES-GFP was inserted into the Rosa26 locus. The floxed allele, and the recombined allele after cre expression is shown. Adapted from Wilhelm et al., 2016[9]

4.1.4 Genetic experiments

For inducible Cre-mediated recombination in lymphatic endothelial cells, flox mice were bred with Prox1-CreERT2 deleter mice. Cre-mediated recombination was induced in newborn mice by intraperitoneal (i.p.) injections of 25µl of a 2mg/ml solution 4-OH-T (Sigma) from postnatal day 1 until 4 (P1-P4). Mice were harvested 10 or 21 days after birth. As control served the Cre-negative littermates.

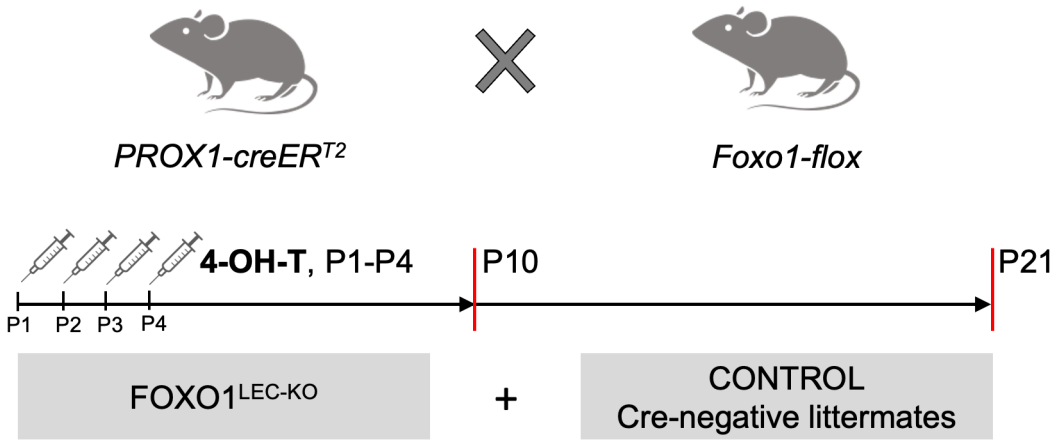

Figure 8: Mating scheme exemplary for *Foxo1* knockout mice. 4-OH-T (4-hydroxy-tamoxifen) was injected at the first four postnatal days. Mice were sacrificed at P10 or P21. A *Prox1-Cre-ER^{T2}- Foxo1$^{fl/fl}$* mouse injected with tamoxifen is referred to as FOXO1$^{iLEC-KO}$

4.1.5 Genotyping

For genotyping, tail biopsies were taken and digested in 190µl lysis buffer (Peqlab) and 10µl Proteinase K (20mg/ml) at 56˚C overnight. After heat inactivation at 85˚C for 45min samples were stored at 4˚C until usage.

One reaction contained the following ingredients:

Component	**Amount (in µl)**
10x PCR Buffer	3
$MgCl_2$ (50mM)	1.3
Primer1	1
Primer2	1
Primer3	1
(Primer4)	1
dNTPs (10mM)	0.6
Taq (5U/l)	0.25
H_2O	18.85

Table 17: Ingredients PCR

The reactions were performed using Primers (Sigma) with a concentration of 20µM listed in Table 18 and conditions mentioned in Table 19 using Thermocyclers (BioRad). All work was performed on ice.

Mouse	**Primers**	**Amplified**

line:		Products
F1dfl	5’ GCTTAGAGCAGAGATGTTCTCACATT 3’	WT 115bp
	5’CCAGAGTCTTTGTATCAGGCAAATAA 3’	Mutant 149bp
	5’CAAGTCCATTAATTCAGCACATTGA 3’	
Prox1-CreERT2	5’GCCTGCATTACCGGTCGATGCAACGA 3’	
	5’GTGGCAGATGGCGCGGCAACACCATT 3’	WT 320bp
	5’ACACCCCAAAGCAACACCACAGGCTC 3’	Cre 720bp
	5’CCTTTCCCCCACTGCCTATTTTCTGATGTC 3’	
RF1fl	5’TGTCGCAAATTAACTGTGAATC 3’	WT 570bp
	5’GATATGAAGTACTGGGCTCTT 3’	Mutant 380bp
	5’AAAGTCGCTCTGAGTTGTTATC 3’	

Table 18: Primers for Genotyping

Mouse line	Step	Temperature	Time	Cycle number
F1dfl	1	94 °C	10 min	1x
	2	94 °C	30 sec	32x
	3	63 °C	1 min	
	4	72 °C	1 min 30 sec	
	5	72 °C	6 min	1x
	6	4 °C	∞	1x
Prox1-CreERT2	1	94 °C	5 min	1x
	2	94 °C	45 sec	40x
	3	70 °C	1 min	
	4	72 °C	1 min	
	5	72 °C	6 min	1x
	6	4 °C	∞	1x
RF1fl	1	94 °C	3 min	1x
	2	94 °C	30 sec	45x
	3	56 °C	45 sec	
	4	72 °C	1 min 30 sec	
	5	72 °C	10 min	1x
	6	4 °C	∞	1x

Table 19: Cycling protocols

The PCR samples were loaded on a 2% Agarose gel supplemented with RedSafe Nucleic Acid Staining solution (1:20.000, Intron Biotechnology). The gel ran at 180V for

approximately 1h, depending on the size of the gel and the length of the amplified DNA products. After separation the gel was imaged using a BiogelDoc analyzer.

4.1.6 Ear model

To study postnatal lymphangiogenesis, mice were harvested 10 (P10) and 21 (P21) days after birth. Then the mouse ear was removed from the mouse head and cut along the Antihelix (Figure 9a, b). All the following steps were performed under a stereomicroscope. The intervening cartilage was carefully separated from the dorsal ear skin by gently pulling the latter (Figure 9d). Next, the dissected dorsal ear skin (Figure 9) was transferred to a 12-well plate filled with PBS with the exposed surface facing down, stretching out the skin due to surface tension.

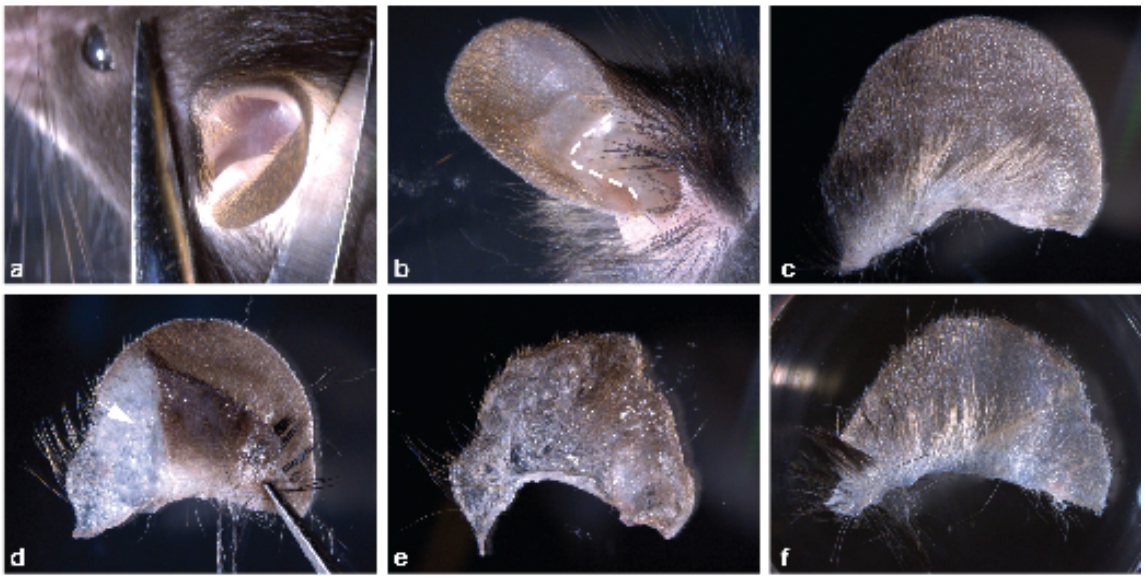

Figure 9: Stepwise dissection of the ear. a, Image showing the mouse head at P21 and scissors. **b,** Close up of the ear and pointing out where to put the first cut. **c,** Overview over the ear cut along the Antihelix. **d,** half dissected ear, showing the intervening cartilage (white arrow). **e,** Freshly dissected, wrinkled ear skin. **f,** Ear skin stretched out on PBS due to surface tension.

The ear skin was fixated in 4% Paraformaldehyde in PBS. After 3h the skin was washed once with PBS and blocked in 3% milk supplemented with 0,3% Tween, preventing unspecific binding of antibodies. Thereupon, the ear skin was incubated in primary antibody solution at 4°C and gentle shaking overnight. On the next day, the ear skin was washed 4 times with PBS supplemented with 0,3% Tween (PBS-T). Afterwards the ear skin was incubated in the secondary antibody solution overnight, being taken care of to expose the samples to as little light as possible. Following day, the ear skin was washed again 4 times and mounted on glass slides, using mounting

medium and coverslips. Image acquisition was performed with Leica SP8 confocal microscope.

4.1.7 EdU labeling

For measuring cells ability to proliferate *in vivo* Click-iT EdU Imaging Kit (ThermoFisher) was used. EdU (5-ethynyl-2'-deoxyuridine) is a nucleoside analogon of thymidine and incorporated into the DNA during the S-phase of cell cycle[245]. Detection is based on a copper-catalyzed covalent reaction between an alkyne (EdU) and an azide.

For *In vivo* experiments, 5μl/g bodyweight of a 6mg/ml EdU solution was injected intraperitoneally in the mice. Mice harvest was performed after 3h incubation and the detection of EdU was performed before secondary antibody incubation, following the manufactures instructions.

4.2 Image acquisition and processing

Stained tissue and cells were imaged at high resolution with a SP8 confocal microscope (Leica). Laser confocal scanning microscopy (LCSM) is a technique where at a specific timepoint only a spatial pinhole is imaged, blocking out-of-focus light in image formation. By a process called optical sectioning, multiple two-dimensional images (called stacks) at different depths in one sample were captured. Afterwards these stacks were superimposed, reconstructing the third dimension of the imaged structure (Maximum projection)[246].

Volocity (Perkin Elmer), Fiji (NIH), Adobe Photoshop and Adobe Illustrator were used for image acquisition and processing. For comparison of immunostaining, settings for laser excitation and scanner detection were kept constant between groups.

4.3 Quantitative analysis of lymphatic vasculature in the ear

Quantifications were conducted on high-resolution confocal images using the Volocity software (Perkin Elmer). In the ear vasculature, the number of vessel branchpoints, vessel diameter, lymphatic area and proliferation was quantified on 3 arbitrary units taken from every ear sample (sized 580 x 580μm). All branchpoints in one arbitrary unit were counted and the mean value per ear was calculated. For assessment of the mean vessel diameter, four randomly chosen lymphatic vessels were measured per unit and averaged. Lymphatic area was determined at P10 measuring the proportion of $LYVE^+$ area to the complete unit area. At P21, $VEGFR3^+$ or $PDPN^+$ was used due to the capillary restricted expression of LYVE1.

For proliferation, cells positive for EdU and the endothelial nucleus marker ERG on lymphatic area were counted and divided by the lymphatic area.

4.4 Cell culture

4.4.1 Cell types

Human dermal lymphatic endothelial cells (HDLECs) were purchased from Lonza and cultured in EBM-2 media (Lonza) supplemented with 10% FBS (Invitrogen) and Hydrocortisone, fibroblast growth factor, vascular endothelial growth factor, insulin-like growth factor, ascorbic acid, epidermal growth factor, gentamycin sulfate and amphotericin-B (EGM-2MV-SingleQuots, Lonza). As of now this will be considered full EBM-2 media in this thesis. HDLECs were tested negative for HIV1, mycoplasma, Hepatitis-B/-C, bacteria, yeast and Fungi and cultured until fifth passage.
Pooled human umbilical vein endothelial cells (HUVECs) were purchased from Lonza and cultured using EBM media (Lonza) supplemented with 10%FBS (Invitrogen) and bovine brain extract, hydrocortisone, epidermal growth factor, gentamycin sulfate, ascorbic acid and amphotericin-B (EGM-SingleQuots, Lonza).

4.4.2 Cell cultivation

Cell cultures were grown in incubators (Eppendorf) maintained at 37°C and 5% CO_2. The cells were thawed at room temperature as fast as possible and then transferred into a T75-flask containing 20ml of prewarmed full EBM-2 media. After 4h a medium change was performed in order to remove cytostatic freezing reagents such as DMSO. Thereupon the cells were cultured until full confluency, performing medium change every second day. For subculture, cells were washed once in PBS (Invitrogen) and detached by Trypsin incubation of 3min at 37°C and 5% CO_2. Trypsin was neutralized by addition of media (4x) and the cell number was determined using the Luna™ Automated Cell Counter (Logos biosystems). 10µl of cell suspension was mixed with equal amount of Tryptan blue and pipetted on Luna™ Cell Counting Slides. After automatized analysis cells were seeded at required densities.

4.5 Adenoviral Transduction

For adenoviral transduction, sub confluent HDLECs were starved for 4h with EBM-2 media supplemented with 0.1% BSA. After starvation cells were incubated in starvation media containing 8 µg/ml Polybrene and the adenovirus for 4h. Following this step cells were washed 5x with HBSS and full EBM-2 media was added.
Amount of adenovirus used was calculated using the following formula:

$$V(Virus) = \frac{Total\ cell\ no. * MOI}{PFU}$$

The PFU (plaque formation unit) was determined by Vector biolabs and is a measure of the number of infectious virus particles (in ml^{-1}). The MOI (multiplicity of infection) refers to the number of virus particles per cell that are added during the infection. The cells were stopped after 16h and 24h by snap freeze in liquid nitrogen and stored at 80˚C until further processing.

4.6 Quantitative real time PCR (qRT-PCR)

4.6.1 RNA Isolation

RNA was isolated from ECs using QIAshredder columns (QIAGEN) and RNeasy Mini Kit (QIAGEN) following the manufactures instructions. Briefly, ECs were rinsed with PBS and lysed in RLT lysis buffer supplemented with 1% β-Mercaptoethanol. After lysis, homogenization was conducted by centrifugation through QIAshredder columns. 1 volume of 70% Ethanol was added before loading the sample on Rnaeasy Mini spin columns. RNA binds preferentially to the silica column, while genomic DNA and proteins were removed by repeated washes and DNAse incubation. After elution of RNA with RNAse free water concentration was determined using a NanoDrop 2000 spectrophotometer. In addition to the nucleic acid concentration in ng/μl sample contamination could be evaluated.

4.6.2 cDNA synthesis

cDNA was synthesized by reverse transcription using the M-MLV reverse transcriptase (Invitrogen). First, 2μg of RNA was diluted with H_2O to 11μl. Thereupon 1μl of dNTPs (Invitrogen) and 1μl of Oligo dT Primer Mix (Invitrogen) was added and incubated for 5min at 65°C. After addition of 2μl DTT and 4μl of First strand buffer the reverse transcriptase was added and incubated for 50min at 37°C, followed by an incubation of 15min at 70°C. Additionally, the sample exhibiting the highest RNA concentration served for a negative control without M-MLV reverse transcriptase.

4.6.3 qPCR

For quantitative assessment of the expression of specific mRNA, qPCR was performed using TaqMan Gene Expression Master Mix (Applied Biosystems) and Taqman probes (Applied Biosystems). The Taqman-principle relies on a hybridization probe binding between the Forward- & Reverse Primer, labeled with a reporter dye on the 5'-end and

a so-called Quencher at the 3'-end. Under these conditions the Quencher eliminates the fluorescent signal of the reporter due to the proximity of both molecules. A Polymerase transcribing DNA in RNA releases the reporter through the 5'-3'Exonuclease activity, leading to a higher signal of light at the wave length of the reporter[247]. One reaction contained the ingredients listed up in Table 20 and was performed under conditions shown in Table 20, using a StepOnePlus real-time PCR instrument (Applied Biosystems).

Taqman qPCR mix (1x)	**Amount (in µl)**
Taqman probe FAM	0,5
Taqman probe actin VIC	0,5
cDNA	1
Taqman Gene Expression Master Mix	5
H_2O	3

Table 20: Taqman qPCR mix

The hybridization probes of the gene of interests were labeled with the fluorescent dye FAM, while the hybridization probe of the internal control of the house keeping gene Actin was labeled with VIC. Using different fluorescent dyes, control gene and gene of interest could be measured in the same reaction.

Temperature (in °C)	**Duration**	**Number of cycles**
50	2min	1x
95	10min	1x
95	15s	40x
60	1min	

Table 21: qPCR Thermocycler protocol

To exclude contamination of qPCR-reagents, for every Taqman probe FAM, one qPCR mix without cDNA was assembled. Amount of DNA contamination in the process of cDNA synthesis was estimated, using one negative control without reverse transcriptase. Data were calculated using the ΔΔCt method.

4.7 RNA-seq

RNA-seq, also called whole transcriptome shotgun sequencing, is a method using next-generation-sequencing in order to analyze the cellular transcriptome at a certain timepoint[248]. RNA-seq experiments were performed in collaboration with the

Bioinformatics and Deep Sequencing Platform at the Max-Planck-institute for Heart- and Lung research in Bad Nauheim.

4.7.1 RNA isolation and quality control

For RNA-seq analysis, total RNA was isolated from ECs using the miRNAeasy micro Kit (Qiagen) combined with on-column DNAse digestion (RNAse-free DNAse set, Qiagen) to avoid contamination by genomic DNA, according to the manufacturer's instructions.

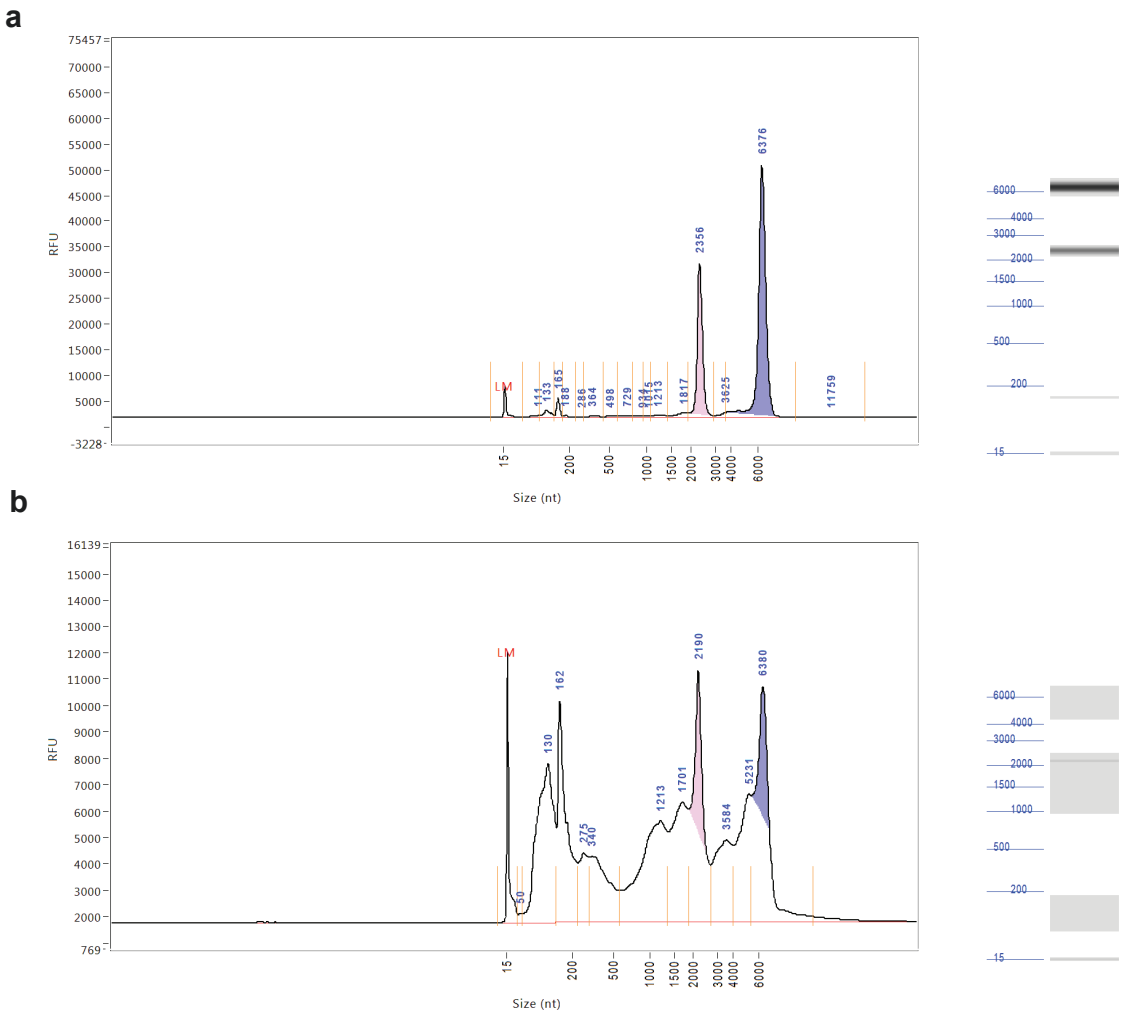

Figure 10: Determination of RNA integrity. a, Good quality RNA (28S/18S=2.1; RIN= 10.0). **b,** Low quality RNA (28S/18S=0.8; RIN= 5.1). RIN = RNA integrity number

RNA integrity was verified with LabChip Gx Touch 24 (Perkin Elmer). This method relies on the electrophoretic separation of RNA on a denaturating agarose gel. While intact RNA exhibits sharp, clear 28S and 18S rRNA bands with a 2:1 ratio, degraded RNA causes a smear.

4.7.2 Library preparation and sequencing

The following steps were performed by the MPI Deep Sequencing Platform, namely by Dr. Stephan Günther. For library preparation, 2μg of RNA was used as input for VAHTS™ Stranded mRNA-seq Library Prep Kit (Vazyme), following manufacturer's protocol. Sequencing was performed on NextSeq500 instrument (Illumina) using v2 chemistry, resulting in average of 30M reads per library with 1x75bp single end setup.

4.7.3 Data analysis

The resulting raw reads were assessed for quality, adapter content and duplication rates with FastQC. Trimmonatic version 0.33 was employed to trim reads after a quality drop below a mean of Q20 in a window of 5 nucleotides[249]. Only reads between 30 and 150 nucleotides were used for further analysis. Trimmed and filtered reads were mapped versus the Ensemble human genome version hg38 (GRCh38) using STAR[250]. The number of reads aligning to genes was counted with featureCounts 1.4.5-p1 tool from the Subread package[251]. Only reads mapping at least partially inside exons were admitted and aggregated per gene. Reads overlapping multiple genes or aligning to multiple regions were excluded.

4.8 Western Blot

Cells were lysed in RIPA-Buffer (150 mM NaCl, 1.0% IGEPAL CA-630, 0.5% sodium deoxycholate, 0.1% SDS, and 50 mM Tris, pH 8.0), supplemented with Phenylmethylsulfonylfluoride and Protease Inhibitor Mix (Complete Mini Protease Inhibitor cocktail tablets, Roche) for 30min on ice. Subsequently the lysate was centrifuged (15min; 14.000rpm; 4˚C), the supernatant was transferred to a new tube and stored at -80 ˚C until further processing. Protein concentration was determined with Bradford assay. This assay underlies the Coomassie Brilliant Blue Dye-G250, which changes its absorption level to 595nm by binding with protein. This absorption change is proportional with protein concentration over a wide range (Roti-Quant, manufactures instructions), and can be quantified using Multiskan FC Microplate Photometer (Thermo Fisher Scientific). The Protein concentration was graphically derived from a standart curve determined from samples with known BSA-concentration. For SDS-PAGE, 1:4 loading buffer (250mM Tris, pH 6.8, 200mM DTT, 8% SDS, 40% Glycerin, 0,04% Bromphenol blue) was mixed with 30µg of protein and heated for 5min up to 95˚C, causing denaturation of the proteins and homogenous noncovalent binding of the negative charged SDS to the proteins.

Proteins were separated using precast gradient gels (Bio-Rad) and then blotted onto nitrocellulose membranes (Bio-Rad), using the Trans-Blot Turbo Transfer System (Bio-Rad). To prevent unspecific binding, the membrane was blocked for 90min in TBS-buffer (50mM Tris/HCL, 150mM NaCl, 2,5mM KCl, pH 8.0), supplemented with 1%Tween and 5% milk powder. This step was followed by the incubation of the membrane in a primary antibody solution (TBS-T and 5% BSA) at 4˚C overnight. Next, the membrane was washed three times with TBS-T and incubated in a solution containing peroxidase-conjugated secondary antibody. The bands were visualized using the Clarity Western ECL Substrate (Bio-Rad) and ChemiDoc (Bio-Rad).

4.9 Statistical Analysis

Statistical analysis was performed by unpaired, two-tailed Student's t-test, or non-parametric one-way ANOVA followed by Bonferroni's multiple comparison test using Prism 5 (Graphpad Software, USA). For all bargraphs, data are represented as mean +/- S.E.M. P values < 0.05 were considered significant. Heatmaps were generated using morpheus, publicly available from the Broad Institute (*https://software.broadinstitute.org/morpheus/*).

5 Results

5.1 The murine ear skin is a suitable model for studying postnatal lymphangiogenesis *in vivo*

To study postnatal lymphangiogenesis, the dorsal site of the murine ear skin was analyzed – a model previously described by other groups[58,252–254]. An advantage of this model is the relatively easy dissection of the thin ear skin from the intervening cartilage, allowing whole-mount visualization with low background signal. The lymphatic vasculature starts to invade the ear at P4 and proliferates until P12, shaping an immature vessel network. Until P21, this primary vascular plexus remodels into a hierarchical network consisting of capillaries and valve-containing collecting vessels[253].

For our studies two timepoints were selected. For the study of the nascent proliferating vasculature, we chose P10. Earlier timepoints were not considered due to difficulties associated with the dissection. The impact of FOXO1 in the remodeling phase was assessed by analyzing the ear skin at P21. Different epitopes, specific for different cell types, were visualized using antibody labelling. A general overview was obtained using antibodies against Platelet endothelial cell adhesion molecule 1 (PECAM, CD31), labelling blood as well as lymphatic endothelial cells (Figure 11, Figure 12). For separation of the different maturation stages of lymphatic vessels, LYVE1 and SMA were used. At P10, LYVE1 is expressed in the entire immature lymphatic network, while at P21 it gets restricted to the capillaries. The collecting vessels start to recruit SMA-expressing smooth muscle cells (Figure 12). The lymphatic valves of the collecting vessels can be visualized using the markers Integrin alpha-9 or Podocalyxin (Figure 13). Podoplanin (PDPN) is expressed by all LECs, serving as a marker of the entire lymphatic system. Also, PROX1 is expressed by all LECs; however, as a transcription factor it is restricted to nucleus, serving as a nuclear marker. VEGFR3 is expressed by LECs but also by some blood endothelial cells.

At P10, the ears show an organized blood vascular network nourishing all parts of the ear, while the lymphatic network is still developing (Figure 11). It starts to invade the ear proximally, spreading out to the distal parts of the ear. The lymphatic vessels are bigger in size then the blood vessels and are still immature (e.g., lack of valves, SMCs).

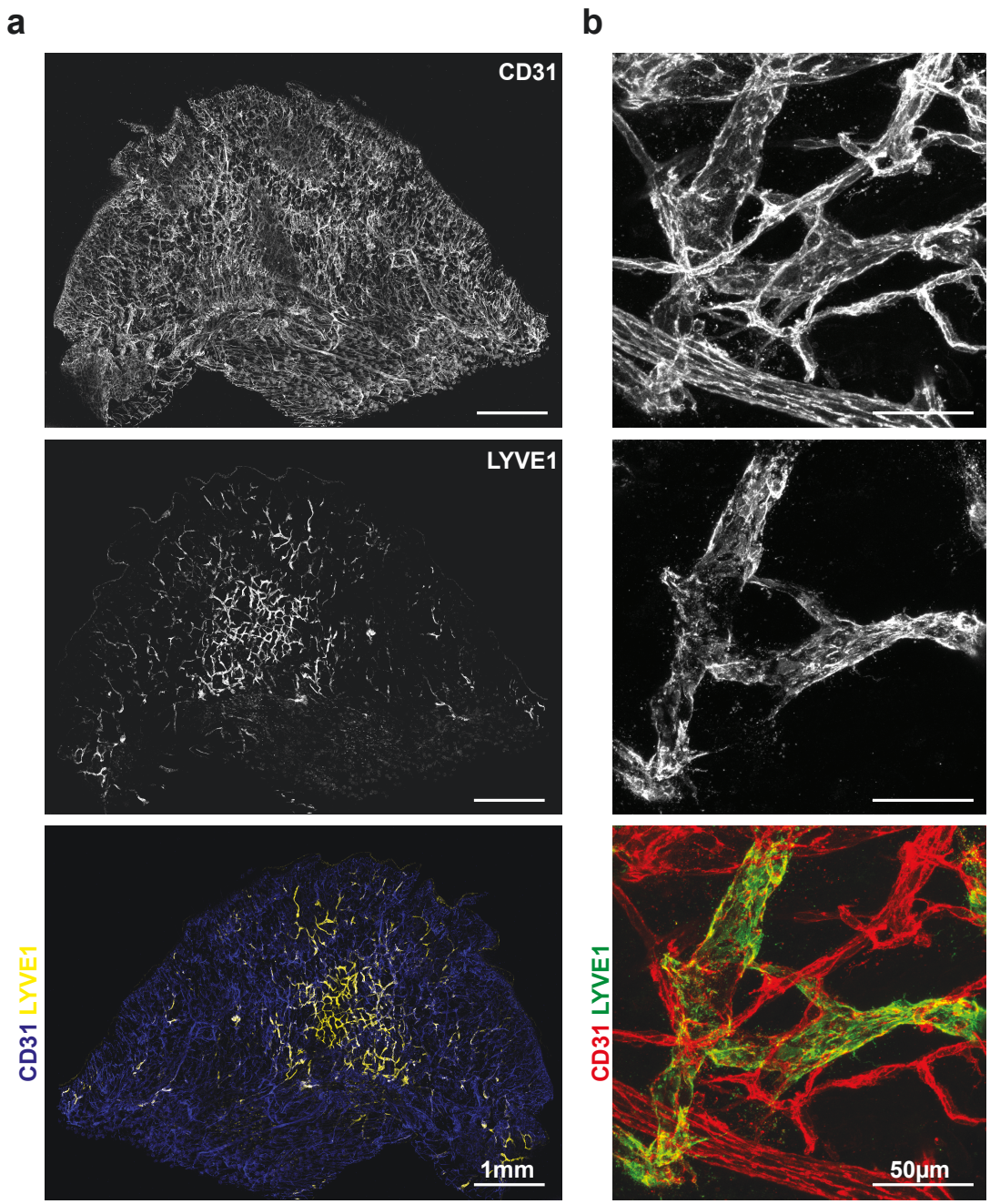

Figure 11: Lymphatic vasculature in the murine ear skin at P10. Overview with 10x (**a**) and 50x magnification (**b**) of the lymphatic system.

At P21, the lymphatic network has reached all parts of the ear. The LYVE1-distribution indicates the position of the capillaries in the periphery of the ear, while the collecting vessels are located at the base. The collecting vessels arise through merging of lymphatic capillaries (Figure 12c). They are bigger than arteries and veins and show smooth muscle cell coverage and lymphatic valves (Figure 12, Figure 13).

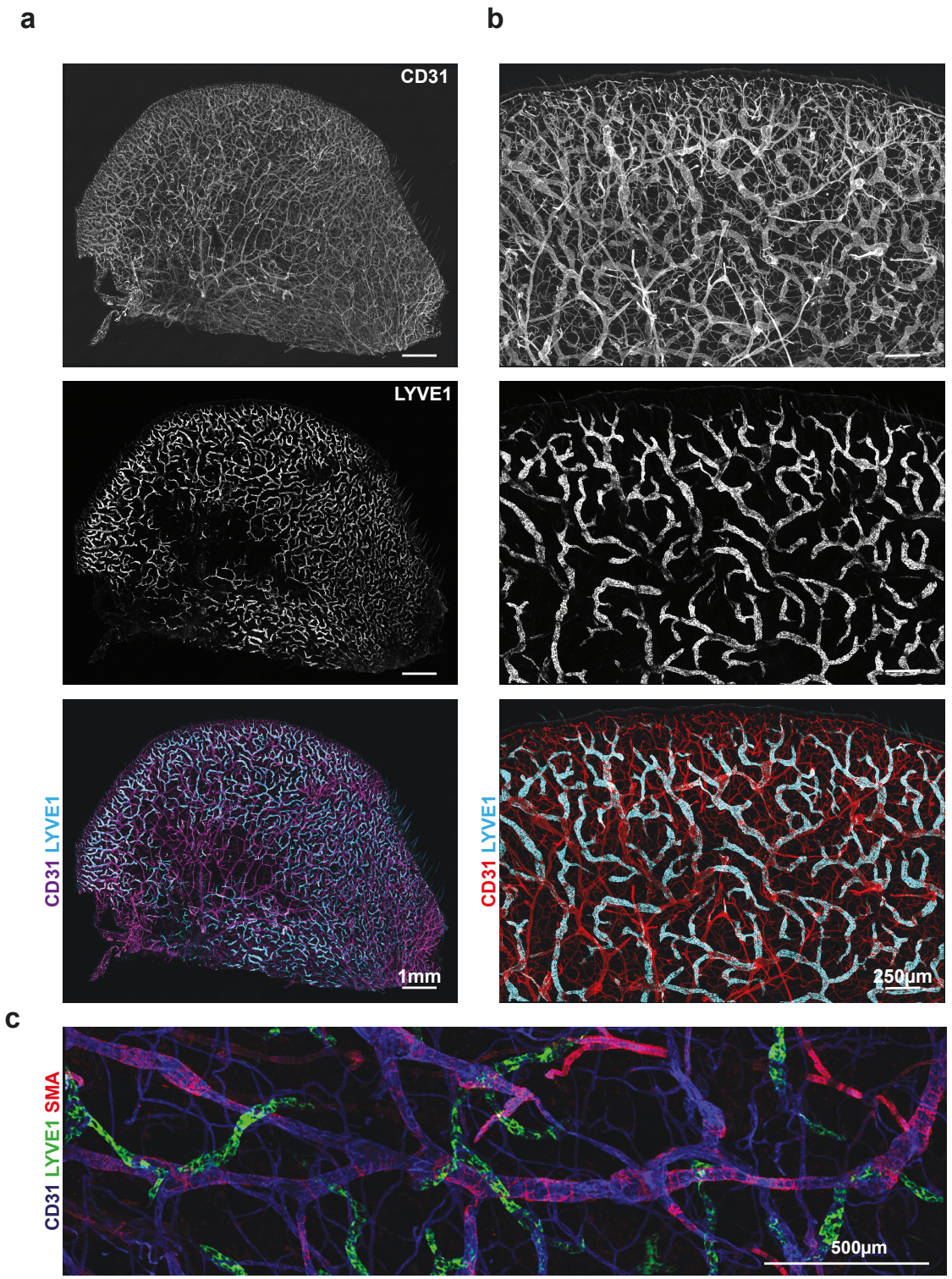

Figure 12: Lymphatic vasculature in the murine ear skin at P21. Overview (**a**) and magnification of the sprouting front (**b**) of the lymphatic system. **c**, tile scan of collecting vessel.

Using lymphatic valve markers (described above), the two semilunar leaflets, composing one lymphatic valve, can be visualized. These valves are formed by specialized LECs, visible due to expression of LEC-specific markers.

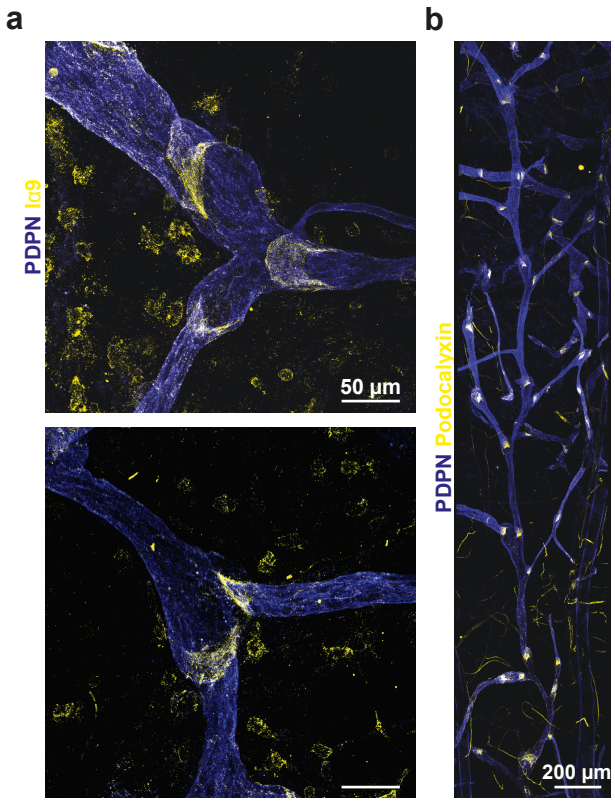

Figure 13: Lymphatic valves in the developed lymphatic system. a, Close up of lymphatic valves, showing the two semilunar leaflets. **b**, Tile scan of a collecting vessel, illustrating the compartmentalization in lymphangions by lymphatic valves.

In summary, the described ear skin model is a system, comprising all hierarchical components of lymphatic vasculature, enabling the detailed analysis of lymphatic morphogenesis. Due to the accessibility of the mouse ear and the thin skin, this model represents a relatively fast way to image the lymphatic vasculature with high resolution and low background signal, enabling quantification at high-resolution.

5.2 FOXO1 expression is dynamically regulated in developmental lymphangiogenesis

FOXO1 immunofluorescence analysis was performed at P10 as well as P21 to assess the expression levels and nucleocytoplasmic distribution of this transcription factor at different stages of developmental lymphangiogenesis. To this end, the FOXO1 labelling was combined with a pan-endothelial as well as a lymphatic endothelial marker, enabling relative comparison of expression between the blood and lymphatic vasculature.

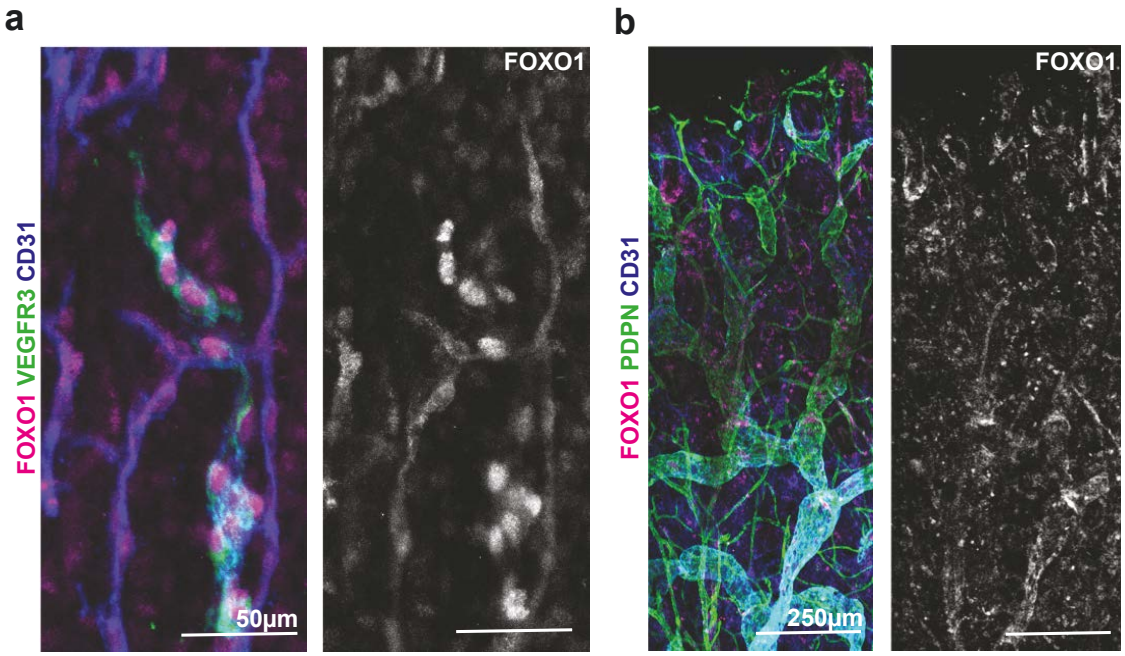

Figure 14: FOXO1 expression is dynamically regulated in developmental lymphangiogenesis. a, Staining for FOXO1, VEGFR3 and CD31 in a postnatal day (P)10 murine ear skin. **b,** Staining for FOXO1, PDPN and CD31 in a postnatal day (P)21 ear skin. The right panel depicts the FOXO1 signal form the left.

At P10, the stainings revealed a distinct FOXO1 signal in the nuclei of $CD31^{+}/VEGFR3^{+}$ lymphatic endothelial cells. Of note, the expression exceeded the levels of FOXO1 in $CD31^{+}/VEGFR3^{-}$ blood endothelial cells. Moreover, a strong nuclear localization suggested crucial functions of FOXO1 during lymphatic vessel morphogenesis. At P21, the expression levels of FOXO1 decreased in most (capillary) LECs. Interestingly, FOXO1 levels remained high in lymphatic valves of collecting vessels, suggesting that valve LECs may differ from those in capillaries.

5.3 Inactivation of FOXO1 in lymphatic endothelial cells leads to a hyperplastic and immature lymphatic vasculature

To further investigate the role of FOXO1 in lymphatics, floxed *Foxo1* mice (*Foxo1*$^{fl/fl}$) were bred with *Prox1-Cre-ER*^{T2} deleter mice. *Prox1-Cre-ER*^{T2}- *Foxo1*$^{fl/fl}$ mice injected with 4-OH-T are hereafter referred to as FOXO1$^{iLEC-KO}$. A strong nuclear signal in the developing lymphatic system suggests efficacy of this experimental setup. These studies (5.3) were performed by Kerstin Wilhelm prior to my work in the project. As mentioned above, the Cre transgene was kept heterozygously in mice to avoid Cre-toxicity and potential off-target effects. Cre and *Foxo1* status was determined via PCR (Figure 15), and *Foxo1*$^{fl/fl}$ littermates lacking Cre expression were used as controls. Pups were sacrificed at P21 and processed as described above.

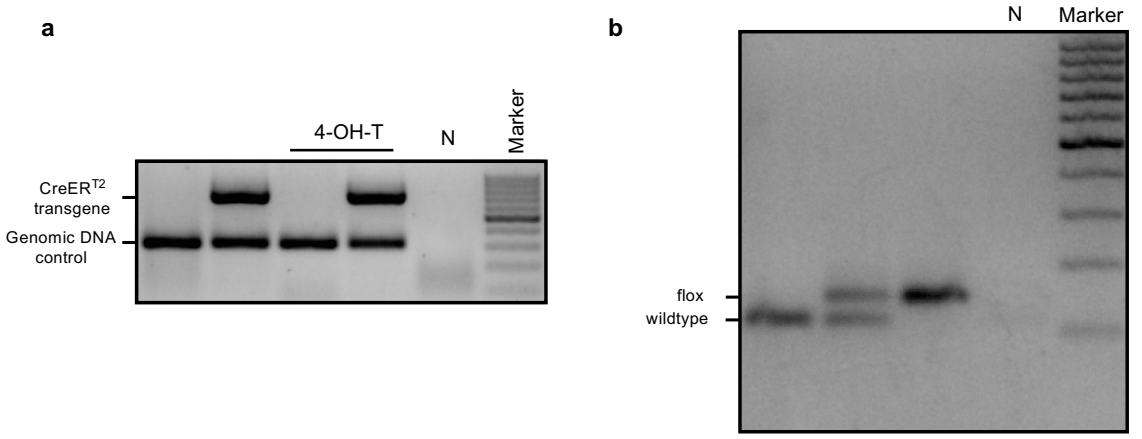

Figure 15: PCR of genomic DNA obtained from tail biopsy of P5 mice. a, Prox1-CreER^{T2} PCR showing the Cre transgene at 720bp and the genomic DNA control at 320bp. **b,** *Foxo1* PCR of a wildtype mice (lane 1, 115 bp), *Foxo1*$^{fl/+}$ (lane 2) and a *Foxo1*$^{fl/fl}$ (lane 3, 149bp) mice. 100bp marker ladder was used, 500bp step is accentuated. 4-OH-T: 4-hydroxy-tamoxifen, N: negative control, bp: base pairs.

Compared to the hierarchically organized lymphatic network in controls, FOXO1-deficient mice showed enlarged lymphatics with a massively increased vessel caliber (Figure 16). Although the lymphatic vessel were bigger, their branching was reduced. Additionally, the process of maturation was perturbed. FOXO1-deficient LECs failed to form proper collecting vessels, evidenced by the persistence of the capillary marker LYVE-1 (Figure 16c). Moreover, these vessels did not acquire smooth muscle actin (SMA) coverage, a hallmark of lymphatic remodeling and maturation. Consistent with these data, the lymphatic valves were absent in these mutants.

Taken together, loss of FOXO1 leads to ballooned and immature lymphatic vessels, impeding the formation of the hierarchical network indispensable for proper function.

To assess whether proliferation contributes to this phenotype, EdU incorporation was assessed (data not shown). This analysis revealed significant increase of proliferation in *Foxo1*-deficient mice, suggesting that enhanced proliferation contributes to the observed phenotype. These data indicate that FOXO1 restricts LEC proliferation and that FOXO1 loss causes lymphatic overgrowth.

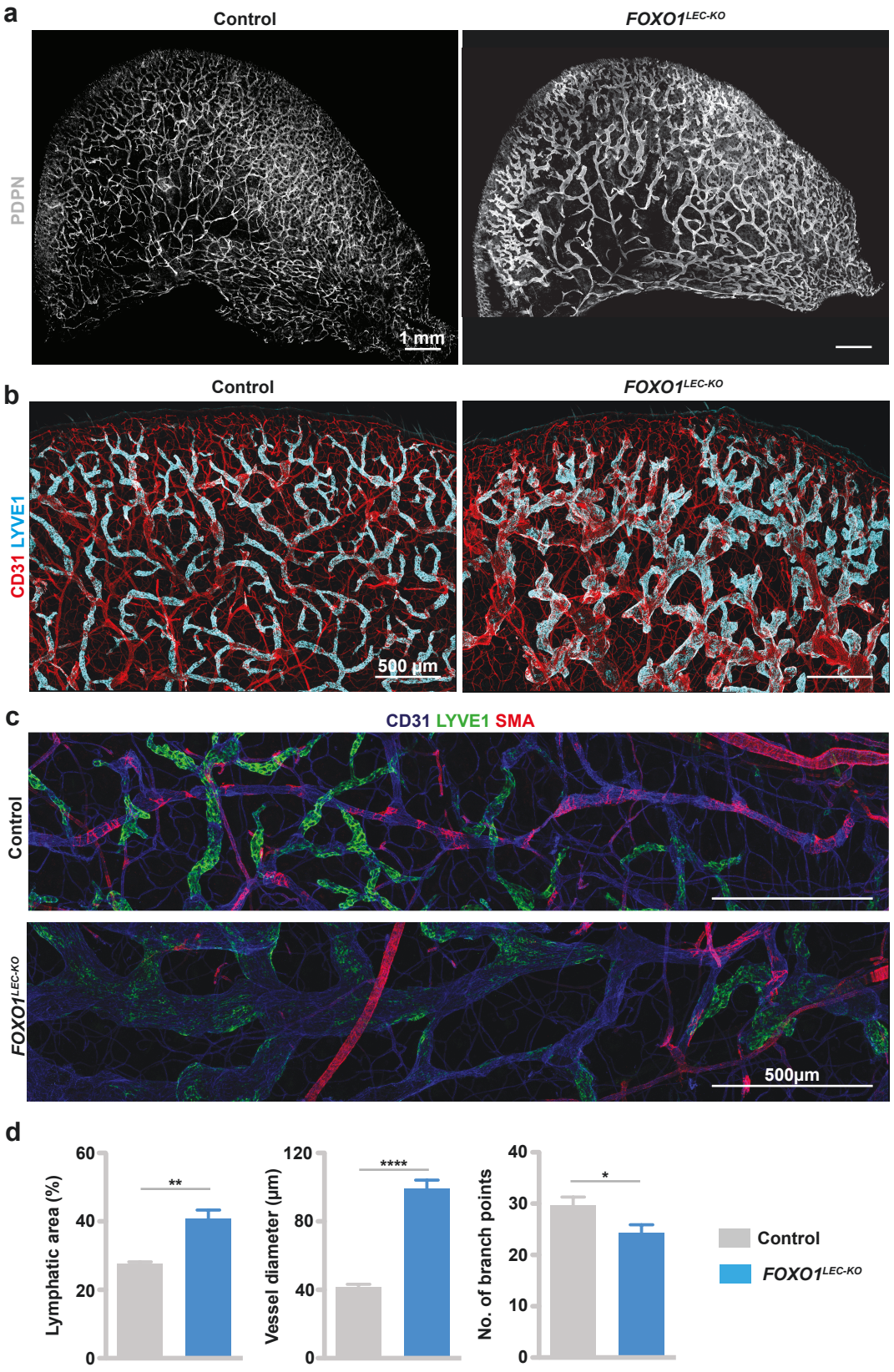

Figure 16: FOXO1 loss causes lymphatic overgrowth and pertubs maturation. Overview (**a**) and higher magnification (**b**) of lymphatic vessels in the murine ear skin. **d**, bar graphs showing mean lymphatic area, vessel diameter and No. of branchpoints. Data represent mean ± s.d., two-tailed unpaired t-test. *P<0.05; ** P<0.01; ****P<0.0001.

5.4 Establishment of a lymphatic FOXO1 gain-of-function model

Next, the consequences of enforced FOXO1 activation in LECs was investigated. To this end *Prox1-CreER*^{T2} deleter mice were crossed with a *Rosa26-Foxo1-ADA-IRES-GFP* strain. This conditional mouse line expresses a FOXO1 mutant in which the AKT-dependent phosphorylation sites in FOXO1 are mutated (Foxo1^{ADA}), preventing nuclear exclusion and subsequent inactivation of FOXO1 signaling. Conditional expression is achieved through a loxP-flanked STOP cassette, ensuring that the FOXO1^{ADA} mutant is only expressed upon Cre-mediated recombination (see 4.1.3.3).

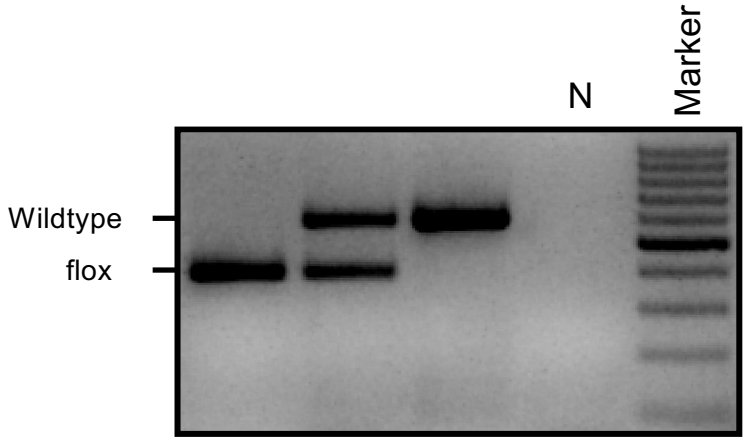

Figure 17: PCR of genomic DNA obtained from tail biopsy of P5 mice. Homozygous *Foxo1*-ADA (lane 1, 380bp), heterozygous (lane 2) and wildtype (lane 3, 570bp). 100bp marker ladder was used, 500bp step is accentuated, N: negative control, bp: base pairs.

Heterozygous Cre-status and homozygous *Foxo1*-ADA-status was confirmed via PCR (Figure 15, Figure 17). A *Prox1-Cre-ER*^{T2} *Rosa26-Foxo1*^{ADA}*-IRES-GFP* mouse injected with 4-OHT from P1-P4 is hereafter referred to as FOXO1$^{iLEC-OE}$.

Mice were sacrificed at P21 and stained for GFP (Figure 18a) and FOXO1 (Figure 18b) to validate successful recombination. The GFP was cloned behind an internal ribosome entry site, allowing independent initiation of translation, thereby indicating recombination without directly influencing FOXO1 functionality. An Anti-GFP-antibody was used for enhancement of the GFP signal.

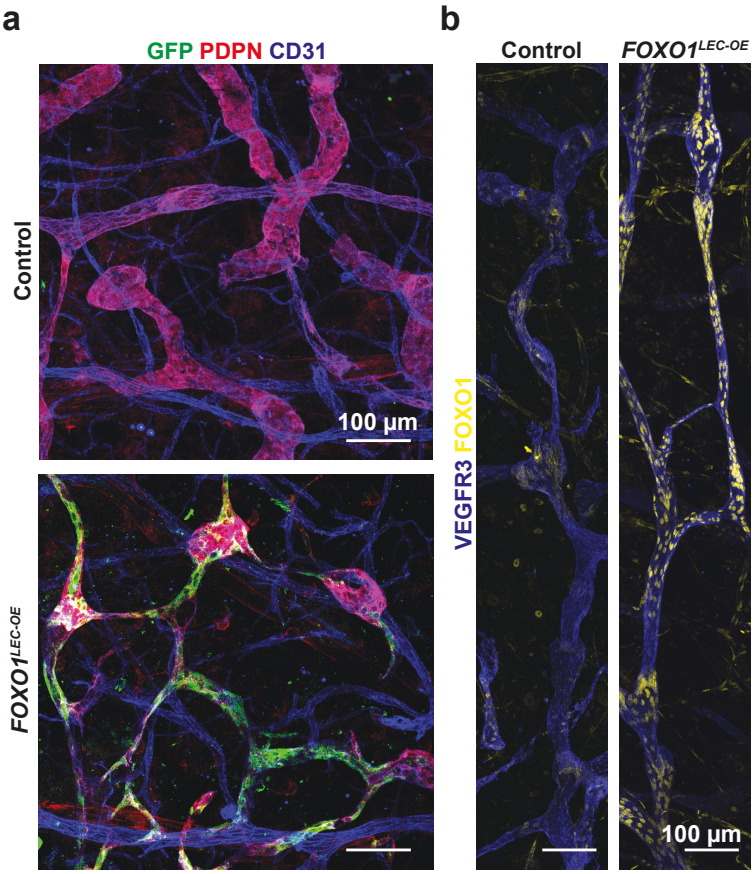

Figure 18: FOXO1-mutant overexpression is lymphendothelial specific and restricted to the nucleus. a, IRES-GFP expression is restricted to lymphatic vessel sections exhibiting FOXO1-induced phenotype. **b**, FOXO1 signal is restricted to the nucleus, indicating disruption of AKT-dependent nucleocytoplasmic shuttling.

Prox1-Cre-ER^{T2}-positive animals exhibited a robust GFP signal restricted to the lymphatic endothelium, whereas Cre negative littermates were GFP negative (Figure 18a). Recombination did not take place in every LEC, as GFP-negative vessel sections suggest. Moreover, the intensity of the FOXO1 staining varied considerably, indicating heterogeneity in of 4-OHT- induced recombination.

As expected, FOXO1 staining was substantially increased in FOXO1$^{iLEC-OE}$ and restricted to the nucleus (Figure 18b). Particularly in the lymphatic capillaries, the GFP-negative segments had a larger vessel diameter, resembling those in the controls. The phenotype characterized below is the result of restricting the analysis to GFP-positive vessel sections.

5.5 Lymphatic endothelial overexpression of FOXO1^{ADA} impairs proliferation and causes a hypoplastic phenotype

After validation of the functionality of this model, the phenotypic consequences of forced FOXO1 activation were examined beginning at P10.

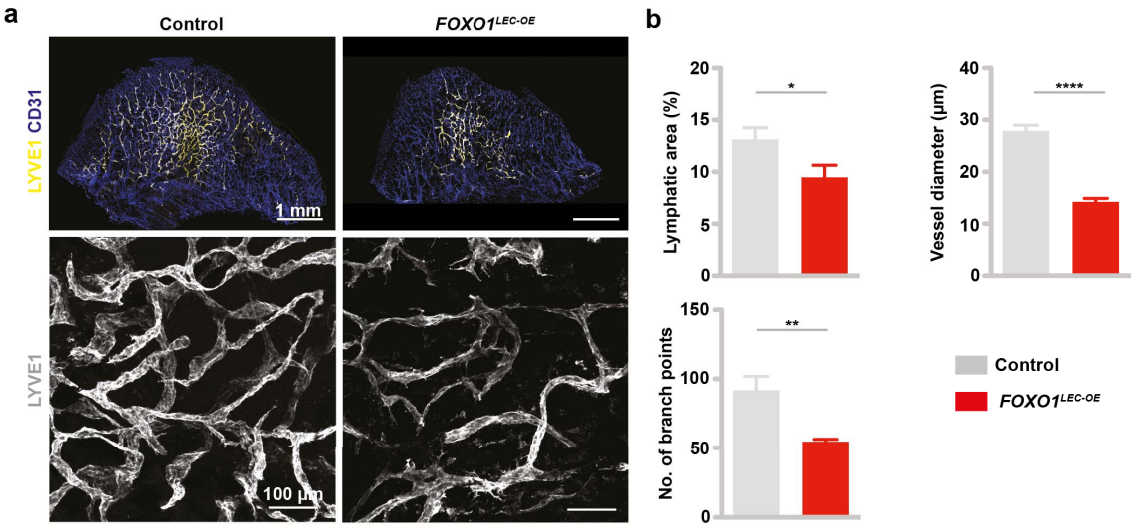

Figure 19: FOXO1 overexpression leads to decreased vessel diameter and reduced number of branchpoints. a, Overview and higher magnification of the vascular system in the murine ear skin **b**, Bar graphs exhibiting mean lymphatic area, vessel diameter and No. of branchpoints. Data represent mean ± s.d., two-tailed unpaired t-test. *P<0.05; ** P<0.01; ****P<0.0001.

Mice ears were stained with pan- and lymphatic-specific endothelial markers, to get an overview of the FOXO1 gain-of-function phenotype at P10. Confocal imaging revealed a hypoplastic lymphatic vasculature characterized by reduced vessel diameter and lymphatic area, suggesting reduced cell plasticity or number. The vessel network appeared disorganized with profound caliber changes, likely caused by differences of FOXO1 levels or activity due to variations in Cre-mediated recombination (Figure 18). In controls, the LYVE1 expression was uniformly distributed, covering large parts of the ear, while in FOXO1$^{iLEC\text{-}OE}$ mice, LYVE1 expression was more centralized and scattered, suggesting less lymphangiogenic activity in these mice.

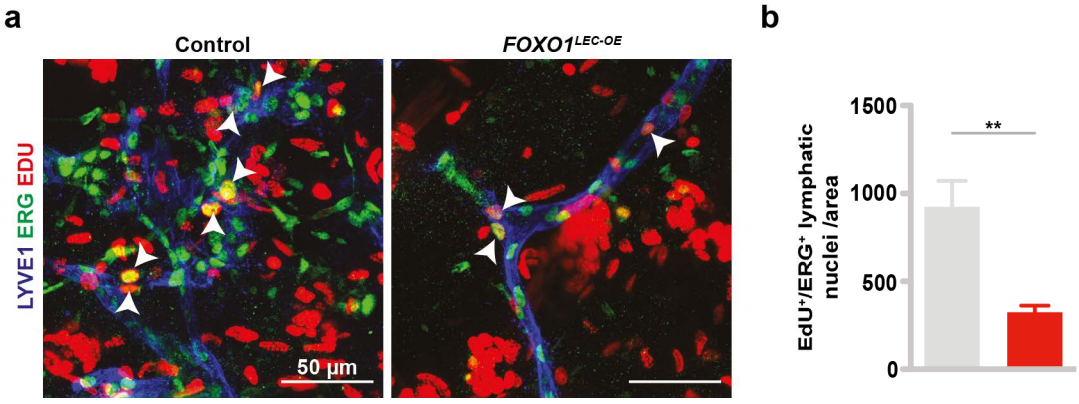

Figure 20: FOXO1 overexpression impairs proliferation of LECs after 10 days significantly. a, EdU (red) and ERG (green) staining in P10 mouse ears in control and FOXO1^{ADA} mice. Co-labelled nuclei are indicated in yellow. **b,** Bar graph showing the number of EdU+/ERG+ nuclei per area. Data represent mean ± s.d., two-tailed unpaired t-test. ** P<0.01.

EdU incorporation in LECs was measured to assess the contribution of proliferation to this phenotype. Consistent with the results in the loss-off-function mutants, proliferation was significantly reduced in FOXO1$^{LEC\text{-}OE}$, suggesting canonical functions of FOXO1 in LECs that contribute to the observed phenotype.

5.6 FOXO1-mutant overexpression deregulates maturation and growth

Next, FOXO1$^{iLEC\text{-}OE}$ mice were sacrificed 21 days after birth, to investigate the consequences of forced FOXO1 activation on lymphatic remodeling and maturation. To this end, lymphatic proliferation, maturation and network organization were analyzed. In comparison to the mature and highly organized network in controls, FOXO1$^{iLEC\text{-}OE}$ ears exhibited a profound phenotype that was even pronounced than at P10, suggesting that the lymphatic defects are time-progressive (Figure 21). The lymphatic vessels were thinner and fewer branched emerged from the lymphatic network. Quantification of the phenotype revealed strong reduction in lymphatic area and vessel diameter (Figure 21). Interestingly, the blood vasculature was also affected (Figure 21b), although the Prox1-CreERT2 deleter does not recombine in these cells (5.4). Especially the veins appeared hyperplastic and overgrown, suggesting potential lymph-angiocrine effects upon LEC-restricted FOXO1 activation.

To assess the maturation state in FOXO1$^{iLEC\text{-}OE}$ mice at P21, we focused on the collecting vessels, because they represent the matured vessel segment and exhibit measurable maturation features.

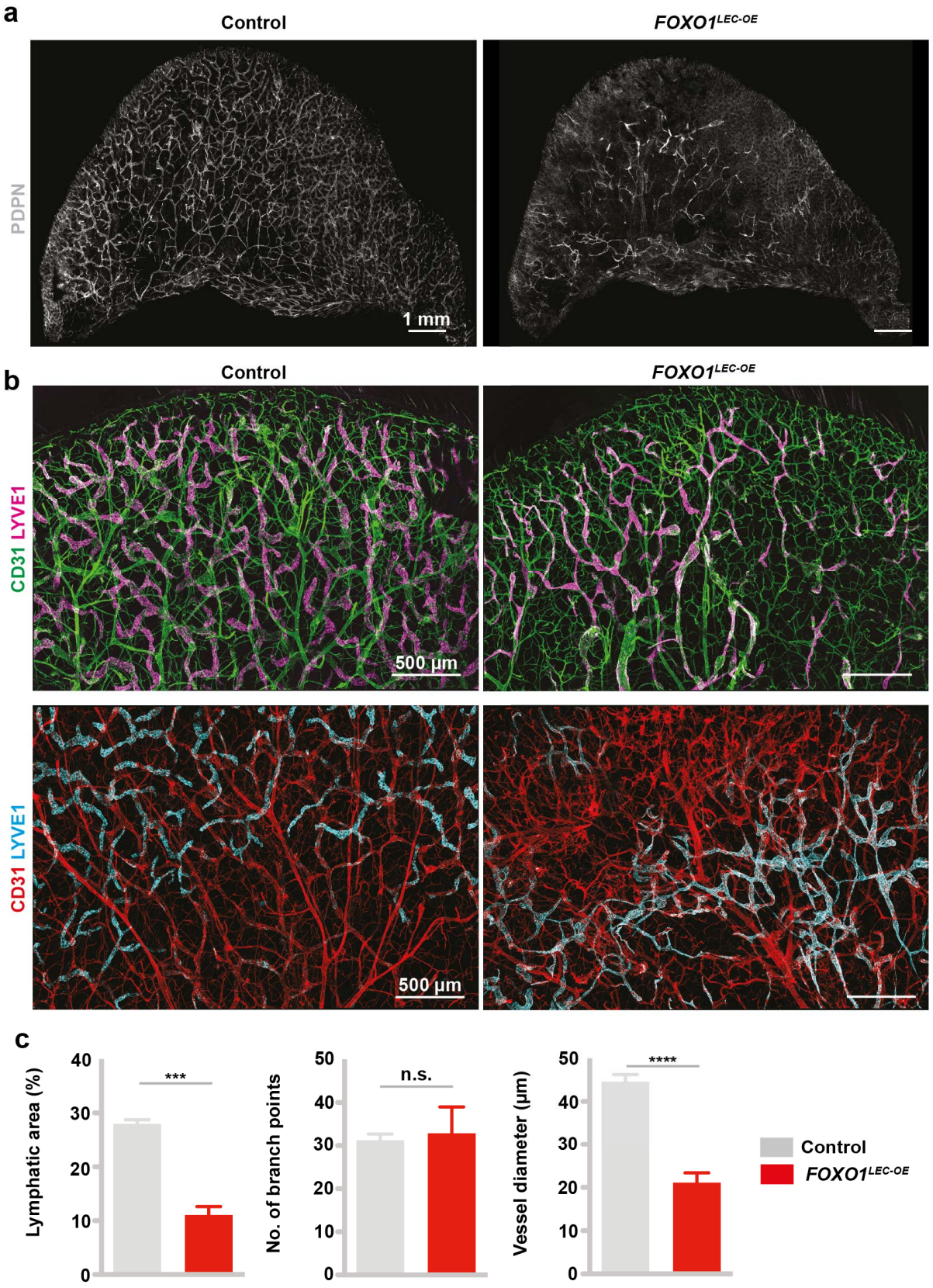

Figure 21: Overactivation of FOXO1 leads to lymphatic vessel rarefactions. Overview (**a**) and higher magnification (**b**) using panendothelial and lymphendothelial specific marker**. c,** Bar graphs exhibiting mean lymphatic area, vessel diameter and No. of branchpoints. Data represent mean ± s.d., two-tailed unpaired t-test. *** P<0.001; ****P<0.0001; n.s. = not significant.

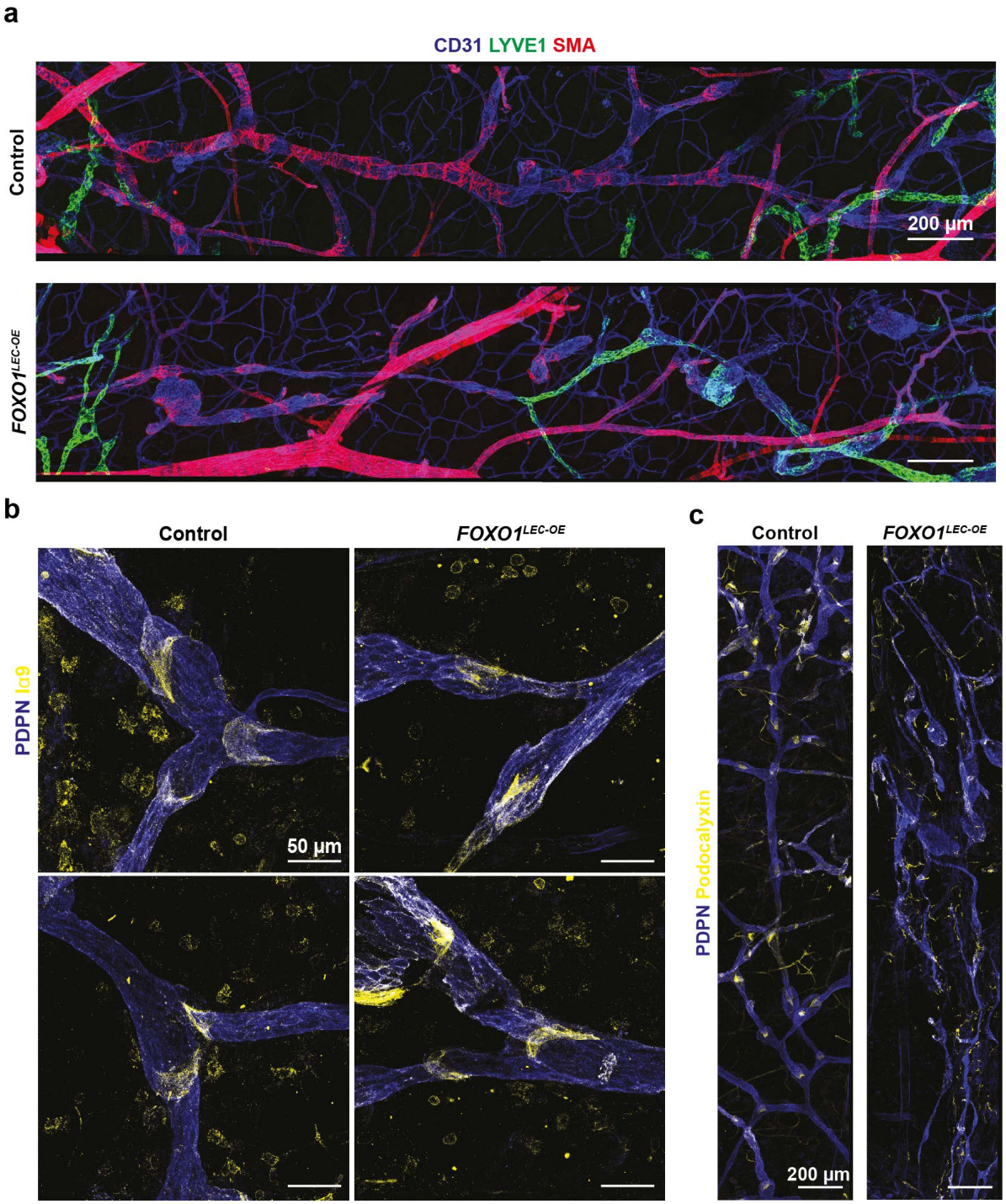

Figure 22: Overexpression of FOXO1 impairs maturation of the lymphatic system. a, Tile scan of collecting vessels using maturation markers such as LYVE1 and SMA **b**, Close up and Tile scan (**c**) of lymphatic valves using the valve marker Integrin α9.

Tile scans, meaning the composition of a defined number of small high-resolution images, were taken to analyze representative collecting vessels of the mouse ear. FOXO1$^{iLEC\text{-}OE}$ mice collecting vessels were very thin and seemed smaller, indicating that the coordinated formation of collecting vessels is deregulated when FOXO1

signaling is over-activated. Consistent with this interpretation, SMC recruitment and valve formations were also affected (Figure 22).

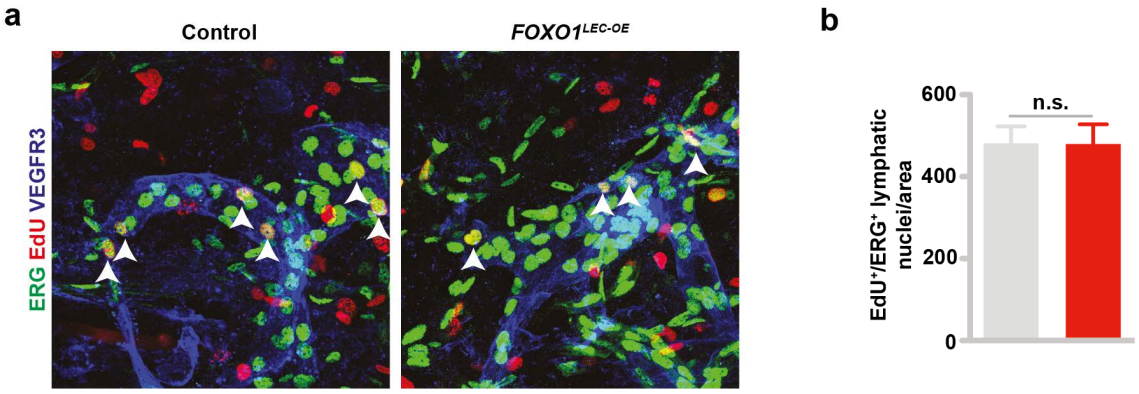

Figure 23: FOXO1 overexpression does not lead to increased proliferation at P21. a, Exemplary image with EdU (red) and ERG (green) staining of arbitrary units in P21 mouse ears. Cocoulered nuclei impress yellow. **b**, Bar graph showing the number of EdU+/ERG+ nuclei per area. Data represent mean ± s.d., two-tailed unpaired t-test. N.s. = not significant.

Proliferation assay revealed low levels of cell division in controls and FOXO1$^{iLEC\text{-}OE}$ mice which did not differ between the two groups, suggesting that the proliferation inhibition caused by FOXO1 is compensated over time (e.g., by non-recombined wildtype LECs).

5.7 Human dermal lymphatic endothelial cells express lymphatic-specific markers and FOXO1

To gain deeper insights into the underlying mechanisms of FOXO1 function in LECs, we employed an *in vitro* approach. In a first step, HDLECs were compared with HUVECs, trying to characterize the cells in the same way the blood and lymphatic vessels *in vivo* were characterized (See 5.1). Epitopes we stained for in vivo were expressed by HDLECs on mRNA and protein level (Figure 24). Additionally, expression levels of FOXO1 *in vitro* were analyzed. The mRNA levels in sub-confluent cells showed higher *FOXO1* levels in HUVECs than in HDLECs. Moreover, expression of *FOXO1* in an RNA-seq dataset of different untreated endothelial subtypes (Figure 24b) was investigated. This RNA-seq data set was produced in our laboratory by Jorge Andrade. The expression levels of *FOXO1* are higher in HDLECs compared to those in HUVECs, reproducing our observation in the developing lymphatic system (Figure 14a). We conclude that the *FOXO1* expression levels are highly dynamical regulated and beside the cell type highly dependent on environmental factors such as oxidative stress, nutrition supply and growth factors.

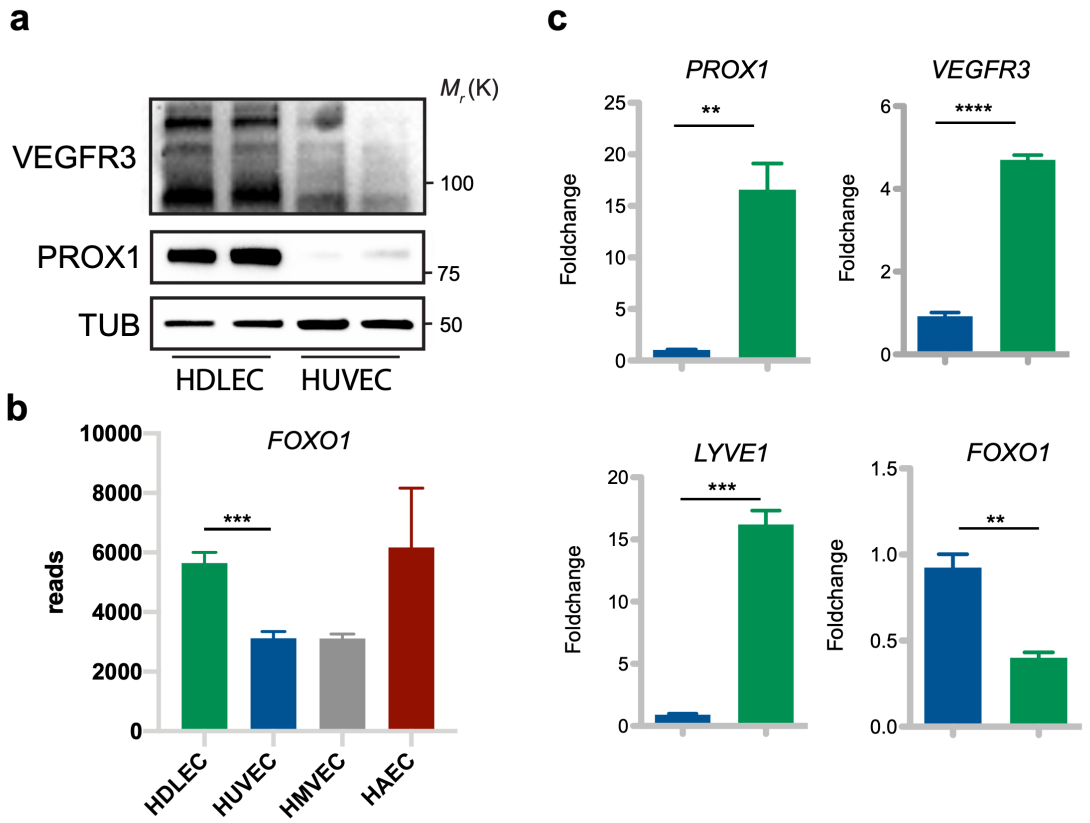

Figure 24: *In vivo* markers are capable to differentiate blood and lymphatic endothelial cells *in vitro*. Western blot (**a**) and qPCR analysis (**c**) of lymphatic marker genes in sub confluent endothelial cells (n=3), fold change normalized to controls. **b**, expression levels of *FOXO1* in different endothelial subtypes. HMVEC: Human microvascular endothelial cells. HAEC: Human aortic endothelial cells. RNA-seq-data extracted from preexisting data set. Data represent mean ± s.d., two-tailed unpaired t-test. ** P<0.01; *** P<0.001; ****P<0.0001.

5.8 Adenoviral overexpression of a constitutively nuclear active FOXO1 mutant leads to the robust regulation of canonical FOXO target genes

In preparation for an unbiased RNA-seq-experiment, a FOXO1 mutant (FOXO1^{A3}) was overexpressed in HDLECs using an adenoviral-based transduction protocol (See 4.5). Similar to the FOXO1^{ADA} mutant used in the *in vivo* studies, FOXO1^{A3} harbors point mutations of the three AKT phosphorylation sites, rendering the protein constitutively nuclear. As a control, an adenovirus encoding for a GFP protein under the control of a CMV-promotor was used. Successful adenoviral transduction was confirmed at the mRNA and protein level using three different MOIs (10, 25 and 50). To investigate dynamic changes in gene expression in FOXO1^{A3}-expressing HDLECs, we analyzed the cells after 16h and 24h. We expected to see primary transcriptional targets of FOXO1 already after 16h post transduction, while after 24h also indirectly regulated pathways could come into play. It should be noted that this experiment was a

preparatory experiment for the large-scale RNA-seq-experiment and was performed only once (n=1).

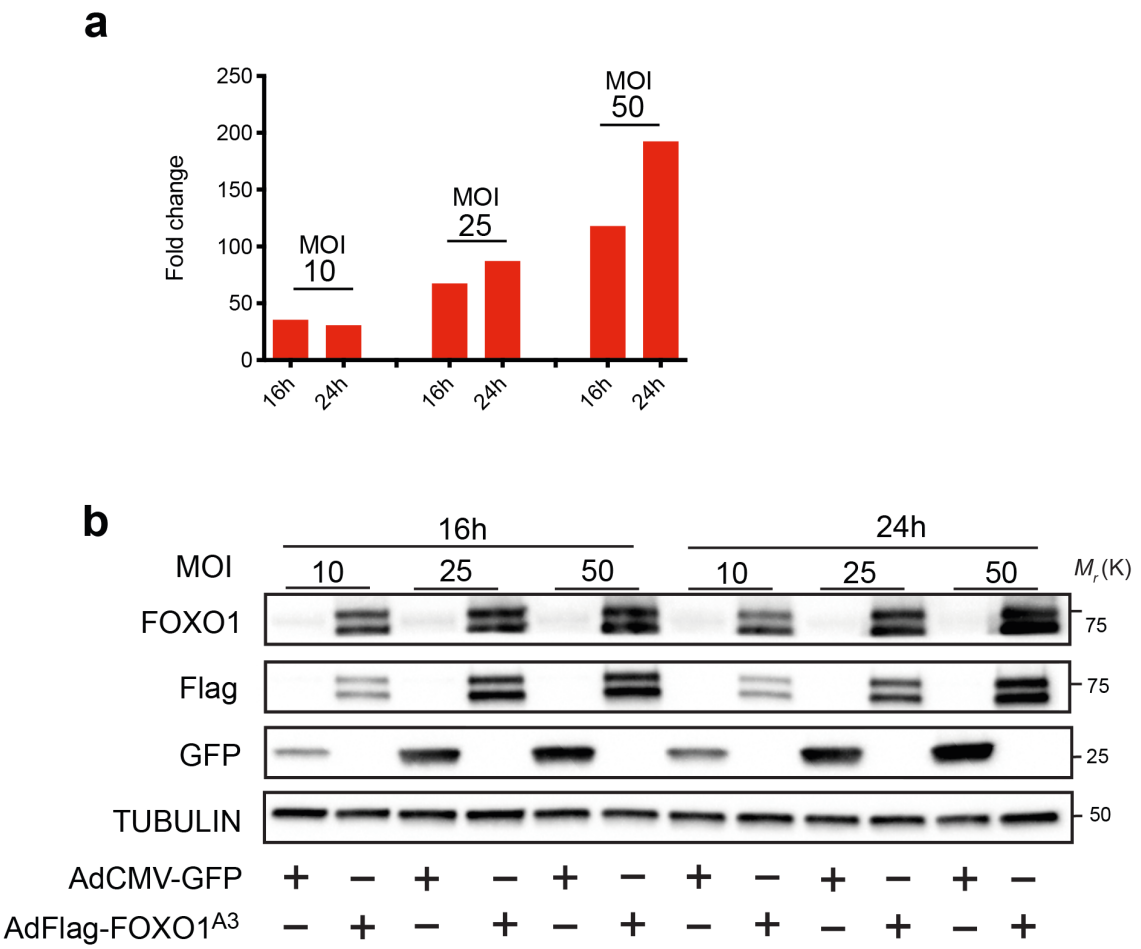

Figure 25: FOXO1^{A3} transduction leads to a robust upregulation of FOXO1 at mRNA and protein level. qPCR (**a**) and Western blot analysis (**b**) of *FOXO1* mRNA (**a**) and FOXO1, Flag and GFP protein levels (**b**) in AdCMV-GFP and AdFlag-FOXO1^{A3} transduced HDLECs (n=1). a, Fold change normalized to controls.

qPCR and Western Blot analysis confirmed that the FOXO1 mutant was highly expressed in HDLECs following adenoviral transduction of the cell (Figure 25a). Western blot analysis indicated functional translation into protein.

In a second step, we analyzed the regulation of canonical FOXO1 target genes on the mRNA and protein level. Bona-fide targets such as *MXI1*, *MYC*, *CITED2*, *SOD2* were regulated as expected. We conclude that the overexpression of FOXO1^{A3} is a suitable model for studying the molecular effects of FOXO1 activation in HDLECs.

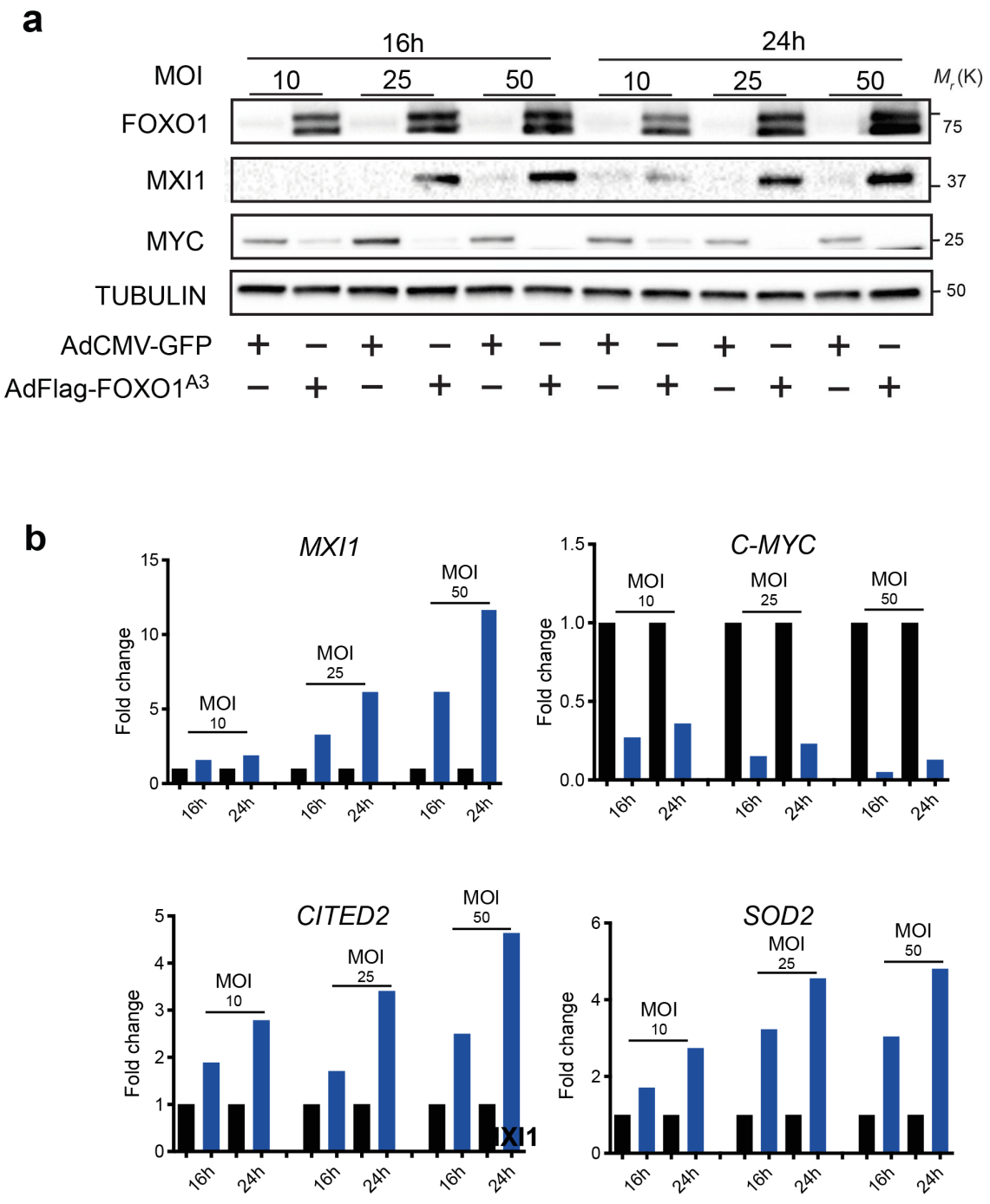

Figure 26: Forced activation of FOXO1 regulates canonical FOXO target genes. a,b, Immunoblot and qPCR analysis showing regulation of well-known FOXO1 target genes. n=1

To exclude the possibility of induction of apoptotic cell death due to high levels of FOXO1 expression after transduction, we immunoblotted for cleaved Caspase 3, one of the central proteases in the execution phase of cell apoptosis (Figure 27). As positive control, we co-stimulated HDLECs with tumor necrosis factor α (TNFα) and Cycloheximide.

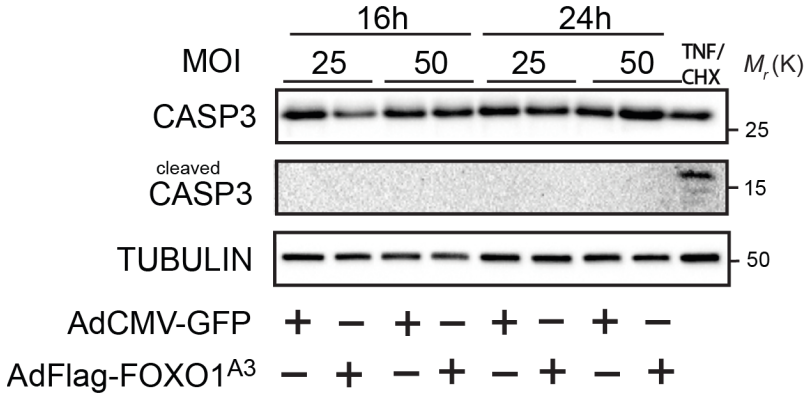

Figure 27: Adenoviral transduction does not induce apoptosis in HDLECs. TNF: Tumor necrosis factor α, CHX: Cycloheximide.

Importantly, no induction of apoptosis was observed. We therefore performed the RNA-seq experiment with an MOI of 50 to elicit a more vigorous FOXO1 response, aiding the bioinformatic analysis of downstream signaling pathways. In addition, an RNA-seq-dataset with FOXO1^{A3} mutant overexpression in HUVECs was already available in our laboratory. For precise comparison of both datasets in future projects, we decided to align the experimental setup as much as possible.

5.9 RNA-sequencing reveals molecular mechanisms of FOXO1 in lymphatic ECs

For RNA-seq, the experiment as shown in Figure 28a was performed six times. Out of the 24 samples, samples with the highest RNA integrity were chosen for sequencing. We decided to analyze gene expression after 16h and 24h to understand the gene expression dynamics following FOXO1 activation.

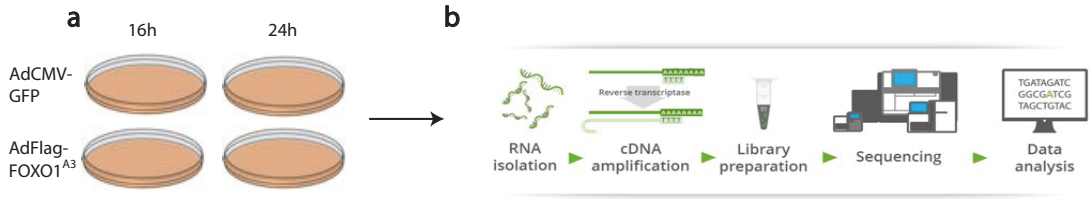

Figure 28: Workflow of for RNA-sequencing of HDLECs transduced with AdCMV or AdFlagFOXO1^{A3}. After transduction with either FOXO1^{A3} or GFP-containing Adenovirus, RNA was isolated and reverse transcribed into DNA. This DNA is preprocessed into a library suitable for the actual sequencing process. Sequencing and parts of data analysis were performed with the Bioinformatics and Deep Sequencing Platform at the Max-Planck-institute for Heart- and Lung research in Bad Nauheim. For further details see above (4.7).

To get a general overview of the data set, we performed a principal component analysis. This bioinformatic procedure enables compression of a large data set onto a smaller set, in this case two, orthogonal variables. Our data set revealed deviation of

one sample of each control group (Figure 29a), suggesting a batch effect affecting one experimental transduction. After applying a batch control, a stringent clustering in Dimension1 (Dim1) was achieved, although more deviation was introduced into Dim2. Therefore, we decided to work with the unprocessed data.

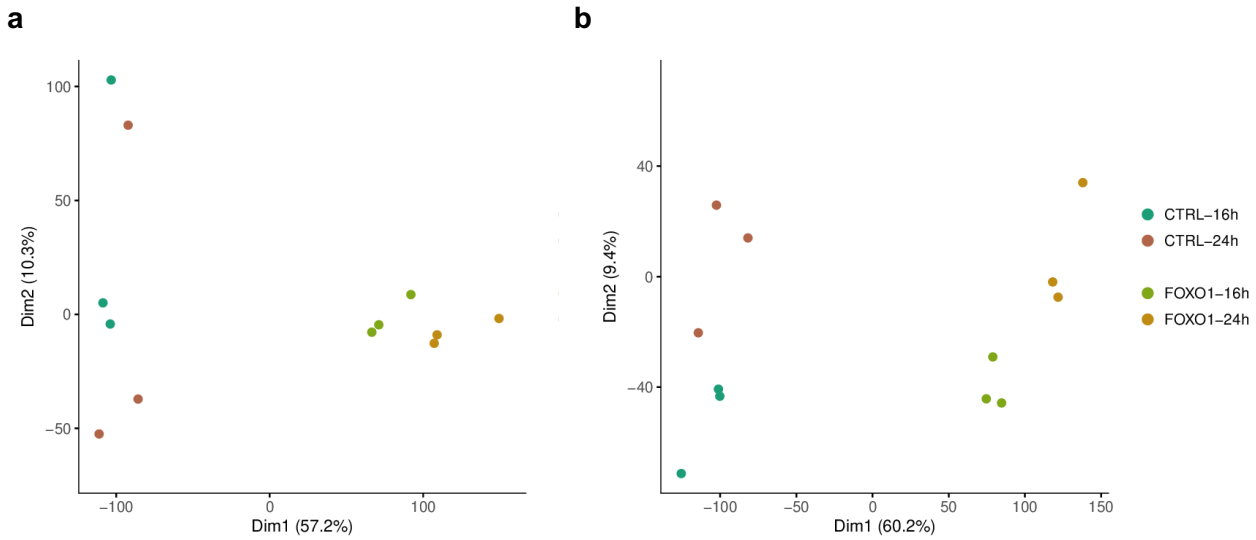

Figure 29: Principal component analysis (PCA) of the RNA-seq data set. a, PCA of raw data, showing batch effect in the control sample. **B**, raw data after application of batch control software.

Per sample between 16.745.283 and 45.745.647 (Mean: 31.369.478, ± S.D. of 7.465.811) reads were processed, aligned to 17.940 genes. After 16h, 11013 genes were differentially expressed using a threshold of adjusted p value (p^{adj}) of <0,05, after 24h 10952 genes.

To visualize the differently expressed genes, we plotted the data as a volcano plot (Figure 30 right scatter plot, **a,** after 16h, **b,** after 24h). This plot emphasizes that a plethora of genes are regulated significantly and with substantial foldchange, but not enabling further clear conclusions about the underlying biological pathways without usage of further bioinformatic analysis. The MA plot emphasizes higher variability in lower expressed genes, as it is expected in most RNA-Seq data sets[255].

Although the plots in Figure 30 are a useful tool to get a general overview about the dataset, the amount of significantly regulated genes makes it difficult to identify key players responsible for the observed phenotype. Due to the abundance of highly significant regulated genes, comparison of the individual top-regulated genes was not promising. Additionally, analysis of single gene expression changes may reveal important biological insights, but many cellular processes require regulation of gene groups. The functional impact of genes regulated in groups might thus be higher than the impact of one strongly regulated gene.

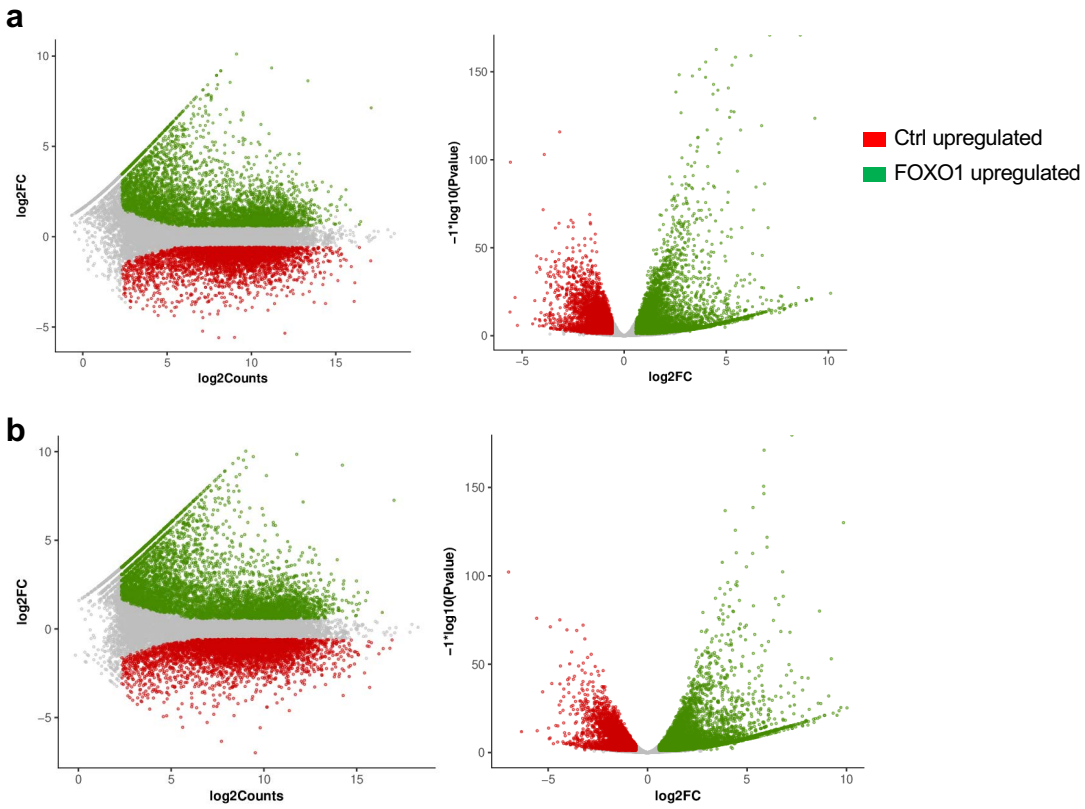

Figure 30: MA and Volcano plot. After 16h (**a**) and after 24h (**b**). All genes <5 counts have been removed. Adjusted p value ≤ 0,05, Log_2FC <>± 0.585. Non-regulated genes are represented in grey.

Given these considerations, gene set enrichment analysis (GSEA) was performed to get insights which cellular programs are controlled by FOXO1. GSEA focuses on the regulation of gene sets sharing similarities, such as regulation of a particular pathway or chromosomal allocation, thereby representing cellular phenotypes more precisely than single gene expression changes[256].

RNA-seq data was analyzed with two different groups of gene sets, one provided by the Molecular Signatures Database (MSigDB)[256], the other by the Kyoto Encyclopedia of Genes and Genomes (KEGG).

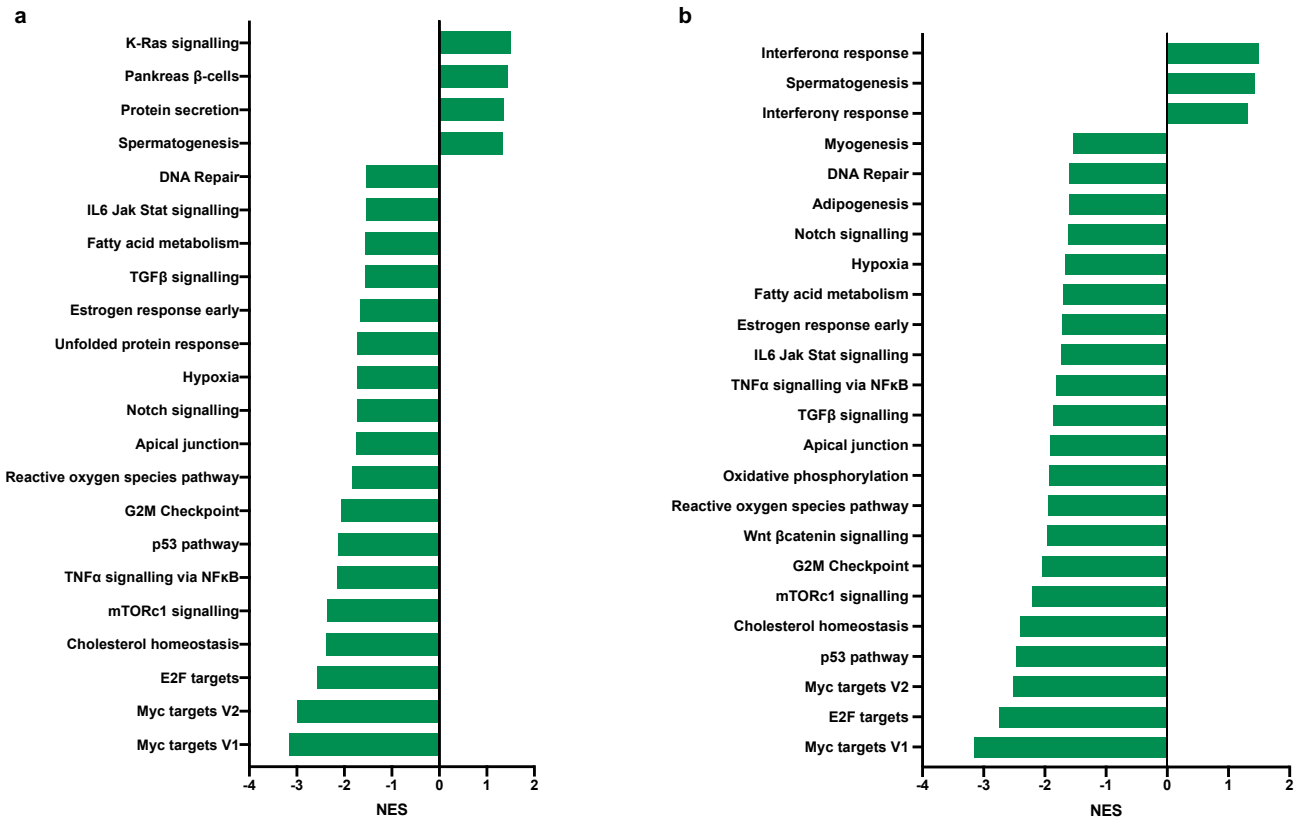

Figure 31: GSEA using the hallmark gene set collection. Top hits after 16h (**a**) and after 24h (**b**) FDR<0.25. NES, normalized enrichment score. FDR, false discovery rate.

In a first attempt, we performed GSEA using the hallmark gene set collection. These gene sets were extracted from over 10000 gene sets, aiming to reproduce well-defined biological states[257]. From the 50 hallmark gene sets, the ones with a false discovery rate <0.25 are shown in Figure 31. Multiple gene sets linked to proliferation were downregulated in the FOXO1^{A3}-overexpressing cells, including MYC targets, E2F targets, mTORC1 signaling or G2M checkpoint, indicating FOXO1-dependent regulation of proliferation at multiple levels. Remarkably, also the cholesterol homeostasis gene set was downregulated, perharps due to a reduced demand for anabolic metabolism and cholesterol-containing cell membranes. Although we chose two timepoints for the analysis, no major differences in the gene sets were observed between the two.

Subsequently, we analyzed the same data set using KEGG gene sets, aiming to get deeper insights into the altered signaling pathways and cellular processes.

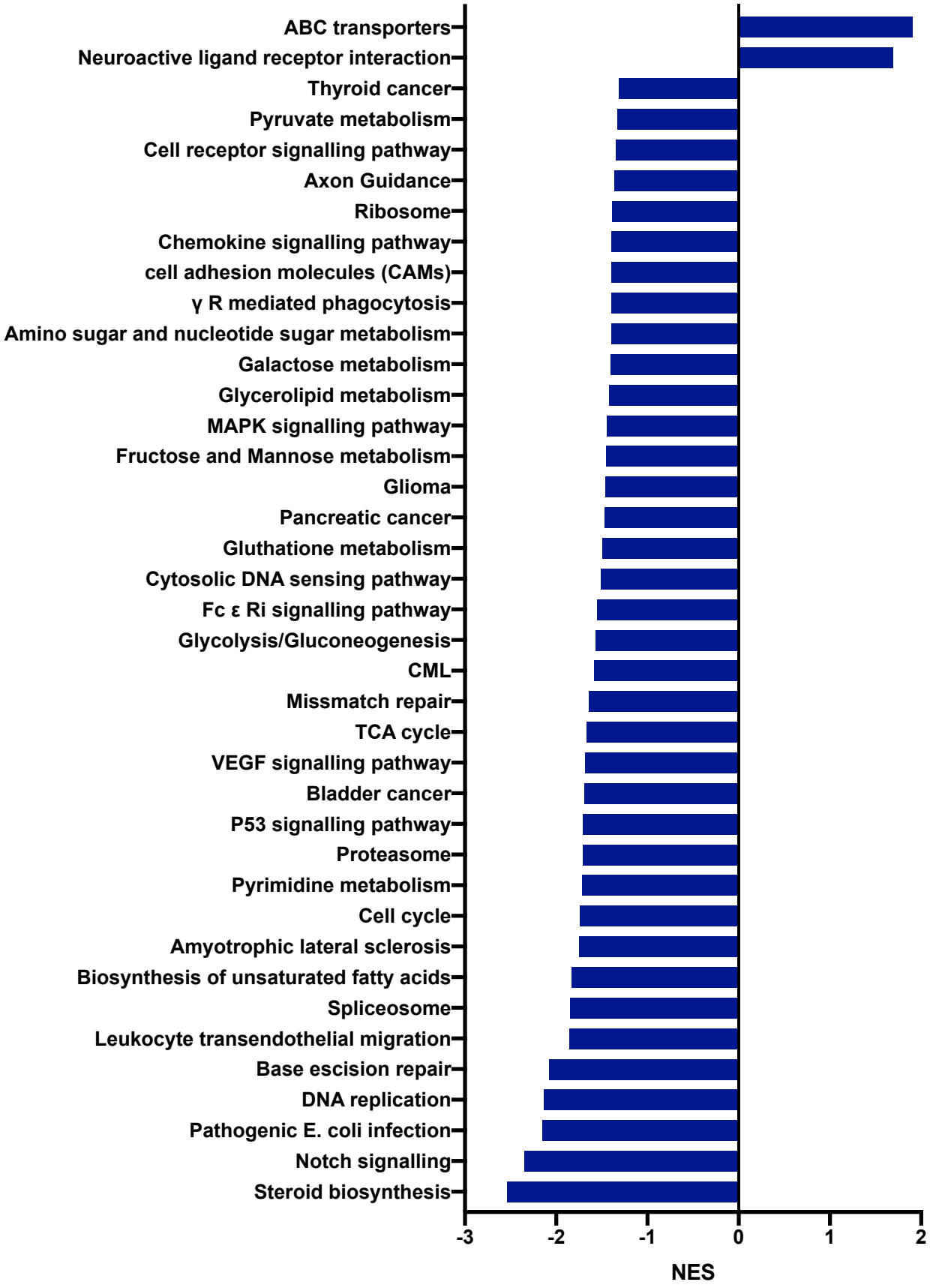

Figure 32: GSEA using KEGG. Top hits after 16h. FDR<0.25. NES, normalized enrichment score. FDR, false discovery rate.

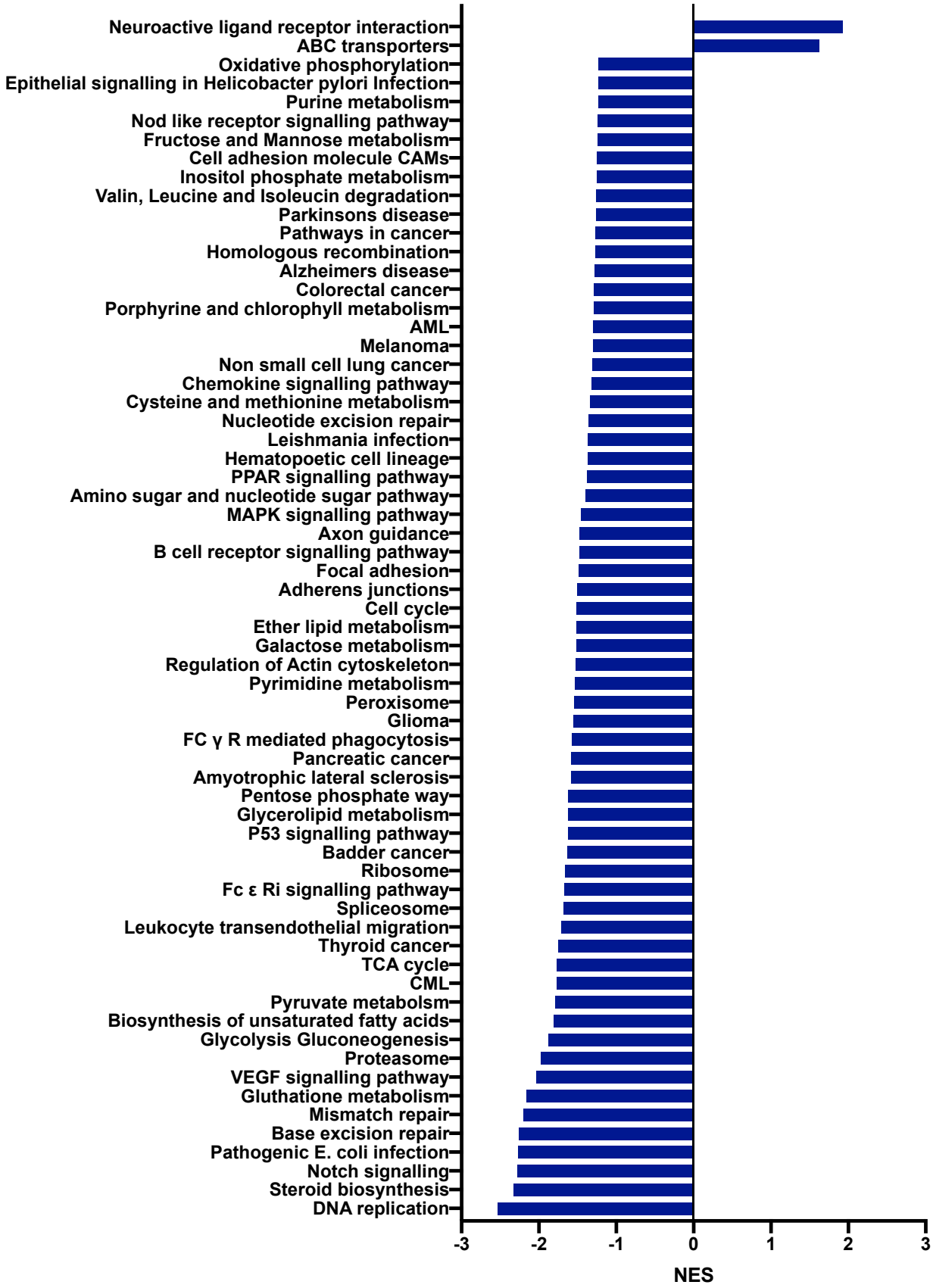

Figure 33: GSEA using KEGG after 24h. Top hits after 24h. FDR<0.25. NES, normalized enrichment score. FDR, false discovery rate.

KEGG projects have developed large pathway databases, aiming to connect genomic information with higher-order functional information[258]. A substantial amount of gene sets here is highly adapted to specific conditions (f.e. pathogenic E- coli infection or specific diseases) and is therefore not considered in the further course.

After 16h and 24h, two gene sets were significantly upregulated, 37 were downregulated after 16h (Figure 32) and 65 after 24h (Figure 33). Also here, no major differences were observed between the two timepoints chosen.

Conspicuously, many downregulated gene sets are linked to proliferation and associated metabolic changes, such as DNA replication, cell cycle, steroid biosynthesis or pyruvate metabolism. This observation matches our previous GSEA results and *in vivo* data, indicating FOXO1 dependent downscaling of proliferation by influencing different regulators of proliferation and growth, such as MYC and mTOR.

Previous work from our lab showed FOXO1 dependent repression of MYC signaling in BECs, which drives the acquisition of a quiescent state[146] . Interestingly, we also see a strong regulation of MYC in LECS in our data, suggesting similar mechanisms of regulation. In addition, FOXO1 activation led to a profound suppression of mTOR signaling. Given mTORs central essential role in the promotion of cellular anabolism and growth[174] , we decided to analyze the regulation of this pathway by FOXO1 in more detail.

5.10 FOXO1 regulates mTOR signaling

A highly downregulated gene set was mTORC1 signaling, a pathway involved in anabolic metabolism, growth and proliferation. The GSEA revealed robust downregulation of genes related to mTORC1 signaling in $FOXO1^{A3}$ overexpressing LECs after 16h and 24h, indicating reduced mTORC1-activity in $FOXO1^{A3}$-overexpressing-LECs.

As FOXO1-dependent regulation of mTOR signaling has been described to take place partly via Sestrins[173], Sestrin transcript levels were analyzed in different endothelial subtypes via RNA-seq (Figure 34b). Strikingly, expression levels of Sestrin 1 and 2 are comparable in different endothelial subtypes, but expression of Sestrin 3 is strongly induced in LECs, suggesting a particular function in this endothelial subtype. $FOXO1^{A3}$ overexpression leads to a profound increase in the mRNA (Figure 34c) and protein levels (Figure 34d) of this inhibitor of mTOR signaling.

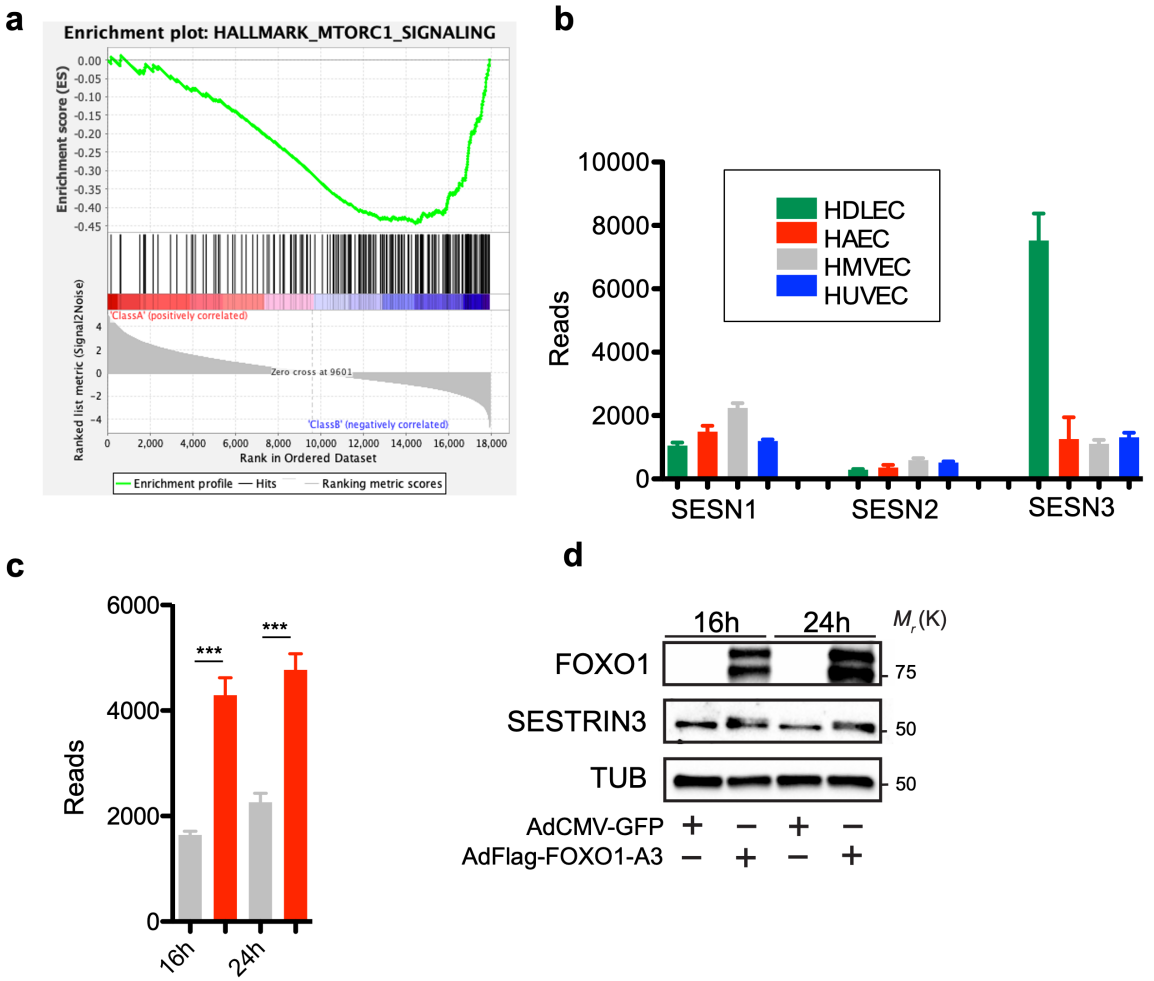

Figure 34: FOXO1 regulates mTor and Sestrin3. a, GSEA of the mTor gene set in AdFOXO1^{A3} or AdCtrl-transduced LECs after 16h with an enrichment score of -0.44 and a normalized enrichment score of -2,35. **b,** expression levels of Sestrin 1,2 and 3 in different endothelial subtypes. **c**, Sestrin 3 expression in AdFOXO1^{A3} (red) - or AdCTRL-transduced (grey) LECs. **d**, immunoblot showing FOXO1 dependent regulation of Sestrin3 in LECs. Data represent mean ± s.d., two-tailed unpaired t-test. *** P<0.001.

Second, the TSC2-independent pathway was analyzed. FOXO1^{A3} led to marked induction of RICTOR, a defining component of the mTORC2 complex that regulates cell survival[173]. We checked the expression levels for all components of mTOR-signaling in the RNA-Seq-data. All components were not affected by FOXO1 except of RICTOR, exhibiting a solid 3,5-fold increase under FOXO1^{A3} overexpression (Figure 35a). As it was done by Chen et al., p27 and Cyclin D, two canonical target genes of FOXO1, were depicted as controls of FOXO1 activity[173]. These data suggests that FOXO1 may reprogramme mTOR signaling away from mTORC1 driven anabolism and growth and towards mTORC1-driven cell survival and feedback regulation (e.g. through AKT) – a model consistent with prior reports in cancer cells[259] .

In conclusion, FOXO1 overexpression might lead to downregulation of mTORC1 in LECs by induction of Sestrin 3 and Rictor.

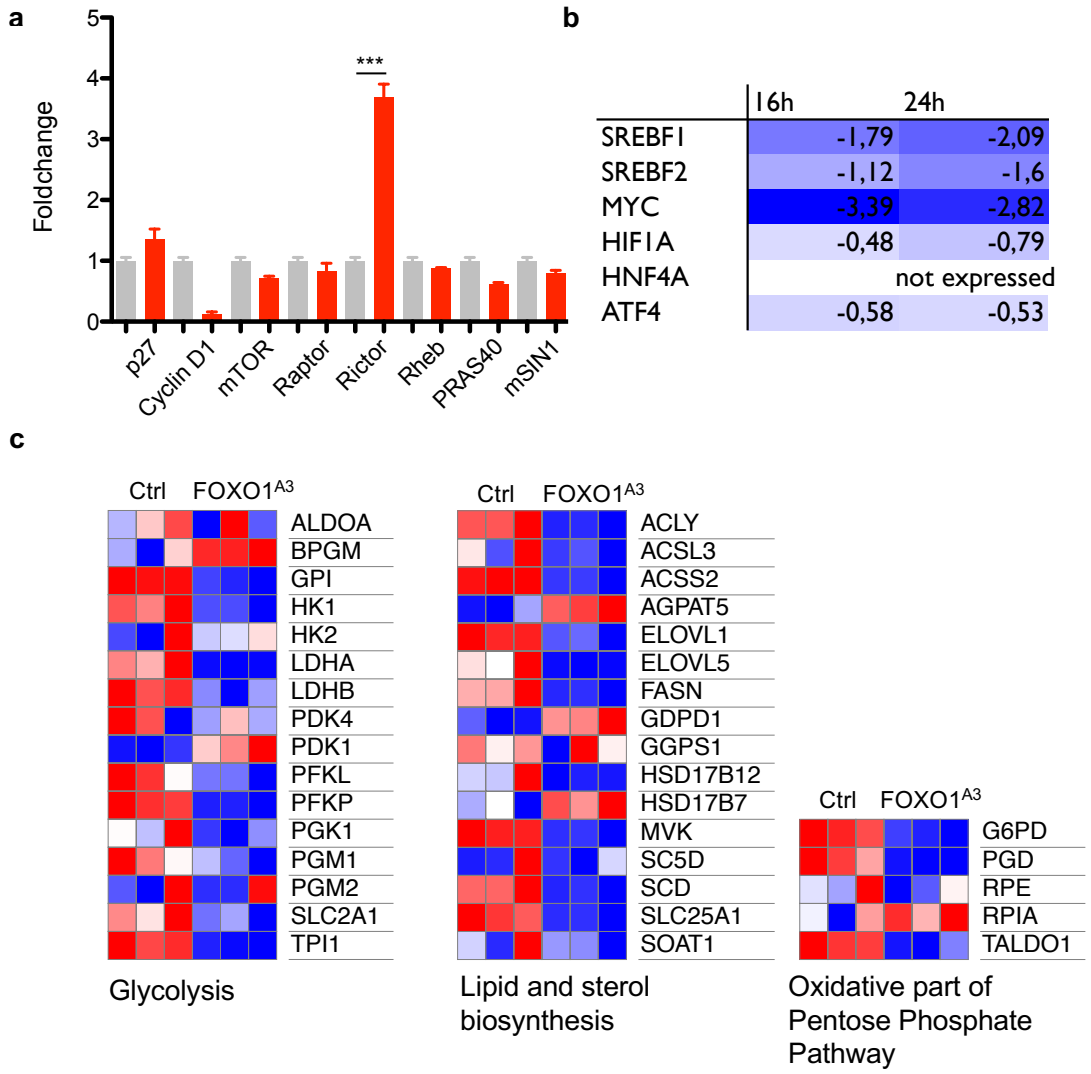

Figure 35: FOXO1 reduces mTORC1 activity by induction of Rictor and mTORC1 reduction leads to downregulation of several metabolic pathways. a, FOXO1 increases mRNA expression of Rictor[173]. **b,** foldchange of transcription factors regulated by mTORC1 after 16h and 24h in FOXO1^{A3} LECs compared to Ctrl-LECs. **c**, Heatmaps of 3 metabolic pathways regulated by mTORC1. Data represent mean ± s.d., two-tailed unpaired t-test. *** P<0.001

To further understand the effects of FOXO1 on mTORC1 signaling, we zoomed into the regulation of metabolic pathways that are tightly linked to the activation of mTORC1 signalling[175]. As Düvel et al. identified glycolysis, lipid and sterol biosynthesis and the pentose phosphate pathway as the main metabolic pathways inducted by mTORC1 activation, we focused our analysis on those[175]. Surrogate readouts of mTORC1 activity such as phosphorylation of the ribosomal protein S6 kinases (S6K1 and S6K2) or the eukaryotic initiation factor 4E (eIF4E)-binding proteins (4E-BP1 and 4E-BP2) have not been performed in this thesis.

Heatmaps, consisting of genes involved in all the above-mentioned pathways, exhibited a clear downregulation of most genes. As depicted in Figure 35, the rate-limiting enzymes of glycolysis, Hexokinase (HK1 and 2), Phosphofructctokinase-1 (heterotetramer consisting of PFKL and PFKP), glucose- 6-phosphat-Dehydrogenase (G6PD) for the pentose phosphate pathway and rate-limiting enzyme of the lipid and sterol biosynthesis are downregulated. This data indicates decrease in mTORC1 regulated metabolic pathways by overactivation of FOXO1. Additionally, we analyzed the expression of specific transcription factors, which have been identified before to be regulated by mTORC1[175](Figure 35). SREBF1 and SREBF2 are known master transcriptional regulators of genes implicated in de lipid and sterol biosynthesis[175]. The transcription factor MYC is a known target of mTORC1 but also of FOXO1 and an important driver of proliferation. MYC is downregulated and - as the Gene set enrichment analysis already showed - MYC gene sets are significantly downregulated. HIF1α, a known inducer of glycolysis has been reported to be induced by mTORC1 signaling[175]. Matching the previous data, this transcription factor is also downregulated after 16h and 24h.

Taken together, all the identified transcription factors in Düvels et al. study have been downregulated in our data (Figure 35b) as well, supporting our hypothesis that FOXO1 is an important suppressor of the mTORC1 pathway.

5.11 Assessment of maturation *in vitro*

As our in vivo data shows, enhanced FOXO1 signaling might be related with disturbed maturation. To assess maturation of lymphatics *in vitro*, we generated a list of genes involved in lymphatic maturation by meticulous literature review of the major publications regarding this topic[9,20,51,52,56,58,59,61,62,66,88]. Interestingly, almost all genes participating in lymphatic maturation were downregulated, implicating inhibited maturation gene expression in HDLECS with activated FOXO1 signaling. Two exceptions can be observed. Angiopoietin 2, a protein required for lymphatic pattering[88], and Reelin, an extracellular matrix glycoprotein implicated in smooth muscle cell recruitment[58].

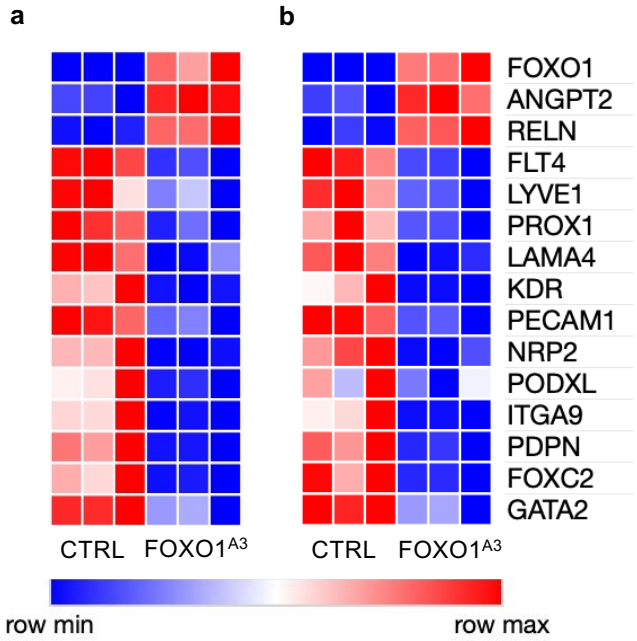

Figure 36: FOXO1 overexpression leads to reduction of lymphatic maturation genes. Selected maturation genes after 16h (**a**) and 24h (**b**). Heatmap color coding shows maximum in red and Minimum in blue. Read values were used as raw data. Heatmap was generated using morpheus, available from the Broad Institute (*https://software.broadinstitute.org/morpheus/*).

6 Discussion

In this study we identified FOXO1 as an essential regulator of lymphatic vascular growth. Using genetic gain- and loss-of-function-models *in vivo* and *in vitro*, we demonstrate that LECs are highly sensitive to changes in FOXO1 signaling and that FOXO1 activation limits lymphatic expansion, resulting in an immature, poorly developed and likely dysfunctional lymphatic network. Unlike in other cell types, FOXO1 overexpression did not induce apoptosis *in vitro.* Instead, we found that FOXO1 orchestrates the transcription of genes involved in cell-cycling and metabolism, including pathways such as glycolysis, lipid and sterol biosynthesis, and the pentose phosphate pathway. Regulation of proliferation and growth seems to be executed via different interaction partners, such as MYC and mTOR.

These findings highlight the central function of FOXO1 in lymphatic systems, where it acts at the intersection of lymphatic endothelial proliferation, metabolism and differentiation. In the following paragraphs, key findings of this thesis will be contextualized and their biomedical implications discussed.

6.1 Dynamic changes in FOXO1 expression and subcellular distribution suggest diverse functions in the lymphatic system

Staining of FOXO1 in wildtype animals at P10 revealed that FOXO1 is highly expressed in LECs – even higher than in BECs (Figure 14) - indicating a decisive role in lymphatic development. Interestingly, FOXO1 subcellular distribution showed a pattern that one would not necessarily predict from previous studies in BECS[146]. Whereas FOXO1 showed a diffuse nucleo-cytoplasmic staining in sprouting blood vessels, FOXO1 was a more nuclear protein in sprouting lymphatic vessels. These observations support the idea that FOXO1 might have specific roles in lymphatic vessels that differ from those in blood vessels. Of note, the expression pattern of FOXO1 changed at later stages of development. At P21, FOXO1 became more restricted to collecting vessels and valves, implying crucial roles in lymphatic remodeling and maturation. These observations go in line with recent publications, reporting important roles of FOXO1 as an important regulatory protein for lymphatic valve formation and maintainance[229,230]. Especially this aspect will be discussed later.

6.2 FOXO1 activation reduces proliferation in developing lymphatics

To observe the consequences of FOXO1 activation during lymphatic development *in vivo*, we analyzed mouse dermal lymphatics at the developing (P10) and the

remodeled state (P21). At P10, the lymphatic vessels were hypoplastic with reduced vessel diameter and smaller size of the sprouts (Figure 19). The reduced proliferation that we observed at this stage fits to the classical role of FOXOs as key controllers of the cell cycle[156]. Micro array analysis in human endometrial stromal cells brought to light that FOXO1 regulates several genes essential for cell cycle progression by controlling G1/S and G2/M phase transition[167] (s. 1.3.2.1).

Interestingly, a murine knock out of AKT, the effector kinases of PI3K signaling, resulted in a very similar lymphatic phenotype characterized by a hypoplastic vessel network with a reduced number of proliferating LECs[218]. Since AKT inhibits FOXOs through direct phosphorylation, these data indicate that the PI3K-AKT-pathway is a critical regulator of FOXO1 in lymphatics, too. This observation also aligns with the observation by Wilhelm et al. in BECs, where forced activation of FOXO1 led to premature BEC quiescence and blood vessel rarefaction[146], highlighting commonalities between these EC types. Differences in FOXO1 biology between blood and lymphatic vessels are addressed later in the discussion. However, other causes of a hypoplastic vessel network need be considered as well. Examples include different forms of cell death, including apoptosis. FOXO1 is a known inductor of apoptosis in certain cell types[187]. Nevertheless, it should be stressed that we did not find evidence for major changes in apoptosis, making this mechanism rather unlikely (Figure 27).

6.3 FOXO1 activation interferes with maturation processes

But how does FOXO1 impact proliferation and maturation of dermal lymphatics? It is well known that proliferation and differentiation do not go hand in hand[260,261]. Differentiation or maturation often involves a restriction in proliferation, and aberrant proliferation can result in a diminution of maturation or specialization[260]. Moreover, in a mature or differentiated state well-tuned proliferation is a prerequisite for maintenance of tissue architecture and organ functionality[261]. On the other hand, reduced proliferation does not automatically lead to increased differentiation. However, some proteins seem to reduce proliferation and induce differentiation at the same time - so called dual function cell cycle regulators[261].

At later stages of lymphatic morphogenesis (P21) the FOXO1 overexpression phenotype is sustained, arguing that FOXO1 is not only pivotal for early development, but also for maturation of the lymphatic system. The lymphatic vessels are thinner in shape, and the whole lymphatic network is sparse. Conspicuously, maturation was massively disturbed, determined from the following observations: Collecting vessels expressed classical lymphatic capillary markers such as LYVE1 and the smooth

muscle actin coverage (SMA) was plainly below average. Moreover, lymphatic valves were reduced in number, disorganized and the expression of the valve specific genes Podocalyxin and Integrin alpha9 was suppressed.

Especially the valve defects have given rise to the suspicion that the system does not function properly (Figure 22). Since there are already some studies on the role of FOXO1 in lymphatic valves, their findings and differences to ours will be briefly presented and discussed. Applicable to this study and our data, Niimi et al. describes FOXO1 as a repressor for lymphatic valve formation and maintenance[230]. Mechanistically, they propose PRDM1 as a repressor downstream of FOXO1. Whether the inhibition of lymphatic valve specific genes is direct or indirect remains, however, unaddressed. Scallan et al. promote a model where FOXO1 suppresses valve formation by suppression of valve-specific genes[229]. This data fits our observations, as forced activation appears to prevent proper valve formation. Although not the focus of this thesis, it should be noted that our FOXO1-Knockout is also devoid of valves, whereas Scallan et al. reports the promotion of lymphatic valve growth upon FOXO1-deletion[229]. This might be explained due to different vascular beds that have been studied, as Scallan et al. performed their studies in the mesentery and axillary lymphatic vessels, an aspect that will be discussed further. Valve morphogenesis and its biophysical function in the mesentery of FOXO1-Knockout mice has also been studied by Davis et al., reporting an increased number of valves in the mesentery, remaining in a not fully matured state of development[262]. Importantly, Scallan et al. and Davis et al. studied lymphatics in the mesentery, which entails some considerations. Whereas postnatal deletion of FOXO1 leads to the phenotype in the mouse ear described in this thesis, Scallan et al. and Davis et al. describe vessels in the mesentery with the same diameter and retained SMA coverage[229]. This could be explained by the timepoint of FOXO1 deletion: Whereas the dermal lymphatic system in the mouse ear starts to develop postnatally, mesenteric vessels were already forming, leading to a FOXO1 Knockout or overexpression in the maturated state.

Although the observed phenotype progresses over time, proliferation measured *in vivo* did normalize compared to wildtypes at P21. FOXO1 staining at P21 (Figure 18b) confirmed continued high levels of FOXO1 expression, making the subsiding of high expression unlikely. Instead, compensation mechanisms seem to be taking effect to counteract reduced proliferation. One well studied pathway cross talking and compensating the PI3K-AKT-pathway is the Ras-ERK pathway[263].

Furthermore, the effect of lymphatic endothelial overexpression of FOXO1 had a profound effect on the dermal blood vascular system, as can be observed in the panendothelial stainings at P21 (Figure 21). The blood vessels appeared disorganized

and hyperbranched, almost exhibiting similarities to blood vessel anomalies. Especially slow-flow venous and lymphatic malformations are most evidently caused by mutations in the PI3K-AKT-mTor signaling pathway[219], thereby opening room for speculations of disease contribution by FOXO1 in blood and lymphatic endothelial cells. Although the mechanism behind this observation is beyond the scope of this thesis, it illustrates the deep interweaving of the different parts of the vascular system.

6.4 *In vitro* experiments reveal mechanistical insights in FOXO1 dependent regulation in LECs

To gain mechanistic insights into the FOXO1-dependent regulation of lymphatic endothelial cells, we established an adenoviral FOXO1-A3 overexpression system. After validating our *in vitro* system by measuring canonical FOXO1 targets on mRNA and protein level, we performed an unbiased genome-wide RNA-seq experiment, providing the FOXO1 transcriptome at different time points.

In a first analysis, most genes are upregulated upon $FOXO1^{A3}$ overexpression. Canonical FOXO1 target genes were regulated as expected (Figure 26).

Comparative transcriptome analysis revealed that FOXO1 is a negative regulator of several signaling pathways, including MYC[146] and E2F targets[168,264]. Wilhelm et al. has identified MYC before as a central regulator of metabolism and growth[146] in BECs. As MYC regulated gene sets are among the most regulated in our data derived from LECs, we assume that MYC also plays an important role in LECs. Nevertheless, it should be noted that FOXO1 distribution in proliferating LECs differs significantly from the pattern seen in BECs, indicating additional functions beside FOXO-MYC signaling.

Moreover, central metabolic pathways such as cholesterol and steroid biosynthesis (Figure 31, Figure 32) were downregulated upon FOXO1 signaling. We surmise that mTORC1, a well-known regulator of anabolic cell metabolism, growth and proliferation - is at least partly responsible for the observed effects. Reasons for this assumption are the strong GSEA score for mTORC1 gene set, the robust downregulation of numerous genes related to activated mTORC1 signaling and the reported regulation of mTORC1 by FOXO1[173].

To analyze the TSC2-dependent pathway of FOXO-dependent mTORC1 regulation, we studied the expression of Sestrin 3 in different endothelial subtypes and our RNA-seq data (Figure 34b, c). We confirmed that Sestrin 3 seems to be a target of FOXO1 (Figure 34c, d)[173] that is highly expressed in LECs (Figure 34b). FOXO1 also induced RICTOR (Figure 35a), promoting mTORC2 assembly on the expense of mTORC1. In summary, the gene expression changes suggest reduced mTORC1 activity,

mechanistically by direct inhibition of mTORC1 activity and by shifting mTOR complex assembly towards mTORC2. However, surrogate readouts such as phosphorylation of the ribosomal protein S6 kinases (S6K1 and S6K2) or the eukaryotic initiation factor 4E (eIF4E)-binding proteins (4E-BP1 and 4E-BP2) are needed to assess the activity of the mTORC1 signaling cascade.

To get further insights into the FOXO1-dependent mTORC1-inhibition, we analyzed the expression of transcription factors known to be regulated by mTORC1 (Figure 35b) and gene expression of exemplary conserved metabolic pathways[175] (Figure 35c). All the three studied pathways exhibited pronounced reduction in mRNA expression, indicating reduced metabolic activity. Glycolysis, the metabolic pathway converting Glucose in pyruvate/lactate, is known to be regulated by FOXO1 in direct and indirect ways. As shown by Wilhelm et al., the observed effect might be partly caused by FOXO1-induced MYC supression[146]. Additionally, FOXO1 directly elevates PDK-4 levels, a kinase phosphorylating pyruvate dehydrogenase (PDH), and thereby regulating glucose metabolism[265]. mTORC1 induces glycolysis mainly by reduction of the transcription factor HIF1α[175], a transcription factor also reduced in our data set (Figure 35b). Regulation of Glycolysis by FOXO1 through different regulation pathways to adjust cell metabolism to lower requirements is appealing, indicating FOXO1-signaling intersects at different levels in regulation of glycolysis.

Lipid and sterol biosynthesis is a well-known downstream metabolic pathway of mTORC1[175,266]. Our data indicates clear downregulation of this pathway in RNA-seq data (Figure 31, Figure 32, Figure 33, Figure 35c), probably due to downregulation of SREBPs (Figure 35b)[267]. These transcription factors have been identified as activators of the cholesterol and lipid biosynthesis program[268], and FOXO1 might also inhibit SREBP1c-transcription directly[269]. Thus, regulation by mTORC1 and FOXO1 might finetune proliferation with the demand of lipid membranes and cholesterol. Previous studies already pointed out the importance of lipid metabolism in the process of lymphangiogenesis, focusing on the role of fatty acid oxidation in LECs[270]. Since the lymphatic vasculature in the intestine (the 'lacteals') is explicitly responsible for fat absorption, special functions might in this vascular area and therefore an appealing vascular bed for further studies.

Additionally, we showed that FOXO1 leads to downregulation of lymphatic maturation genes in our experimental setup. As an exception, Reelin is highly upregulated. On closer inspection, MCP1 (corresponds to CCL2), the major interaction partner of Reelin and responsible for Reelin dependent SMC recruitment[58], is downregulated -3,2 foldchange after 16h (data not shown). Mechanistically, Reelin might be elevated compensatory due to FOXO1 dependent downregulation of CCL2. This might explain

partially the loss of SMCs in our *in vivo* model. Although we are not able to differentiate between direct or indirect regulation, the observed downregulation is more pronounced after 16h, arguing in favor of direct regulation.

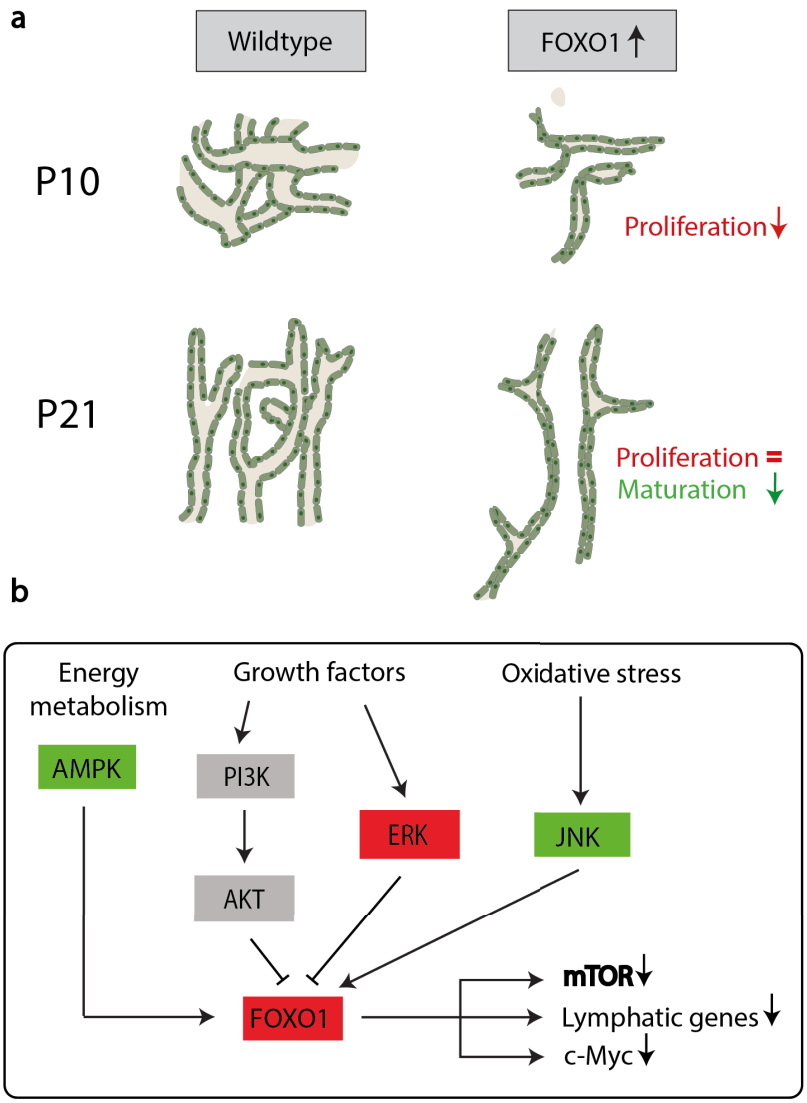

Figure 37: FOXO1 orchestrates proliferation and maturation in lymphatics. a, Summary of our *in vivo* studies in developing (P10) and mature (P21) lymphatics **b,** FOXO1 negatively regulates mTOR, Lymphatic genes and c-Myc, causing an immature lymphatic system.

But is this observation result of a direct inhibition of lymphatic maturation genes by FOXO1, or a secondary effect due to FOXO1 dependent influences in other cell biological processes, such as oxidation resistance? Although our findings in combination with recent studies[229,230] suggest a direct influence of FOXO1 on maturation, our technical approach does not allow to answer this question in conclusion. On one hand, FOXO1 chromatin immunoprecipitation studies are needed to provide further insight which of the FOXO-regulated transcripts are direct – an important approach for future FOXO studies in lymphangiogenesis and maturation.

Additionally, it should be noted, that the quantity of FOXO1 activation in our experimental approach significantly exceeded the physiological amounts. Maturation might be related to finetuned FOXO1-regulated proliferation at the cellular level. The disturbed maturation might not be caused by high levels of FOXO1 itself, but rather by loss of FOXO1-dependet finetuned proliferation.

In summary, our *in vitro* data reveals downregulation of several metabolic pathways, presumably to adjust cell metabolism to the reduced proliferative state. Mechanistically, we propose the FOXO 1-dependent downregulation of MYC and mTORC1, two well-known regulators of cell growth.

6.5 Strengths, weaknesses and limitations of the study design

Before starting our research, we decided for an exploratory approach of our project. In contrast to confirmatory research, where a hypothesis formulated before is tested, our exploratory approach pursued the goal to generate inductively derived insights about the research object and develop new theoretic concepts from them. To ensure reliable results with high validity, we used quantitative analysis methods in every *in vivo* and *in vitro* experiment, balancing researcher biases, for which f. e. especially *in vivo* microscopy work might be susceptible.

For our *in vivo* approach, we used an inducible, conditional mouse model, enabling us to decide the timepoint when FOXO1 signaling is activated in a given cell type. Taking advantage of this technology, we ensured that the observed effects were likely caused by changes in FOXO1 signaling in LECs. GFP-labeling excluded confounded results due to artificial FOXO1 expression in other tissues (Figure 18). It should be noted, however, that PROX1 is not only expressed in lymphatics, but also in the brain, liver, eye and skeletal muscle[242], among other tissues. Expression of the FOXO1 mutant allele in these tissues raises the possibility of systemic effects on the lymphatic vasculature that are not the consequence of altered FOXO1 activity in LECs. As a control Cre-negative littermates were used and the animal care takers were blinded for the genotype of the mice during the 4-OHT administration. Thus, an information bias was eliminated.

Regarding the validity of our results, it has become more and more evident over the last years, that EC function is highly depended on the tissue it is embedded in[2,271]. This specialization is sometimes expressed in their names, e.g. ‘lacteals’ for lymphatic capillaries in the gut. The two studies of 2021 studying the role of FOXO1 in lymphatics, obtained their data from mesentery lymphatics[229,230]. As discussed above, different vascular beds develop at different embryonic (mesenteric lymphatics) or

postnatal (dermal lymphatics) stages in mouse model. This consideration allows to conclude, that the differences seen in different vascular beds, are not only caused due to their differences in vascular microenvironment, but also due to experimental intervention at different developmental stages. By studying one vascular bed in detail, we increased the internal validity of our results, while potentially ignoring specialties of other vascular beds (e.g. mesentery). This should be taken into account when generalizations are being made from our results.

Our *in vitro* data has been acquired using single donor human dermal lymphatic endothelial cells, purchased from commercial vendors. In contrast to pooled cells, where individual variation of cell phenotype and behavior is balanced due to combination of different genetic donors, it can be assumed for single donor cells higher intervariablity due to greater influence of genetic background and clinical history of the donor. To keep the experimental setting comparable and maintain high internal validity, we paid great attention using the same cell lot for our *in vitro* experiments. Additionally, it should be considered, that the *in vivo* part of this work has been conducted in a murine model, whereas the *in vitro* data has been acquired using human cells. Although comparability of murine and human cells has been reported many times in the last decades, differences exist in experimental output and data analysis.

RNA-seq experiments provide the expression level of mRNA in the analyzed number of cells (or single cell) at a specific timepoint. Although the analysis can be challenging, this method provides plenty of information about the current state of the cell. Nevertheless, the researcher must keep in mind, that fundamental regulatory processes take place at the posttranslational level and thereby remain invisible when using RNA-seq exclusively. Especially for the analysis of kinases such as mTORC1, further experimental evidence is needed to make conclusion about the regulation or activity of a particular signaling cascade, since a large part of the mTORC1 regulation takes place at the posttranslational level[174,178]. To understand its state of activity, immunoblot analyses with phospho-specific antibodies of mTORC1 substrates are required.

GSEA is a powerful tool for extraction of biological information out of gene expression data[256]. In contrast to traditional strategies, mainly focusing on the fold-change of individual genes, this approach analyses groups of genes, belonging together because of a biological function or type of regulation. An example are all components of a metabolic pathway (e.g. cholesterol biosynthesis). This enables the scientist to uncover mechanisms of regulation that are not obvious when just looking for changes of individual genes. Of course, as a knowledge-based approach, every gene set consists of a list of genes and thus relies on the current state of science. To enable rapid

development, every scientist can develop gene sets and make them online available. In summary, GSEA is a reliable bioinformatic method for gene expression analysis, although special attention has to be paid to the input quality.

6.6 FOXO1, a future therapeutic target in diseases?

Although the literature describing clinical implications of FOXO1 dysregulation or lymphatic malfunction is tremendous, only three papers[228–230] have speculated about a potential involvement of FOXO1 in lymphatic disease. Pathological lymphangiogenesis plays a decisive role in diverse disease pathologies and might be caused as well as prevented by changes in FOXO1 activity or function. In the next paragraphs, possible implications for two diseases in which lymphatics play a major role will be discussed: cancer and inflammation.

6.6.1 Cancer

Metastasis of a primary tumor is the leading cause of cancer-related death. Indeed, most carcinomas metastasize primarily via the lymphatic system, followed by metastasis through the bloodstream. Therefore, lymphangiogenesis is considered a critical step in the progression of malignant disorders. Tumor cells express mediators for lymph vessel formation. Due to the plethora of mediators implicated in lymphangiogenesis promotion in a tumor environment, such as PDGF-BB, IGF-1 and -2, FGF2, HGF, angiopoetin-2, shingosine-1-phosphate, IL-7, and others[130], inhibition of one single target seems ambitious due to possible bypass effects of other mediators. Indeed, this experience has been made with VEGF blockers in blood vessels, where the emergence of resistance often limits sustained therapy success[272].

As we have shown in our work, FOXO1 slows down proliferation in the developing lymphatic system, which could result in slower tissue invasion in solid tumors. As an integrator of several signaling pathways, targeting FOXO1 might reduce bypass effects and prevent tumor lymphangiogenesis more efficiently. Additionally, an immature lymphatic system might be reduced in functionality and thereby additively support disease combat. However, challenging in this approach is the targeting of one specific transcription factor in a specific cell type in a living organism. Although gene therapeutic approaches are a rapidly developing field of research, it is currently difficult to target transcription factors with conventional drugs. Therefore, our observations might rather create a base for more translational research projects, before being able to be clinically applied.

6.6.2 Inflammation

Inflammation requires lymphangiogenesis for an adequate inflammatory response and blocking of VEGFR3 aggravates inflammation. On the other hand, resolution of inflammation requires antilymphangiogenic regulators, as has been reported in previous studies[121,273]. Additionally, inflammation associated remodeling of lymphatic vessels leads to impaired vessel function and thereby oedema[34]. The antiproliferative effects of FOXO1, presented in our study, could be a contributing factor in the resolution of inflammation. In addition, the remodeling of lymphatics under inflammatory conditions might be partially influenced by changes in FOXO1 status, phenotype correlations of dermal lymphatics under inflammatory conditions might provide hints regarding this question.

Moreover, especially the dermal lymphatic system, studied in this thesis, is of mayor importance for mounting a humoral immune response following vaccination. Lack or impairment in function of dermal lymphatic vessel leads to decreased antibody titers, thereby reducing effectiveness of vaccines[77], underlining importance of proper FOXO1 functionality in the lymphatic vascular system.

These considerations on two exemplary diseases suggest broad application opportunities under pathological conditions, although data on potential clinical applications is not yet available. Our data, thus, supports further scientists to disentangle the contribution of disturbed lymphangiogenesis to most different mammalian pathologies.

6.7 Conclusion

The mature lymphatic vasculature permeates almost all tissues of the mammalian body, carrying out various tasks essential for fluid homeostasis, immune surveillance, and intestinal fat absorption. Previous studies in our laboratory revealed the role of FOXO1 in blood endothelial cells as inducer of quiescence. Stainings of FOXO1 revealed that the expression levels of FOXO1 in the lymphatic vasculature exceeded those of the blood vasculature. Moreover, FOXO1 exhibited a different nucleocytoplasmic pattern in lymphatic endothelial cells. These observations suggested a specialized function of FOXO1 in LECs and established the basis for illuminating its role during the development of the lymphatic system.

Lymphendothelial overexpression of FOXO1 causes a profound reduction in LEC proliferation in the developing lymphatic system. Proliferation normalizes after 21 days, but the lymphatic vessels are impoverished and exhibit maturation defects. We find that FOXO1 represses metabolic pathways such as glycolysis, pentose phosphate

pathway and sterol biosynthesis, probably to adjust metabolism to the current growth state of the cell. Mechanistically, we propose MYC and mTORC1 as crucial downstream effectors of FOXO1 to synchronize cell cycle and metabolic activity in LECs.

Conspicuously, the blood vasculature exhibits a hyperplastic phenotype with increased vessel number, highlighting the tight, highly interdependent affiliation of different components of the vascular system.

Our findings identify FOXO1 as an inhibitor of proliferation in lymphatic endothelial cells. The decrease of proliferation, detected *in vivo*, establishes FOXO1 as an inhibitor of growth and regulator of lymphendothelial metabolism and maturation. It will be interesting to unravel the role of FOXO1 in the pathogenesis of lymphatic diseases and other vascular abnormalities.

Summary

The lymphatic vascular system is a unidirectional vascular network connecting the extracellular space with the venous blood circulation. It is essential for accurate regulation of homeostasis, intestinal fat absorption and immune response. Accurate development and maturation of these vessels is indispensable for growth and survival of the organism. Increased lymphangiogenesis is a hallmark of many tumor entities, whereas decreased lymphatic function can lead to lymphedema. Previous work from our laboratory has revealed the function of the transcription factor Forkhead Box O1 (FOXO1) in blood endothelial cells as an inductor of quiescence. Using lymphendothelial cell-specific overexpression *in vitro* and *in vivo*, we investigate the function of FOXO1 in the development and maturation of the lymphatic vasculature. *In vivo*, FOXO1 overexpression resulted in a sparse lymphatic network, exhibiting reduced proliferation. *In vitro*, we demonstrated downregulation of many genes involved in lymphatic vessel maturation. In addition, FOXO1 appears to reduce MYC and mTORC1 signaling and thereby diverse metabolic pathways, such as lipid and sterol biosynthesis, which may explain reduced cell growth.

This study reveals FOXO1 as a regulator of proliferation and maturation in the lymphatic vasculature. Our results demonstrate that proper development and maintenance of the lymphatic vascular network requires precise regulation of FOXO1, and alterations lead to defects in proliferation and maturation. Thus, FOXO1 might have a role in the pathogenesis of lymphatic diseases such as hereditary lymphedema and might evolve as an appealing target to treat these disorders.

Zusammenfassung

Das lymphatische Gefäßsystem ist ein unidirektionales Gefäßnetzwerk, welches den extrazellulären Raum mit dem venösen Blutkreislauf verbindet. Dabei erfüllt es unerlässliche Funktionen für die Regulation der Homöostase, die intestinale Fettresorption und Immunantwort. Korrekte Entwicklung und Reifung dieser Gefäße ist unverzichtbar für das Wachstum und das Überleben des Organismus. So ist vermehrte Lymphangiogenese ein Kennzeichen vieler Tumorentitäten, wohingegen verminderte Lymphsystemfunktion zu Lymphödemen führen kann. Vorhergehende Arbeiten aus unserem Labor konnten die Funktion des Transkriptionsfaktors Forkhead Box O1 (FOXO1) als Induktor von Quieszenz in Blutendothelzellen offenlegen. Unter der Zuhilfenahme einer lymphendothelzellspezifischen Überexpression *in vitro* & *in vivo* untersuchen wir die Funktion von FOXO1 in der Entwicklung und Reifung des lymphatischen Gefäßsystems. *In vivo* führte die FOXO1-Überexpression zu einer Verarmung an Lymphgefäßen, welche im Wachstum eingeschränkt waren und in einem undifferenzierten Stadium verharrten. *In vitro* konnten wir die Herunterregulierung beinahe sämtlicher an der Lymphgefäßreifung beteiligter Gene nachweisen. Darüber hinaus reduzierte FOXO1 mTORC1 und diverse Stoffwechselwege wie den Cholesterin- und Glukosestoffwechsel, was das reduzierte Zellwachstum erklären könnte.

Diese Studie offenbart die Funktion von FOXO1 als Regulator von Proliferation und Reifung im lymphatischen Gefäßsystem. Unsere Ergebnisse zeigen deutlich, dass eine korrekte Entwicklung und Instandhaltung des lymphatischen Gefäßnetzwerkes eine genaue Regulation von FOXO1 voraussetzt, und Änderungen zu Defekten in Wachstum und Reifung führen. Möglicherweise kommt somit FOXO1 auch eine Rolle in der Pathogenese hereditärer Lympherkrankungen zu, und könnte eine mögliche Funktion in der Therapieentwicklung sekundärer Lymphödeme einnehmen.

Acknowledgement

This work was carried out as a member of the independent research group “Angiogenesis and metabolism laboratory” at the Max-Planck-Institute for Heart and Lung research in Bad Nauheim, Germany, where I was supported by a fellowship by the DZHK. Working in this laboratory provided me an invaluable opportunity to work in a unique scientific environment and has shaped my way of thinking for my whole professional life. First, I would like to thank my advisor Prof. Michael Potente for his support and guidance. His enthusiasm for science, his motivation and kindness made him the best advisor I could have imagined. Thank you. Second, I would like to thank my supervisor Prof. Kerstin Wilhelm for entrusting me to work on her project and her constant support. You showed me what passion for science is, you taught me perseverance. Many thanks. Prof. Preissner sparked my interest in biomedical research in my first two years of medical school. Thank you for motivating me to ask, discuss and develop ideas to the complex world of angiogenesis, thank you for sharing all your experience. I would also like to thank all the PhD students, postdocs, technicians and animal care takers of the Angiogenesis and Metabolism lab and the Department 1 of the Max-Planck-Institute in Bad Nauheim, particularly Dr. Jorge Andrade, Dr. Anuradha Doddaballapur, Dr. Toshiya Sugino, Dr. Yang Zhang, Dr. Mareike Pötsch, Silke Kreher and Julian Malchow. Special thanks to Barbara Zimmermann, the heart of the angiogenesis and metabolism laboratory.

It is impossible to overestimate the importance of constant support, understanding and encouragement of my family. I am very grateful to everything I have and for their trust in my judgement for the bigger things in life. Anke, Christoph, Jakob, Jelte – you are my tower of strength, this work is dedicated to you.

Curriculum vitae

List of publications

Anne Schneider, Jannik Fasse, Dennis Tappe, Christoph Lübbert, Henning Trawinski, Case report: Dirofilarial infection of the face, IDCases, Volume 39, 2025, e02142, ISSN 2214-2509, https://doi.org/10.1016/j.idcr.2024.e02142.

Trawinski, H., Fasse, J. & Nenoff, P. Blasen am Fuß als Urlaubssouvenir. *Dermatologie* **75**, 942 (2024). https://doi.org/10.1007/s00105-024-05414-8

Fasse, J., Trawinski, H., Hardt, M. *et al.* Postexpositionsprophylaxe nach Biss einer Breitflügelfledermaus mit Nachweis des Europäischen Fledermaus-Lyssavirus 1 (EBLV-1).*Innere Medizin* **65**, 608–611 (2024). https://doi.org/10.1007/s00108-023-01638-3

Lim R, Sugino T, Nolte H, Andrade J, Zimmermann B, Shi C, Doddaballapur A, Ong YT, Wilhelm K, Fasse JWD, Ernst A, Kaulich M, Husnjak K, Boettger T, Guenther S, Braun T, Krüger M, Benedito R, Dikic I, Potente M. Deubiquitinase USP10 regulates Notch signaling in the endothelium. **Science.** 2019 Apr 12;364(6436):188-193.doi:10.1126/science.aat0778. PMID: 30975888.

List of figures

List of tables

List of abbreviations

2D	2 dimensional
3D	3 dimensional
ARMS	Alveolar rhabdomyosarcoma
BEC	Blood endothelial cell
CD31	PECAM
CDK	Cyclin-dependent kinase
CKI	Cycklin-dependent kinase inhibitors
CV	Cardinal vein
DC	Dendritic cell
E	Embryonic day
ECM	Extracellular matrix
ES	Embryonic stem cells
FH DBD	Forkhead DNA binding domain
HBSS	Hank's balanced salt solution
HDL	High-density lipoprotein
HDLEC	Human dermal lymphatic endothelial cells
HUVEC	Human umbilical vein endothelial cells
IAL	Inflammation-associated lymphangiogenesis
KEGG	Kyoto Encyclopedia of Genes and Genomes
KO	Knock out
L	Liter
LC	Lymphatic capillary
LEC	Lymphatic endothelial cell
LN	Lymph node
LV	Lymph vessel
LYVE-1	Lymphatic vessel endothelial hyaluronan receptor 1
MFE	Microvascular fluid exchange
mTOR	Mammalian target of rapamycin
NES	Nuclear export sequence
NLS	Nuclear localization sequence
P	Postnatal day
PDPN	Integral membrane glycoprotein Podoplanin
PECAM	Platelet endothelial cell adhesion molecule-1

PH domain	Pleckstrin homology domain
PTA	Peripheral tissue antigen
PTM	Posttranslational modification
RCT	Reverse cholesterol transport
SMA	Smooth muscle actin
SMC	Smooth muscle cell
SLN	Sentinel lymph node
TA	Transactivation domain
OMIM	Online mendelian Inheritance in Man

Table 22: List of abbreviations

References

1. Udan, R. S., Culver, J. C. & Dickinson, M. E. Understanding vascular development. *Wiley Interdiscip Rev Dev Biology* **2**, 327–46 (2012).

2. Potente, M. & Mäkinen, T. Vascular heterogeneity and specialization in development and disease. *Nature Reviews Molecular Cell Biology* **18**, 477–494 (2017).

3. Kukk, E. *et al.* VEGF-C receptor binding and pattern of expression with VEGFR-3 suggests a role in lymphatic vascular development. *Dev Camb Engl* **122**, 3829–37 (1996).

4. Wigle, J. T. & Oliver, G. Prox1 Function Is Required for the Development of the Murine Lymphatic System. *Cell* 1–10 (1999).

5. Breiteneder-Geleff, S. *et al.* Angiosarcomas Express Mixed Endothelial Phenotypes of Blood and Lymphatic Capillaries. *Am J Pathology* **154**, 385–394 (1999).

6. Banerji, S. *et al.* LYVE-1, a New Homologue of the CD44 Glycoprotein, Is a Lymph-specific Receptor for Hyaluronan. *J Cell Biol* **144**, 789–801 (1999).

7. Zawieja, D. C. Contractile physiology of lymphatics. *Lymphat Res Biol* **7**, 87–96 (2009).

8. Geng, X. *et al.* Multiple mouse models of primary lymphedema exhibit distinct defects in lymphovenous valve development. *Dev Biol* **409**, 218–33 (2015).

9. Aspelund, A., Robciuc, M. R., Karaman, S., Makinen, T. & Alitalo, K. Lymphatic System in Cardiovascular Medicine. *Circulation Research* **118**, 515–530 (2016).

10. Liu, X. *et al.* Lymphoangiocrine signals promote cardiac growth and repair. *Nature* **588**, 705–711 (2020).

11. Sabin, F. R. On the origin of the lymphatic system from the veins and the development of the lymph hearts and thoracic duct in the pig. *Am J Anat* **1**, 367–389 (1902).

12. Srinivasan, R. S. *et al.* Lineage tracing demonstrates the venous origin of the mammalian lymphatic vasculature. *Genes Amp Dev* **21**, 2422–2432 (2007).

13. Yang, Y. *et al.* Lymphatic endothelial progenitors bud from the cardinal vein and intersomitic vessels in mammalian embryos. *Blood* **120**, 2340–2348 (2012).

14. Hägerling, R. *et al.* A novel multistep mechanism for initial lymphangiogenesis in mouse embryos based on ultramicroscopy. *Embo J* **32**, 629–644 (2013).

15. Wilting, J. *et al.* Dual origin of avian lymphatics. *Dev Biol* **292**, 165–173 (2006).

16. Mahadevan, A. *et al.* The Left-Right Pitx2 Pathway Drives Organ-Specific Arterial and Lymphatic Development in the Intestine. *Dev Cell* **31**, 690–706 (2014).

17. Martinez-Corral, I. *et al.* Nonvenous origin of dermal lymphatic vasculature. *Circ Res* **116**, 1649–54 (2015).

18. Stanczuk, L. *et al.* cKit Lineage Hemogenic Endothelium-Derived Cells Contribute to Mesenteric Lymphatic Vessels. *Cell Reports* **10**, 1708–1721 (2015).

19. Semo, J., Nicenboim, J. & Yaniv, K. Development of the lymphatic system: new questions and paradigms. *Development* **143**, 924–935 (2016).

20. Yang, Y. & Oliver, G. Development of the mammalian lymphatic vasculature. *J Clin Invest* **124**, 888–897 (2014).

21. Harvey, N. L. *et al.* Lymphatic vascular defects promoted by Prox1 haploinsufficiency cause adult-onset obesity. *Nat Genet* **37**, 1072–1081 (2005).

22. Petrova, T. V. *et al.* Lymphatic endothelial reprogramming of vascular endothelial cells by the Prox-1 homeobox transcription factor. *The EMBO Journal* **21**, 4593–4599 (2002).

23. Hong, Y.-K. *et al.* Prox1 is a master control gene in the program specifying lymphatic endothelial cell fate. *Dev Dynam* **225**, 351–357 (2002).

24. Kim, H. *et al.* Embryonic vascular endothelial cells are malleable to reprogramming via Prox1 to a lymphatic gene signature. *Bmc Dev Biol* **10**, 72 (2010).

25. You, L.-R. *et al.* Suppression of Notch signalling by the COUP-TFII transcription factor regulates vein identity. *Nature* **435**, 98–104 (2005).

26. Bowles, J., Schepers, G. & Koopman, P. Phylogeny of the SOX Family of Developmental Transcription Factors Based on Sequence and Structural Indicators. *Dev Biol* **227**, 239–255 (2000).

27. Irrthum, A. *et al.* Mutations in the Transcription Factor Gene SOX18 Underlie Recessive and Dominant Forms of Hypotrichosis-Lymphedema-Telangiectasia. *Am J Hum Genetics* **72**, 1470–1478 (2003).

28. Srinivasan, R. S. *et al.* The nuclear hormone receptor Coup-TFII is required for the initiation and early maintenance of Prox1 expression in lymphatic endothelial cells. *Gene Dev* **24**, 696–707 (2010).

29. François, M. *et al.* Sox18 induces development of the lymphatic vasculature in mice. *Nature* **456**, 643–647 (2008).

30. Zheng, W. *et al.* Notch restricts lymphatic vessel sprouting induced by vascular endothelial growth factor. *Blood* **118**, 1154–1162 (2011).

31. Kang, J. *et al.* An exquisite cross-control mechanism among endothelial cell fate regulators directs the plasticity and heterogeneity of lymphatic endothelial cells. *Blood* **116**, 140–150 (2010).

32. Murtomaki, A. *et al.* Notch1 functions as a negative regulator of lymphatic endothelial cell differentiation in the venous endothelium. *Development* **140**, 2365–2376 (2013).

33. Karkkainen, M. J. *et al.* Vascular endothelial growth factor C is required for sprouting of the first lymphatic vessels from embryonic veins. *Nature Immunology* **5**, 74–80 (2003).

34. Yao, L.-C., Baluk, P., Srinivasan, R. S., Oliver, G. & McDonald, D. M. Plasticity of Button-Like Junctions in the Endothelium of Airway Lymphatics in Development and Inflammation. *Am J Pathology* **180**, 2561–2575 (2012).

35. Jeltsch, M. *et al.* Hyperplasia of Lymphatic Vessels in VEGF-C Transgenic Mice. *Science* **276**, 1423–1425 (1997).

36. Srinivasan, R. S. *et al.* The Prox1–Vegfr3 feedback loop maintains the identity and the number of lymphatic endothelial cell progenitors. *Genes & Development* **28**, 2175–2187 (2014).

37. Wigle, J. T. *et al.* An essential role for Prox1 in the induction of the lymphatic endothelial cell phenotype. *Embo J* **21**, 1505–1513 (2002).

38. Srinivasan, R. S. & Oliver, G. Prox1 dosage controls the number of lymphatic endothelial cell progenitors and the formation of the lymphovenous valves. *Genes & Development* **25**, 2187–2197 (2011).

39. Karpanen, T. *et al.* Functional interaction of VEGF-C and VEGF-D with neuropilin receptors. *Faseb J* **20**, 1462–1472 (2006).

40. Xu, Y. *et al.* Neuropilin-2 mediates VEGF-C–induced lymphatic sprouting together with VEGFR3. *J Cell Biology* **188**, 115–130 (2010).

41. Bos, F. L. *et al.* CCBE1 Is Essential for Mammalian Lymphatic Vascular Development and Enhances the Lymphangiogenic Effect of Vascular Endothelial Growth Factor-C In Vivo. *Circ Res* **109**, 486–491 (2011).

42. Hogan, B. M. *et al.* Ccbe1 is required for embryonic lymphangiogenesis and venous sprouting. *Nat Genet* **41**, 396–8 (2009).

43. Kulkarni, R. M., Greenberg, J. M. & Akeson, A. L. NFATc1 regulates lymphatic endothelial development. *Mechanisms of Development* **126**, 350–365 (2009).

44. Lim, K.-C. *et al.* Conditional Gata2 inactivation results in HSC loss and lymphatic mispatterning. *J Clin Invest* **122**, 3705–3717 (2012).

45. Frye, M. *et al.* Matrix stiffness controls lymphatic vessel formation through regulation of a GATA2- dependent transcriptional program. *Nature Communications* **9**, 1–16 (2018).

46. Trzewik, J., Mallipattu, S. K., Artmann, G. M., Delano, F. A. & Schmid-Schonbein, G. W. Evidence for a second valve system in lymphatics: endothelial microvalves. *Faseb J* **15**, 1711–1717 (2001).

47. Baluk, P. *et al.* Functionally specialized junctions between endothelial cells of lymphatic vessels. *J Exp Medicine* **204**, 2349–2362 (2007).

48. Leak, L. V. & Burke, J. F. Ultrastructural studies on the lymphatic anchoring filaments. *J Cell Biology* **36**, 129–149 (1968).

49. Lim, H. Y. *et al.* Lymphatic Vessels Are Essential for the Removal of Cholesterol from Peripheral Tissues by SR-BI-Mediated Transport of HDL. *Cell Metab* **17**, 671–684 (2013).

50. Wiig, H. & Swartz, M. A. Interstitial fluid and lymph formation and transport: physiological regulation and roles in inflammation and cancer. *Physiol Rev* **92**, 1005–60 (2012).

51. Norrmén, C. *et al.* FOXC2 controls formation and maturation of lymphatic collecting vessels through cooperation with NFATc1. *The Journal of Cell Biology* **185**, 439–457 (2009).

52. Sabine, A. *et al.* Mechanotransduction, PROX1, and FOXC2 Cooperate to Control Connexin37 and Calcineurin during Lymphatic-Valve Formation. *Developmental Cell* **22**, 430–445 (2012).

53. Petrova, T. V. *et al.* Defective valves and abnormal mural cell recruitment underlie lymphatic vascular failure in lymphedema distichiasis. *Nature Medicine* **10**, 974–981 (2004).

54. Fang, J. *et al.* Mutations in FOXC2 (MFH-1), a Forkhead Family Transcription Factor, Are Responsible for the Hereditary Lymphedema-Distichiasis Syndrome. *Am J Hum Genetics* **67**, 1382–1388 (2000).

55. Brice, G. *et al.* Analysis of the phenotypic abnormalities in lymphoedema-distichiasis syndrome in 74 patients with FOXC2 mutations or linkage to 16q24. *J Med Genet* **39**, 478–483 (2002).

56. Ranger, A. M. *et al.* The transcription factor NF-ATc is essential for cardiac valve formation. *Nature* **392**, 186–190 (1998).

57. Kanady, J. D., Dellinger, M. T., Munger, S. J., Witte, M. H. & Simon, A. M. Connexin37 and Connexin43 deficiencies in mice disrupt lymphatic valve development and result in lymphatic disorders including lymphedema and chylothorax. *Dev Biol* **354**, 253–266 (2011).

58. Lutter, S., Xie, S., Tatin, F. & Mäkinen, T. Smooth muscle–endothelial cell communication activates Reelin signaling and regulates lymphatic vessel formation. *The Journal of Cell Biology* **197**, 837–849 (2012).

59. Hynes, R. O. Integrins. *Cell* **110**, 673–687 (2002).

60. Huang, X. Z. *et al.* Fatal Bilateral Chylothorax in Mice Lacking the Integrin α9β1. *Mol Cell Biol* **20**, 5208–5215 (2000).

61. Mishima, K. *et al.* Prox1 Induces Lymphatic Endothelial Differentiation via Integrin α9 and Other Signaling Cascades. *Mol Biol Cell* **18**, 1421–1429 (2007).

62. Zhang, X., Groopman, J. E. & Wang, J. F. Extracellular matrix regulates endothelial functions through interaction of VEGFR-3 and integrin ?5?1. *J Cell Physiol* **202**, 205–214 (2004).

63. Dietrich, T. *et al.* Inhibition of Inflammatory Lymphangiogenesis by Integrin α5 Blockade. *Am J Pathology* **171**, 361–372 (2007).

64. Okazaki, T. *et al.* α5β1 Integrin Blockade Inhibits Lymphangiogenesis in Airway Inflammation. *Am J Pathology* **174**, 2378–2387 (2009).

65. Planas-Paz, L. *et al.* Mechanoinduction of lymph vessel expansion. *The EMBO Journal* **31**, 788–804 (2011).

66. Bazigou, E. *et al.* Integrin-α9 Is Required for Fibronectin Matrix Assembly during Lymphatic Valve Morphogenesis. *Dev Cell* **17**, 175–186 (2009).

67. Oliver, G., Kipnis, J., Randolph, G. J. & Harvey, N. L. The Lymphatic Vasculature in the 21st Century: Novel Functional Roles in Homeostasis and Disease. *Cell* **182**, 270–296 (2020).

68. Levick, J. R. & Michel, C. C. Microvascular fluid exchange and the revised Starling principle. *Cardiovasc Res* **87**, 198–210 (2010).

69. Starling, E. H. On the Absorption of Fluids from the Connective Tissue Spaces. *J Physiology* **19**, 312–326 (1896).

70. Renkin, E. M. Some consequences of capillary permeability to macromolecules: Starling's hypothesis reconsidered. *Am J Physiol-heart C* **250**, H706–H710 (1986).

71. Bernier-Latmani, J. *et al.* DLL4 promotes continuous adult intestinal lacteal regeneration and dietary fat transport. *J Clin Investigation* **125**, 4572–86 (2015).

72. Dixon, J. B. Lymphatic lipid transport: sewer or subway? *Trends Endocrinol Metabolism Tem* **21**, 480–7 (2010).

73. Choe, K. *et al.* Intravital imaging of intestinal lacteals unveils lipid drainage through contractility. *J Clin Investigation* **125**, 4042–52 (2015).

74. Porter, C. J. H., Trevaskis, N. L. & Charman, W. N. Lipids and lipid-based formulations: optimizing the oral delivery of lipophilic drugs. *Nat Rev Drug Discov* **6**, 231–248 (2007).

75. Card, C. M., Yu, S. S. & Swartz, M. A. Emerging roles of lymphatic endothelium in regulating adaptive immunity. *J Clin Investigation* **124**, 943–52 (2014).

76. Förster, R., Davalos-Misslitz, A. C. & Rot, A. CCR7 and its ligands: balancing immunity and tolerance. *Nat Rev Immunol* **8**, 362–371 (2008).

77. Thomas, S. N. *et al.* Impaired humoral immunity and tolerance in K14-VEGFR-3-Ig mice that lack dermal lymphatic drainage. *J Immunol Baltim Md 1950* **189**, 2181–90 (2012).

78. Takeda, A. *et al.* Single-Cell Survey of Human Lymphatics Unveils Marked Endothelial Cell Heterogeneity and Mechanisms of Homing for Neutrophils. *Immunity* **51**, 561-572.e5 (2019).

79. Jalkanen, S. & Salmi, M. Lymphatic endothelial cells of the lymph node. *Nat Rev Immunol* 1–13 (2020) doi:10.1038/s41577-020-0281-x.

80. Rantakari, P. *et al.* The endothelial protein PLVAP in lymphatics controls the entry of lymphocytes and antigens into lymph nodes. *Nat Immunol* **16**, 386–396 (2015).

81. Forkert, P.-G., Thliveris, J. A. & Bertalanffy, F. D. Structure of sinuses in the human lymph node. *Cell Tissue Res* **183**, 115–130 (1977).

82. Cohen, J. N. *et al.* Lymph node-resident lymphatic endothelial cells mediate peripheral tolerance via Aire-independent direct antigen presentation. *J Exp Medicine* **207**, 681–8 (2010).

83. Tewalt, E. F. *et al.* Lymphatic endothelial cells induce tolerance via PD-L1 and lack of costimulation leading to high-level PD-1 expression on CD8 T cells. *Blood* **120**, 4772–82 (2012).

84. Rouhani, S. J. *et al.* Roles of lymphatic endothelial cells expressing peripheral tissue antigens in CD4 T-cell tolerance induction. *Nat Commun* **6**, 6771 (2015).

85. Brouillard, P., Boon, L. & Vikkula, M. Genetics of lymphatic anomalies. *J Clin Investigation* **124**, 898–904 (2014).

86. Karkkainen, M. J. *et al.* A model for gene therapy of human hereditary lymphedema. *Proc National Acad Sci* **98**, 12677–12682 (2001).

87. Dellinger, M. T., Hunter, R. J., Bernas, M. J., Witte, M. H. & Erickson, R. P. Chy - 3 mice are Vegfc haploinsufficient and exhibit defective dermal superficial to deep lymphatic transition and dermal lymphatic hypoplasia. *Dev Dynam* **236**, 2346–2355 (2007).

88. Gale, N. W. *et al.* Angiopoietin-2 Is Required for Postnatal Angiogenesis and Lymphatic Patterning, and Only the Latter Role Is Rescued by Angiopoietin-1. *Dev Cell* **3**, 411–423 (2002).

89. Mendola, A. *et al.* Mutations in the VEGFR3 Signaling Pathway Explain 36% of Familial Lymphedema. *Mol Syndromol* **4**, 257–266 (2013).

90. Connell, F. *et al.* The classification and diagnostic algorithm for primary lymphatic dysplasia: an update from 2010 to include molecular findings: The classification and diagnostic algorithm for primary lymphatic dysplasia. *Clin Genet* **84**, 303–314 (2013).

91. Carver, C. *et al.* Three children with Milroy disease and de novo mutations in VEGFR3. *Clin Genet* **71**, 187–189 (2007).

92. Ghalamkarpour, A. *et al.* Recessive primary congenital lymphoedema caused by a VEGFR3 mutation. *J Med Genet* **46**, 399–404 (2009).

93. Ghalamkarpour, A. *et al.* Sporadic In Utero Generalized Edema Caused by Mutations in the Lymphangiogenic Genes VEGFR3 and FOXC2. *J Pediatrics* **155**, 90–93 (2009).

94. Ghalamkarpour, A. *et al.* Hereditary lymphedema type I associated with VEGFR3 mutation: the first de novo case and atypical presentations. *Clin Genet* **70**, 330–335 (2006).

95. Irrthum, A., Karkkainen, M. J., Devriendt, K., Alitalo, K. & Vikkula, M. Congenital Hereditary Lymphedema Caused by a Mutation That Inactivates VEGFR3 Tyrosine Kinase. *Am J Hum Genetics* **67**, 295–301 (2000).

96. Karkkainen, M. J. *et al.* Missense mutations interfere with VEGFR-3 signalling in primary lymphoedema. *Nat Genet* **25**, 153–159 (2000).

97. Gordon, K. *et al.* Mutation in Vascular Endothelial Growth Factor-C, a Ligand for Vascular Endothelial Growth Factor Receptor-3, Is Associated With Autosomal Dominant Milroy-Like Primary Lymphedema. *Circ Res* **112**, 956–960 (2013).

98. Alders, M. *et al.* Evaluation of Clinical Manifestations in Patients with Severe Lymphedema with and without CCBE1 Mutations. *Mol Syndromol* **4**, 107–13 (2012).

99. Consortium, L. *et al.* Linkage and sequence analysis indicate that CCBE1 is mutated in recessively inherited generalised lymphatic dysplasia. *Hum Genet* **127**, 231–241 (2009).

100. Au, A. C. *et al.* Protein Tyrosine Phosphatase PTPN14 Is a Regulator of Lymphatic Function and Choanal Development in Humans. *Am J Hum Genetics* **87**, 436–444 (2010).

101. Ferrell, R. E. *et al.* GJC2 missense mutations cause human lymphedema. *Am J Hum Genet* **86**, 943–8 (2010).

102. Ostergaard, P. *et al.* Rapid identification of mutations in GJC2 in primary lymphoedema using whole exome sequencing combined with linkage analysis with delineation of the phenotype. *J Med Genet* **48**, 251–5 (2011).

103. Brice, G. *et al.* A novel mutation in GJA1 causing oculodentodigital syndrome and primary lymphoedema in a three generation family: A novel mutation in GJA1. *Clin Genet* **84**, 378–381 (2013).

104. Fotiou, E. *et al.* Novel mutations in PIEZO1 cause an autosomal recessive generalized lymphatic dysplasia with non-immune hydrops fetalis. *Nat Commun* **6**, 8085 (2015).

105. Du, J. *et al.* The mechanosensory channel PIEZO1 functions upstream of angiopoietin/TIE/FOXO1 signaling in lymphatic development. *J. Clin. Investig.* **134**, e176577 (2024).

106. Hosking, B. *et al.* Sox7 and Sox17 are strain-specific modifiers of the lymphangiogenic defects caused by Sox18 dysfunction in mice. *Dev Camb Engl* **136**, 2385–91 (2009).

107. Rockson, S. G. & Rivera, K. K. Estimating the Population Burden of Lymphedema. *Ann Ny Acad Sci* **1131**, 147–154 (2008).

108. Pfarr, K. M., Debrah, A. Y., Specht, S. & Hoerauf, A. Filariasis and lymphoedema. *Parasite Immunol* **31**, 664–72 (2009).

109. Karpanen, T. & Alitalo, K. Molecular Biology and Pathology of Lymphangiogenesis. *Annual Review of Pathology: Mechanisms of Disease* **3**, 367–397 (2008).

110. Dreyer, G., Norões, J., Figueredo-Silva, J. & Piessens, W. F. Pathogenesis of Lymphatic Disease in Bancroftian Filariasis: *Parasitol Today* **16**, 544–548 (2000).

111. Petrek, J. A. & Heelan, M. C. Incidence of breast carcinoma-related lymphedema. *Cancer* **83**, 2776–81 (1998).

112. Finegold, D. N. *et al.* Connexin 47 mutations increase risk for secondary lymphedema following breast cancer treatment. *Clin Cancer Res Official J Am Assoc Cancer Res* **18**, 2382–90 (2012).

113. Ayele, F. T. *et al.* HLA class II locus and susceptibility to podoconiosis. *New Engl J Medicine* **366**, 1200–8 (2012).

114. Becker, C., Assouad, J., Riquet, M. & Hidden, G. Postmastectomy Lymphedema. *Ann Surg* **243**, 313–315 (2006).

115. Tammela, T. *et al.* Therapeutic differentiation and maturation of lymphatic vessels after lymph node dissection and transplantation. *Nat Med* **13**, 1458–1466 (2007).

116. Medzhitov, R. Inflammation 2010: new adventures of an old flame. *Cell* **140**, 771–6 (2010).

117. Hansson, G. K., Libby, P. & Tabas, I. Inflammation and plaque vulnerability. *J Intern Med* **278**, 483–93 (2015).

118. Kim, H., Kataru, R. P. & Koh, G. Y. Inflammation-associated lymphangiogenesis: a double-edged sword? *J Clin Investigation* **124**, 936–42 (2014).

119. Baluk, P. *et al.* Pathogenesis of persistent lymphatic vessel hyperplasia in chronic airway inflammation. *J Clin Invest* **115**, 247–257 (2005).

120. Kang, S. *et al.* Toll-like receptor 4 in lymphatic endothelial cells contributes to LPS-induced lymphangiogenesis by chemotactic recruitment of macrophages. *Blood* **113**, 2605–13 (2008).

121. Guo, R. *et al.* Inhibition of lymphangiogenesis and lymphatic drainage via vascular endothelial growth factor receptor 3 blockade increases the severity of inflammation in a mouse model of chronic inflammatory arthritis. *Arthritis Rheum* **60**, 2666–76 (2009).

122. Huggenberger, R. *et al.* Stimulation of lymphangiogenesis via VEGFR-3 inhibits chronic skin inflammation. *J Exp Medicine* **207**, 2255–69 (2010).

123. Kajiya, K. & Detmar, M. An Important Role of Lymphatic Vessels in the Control of UVB-Induced Edema Formation and Inflammation. *J Invest Dermatol* **126**, 920–922 (2006).

124. Baluk, P. *et al.* Pathogenesis of persistent lymphatic vessel hyperplasia in chronic airway inflammation. *J Clin Invest* **115**, 247–257 (2005).

125. Kerjaschki, D. *et al.* Lymphatic Neoangiogenesis in Human Kidney Transplants Is Associated with Immunologically Active Lymphocytic Infiltrates. *J Am Soc Nephrol* **15**, 603–612 (2004).

126. Yin, N. *et al.* Targeting Lymphangiogenesis After Islet Transplantation Prolongs Islet Allograft Survival. *Transplantation* **92**, 25–30 (2011).

127. Nykänen, A. I. *et al.* Targeting lymphatic vessel activation and CCL21 production by vascular endothelial growth factor receptor-3 inhibition has novel immunomodulatory and antiarteriosclerotic effects in cardiac allografts. *Circulation* **121**, 1413–22 (2010).

128. Dillekås, H., Rogers, M. S. & Straume, O. Are 90% of deaths from cancer caused by metastases? *Cancer Med-us* **8**, 5574–5576 (2019).

129. Alitalo, K. The lymphatic vasculature in disease. *Nature Medicine* **17**, 1371–1380 (2011).

130. Karaman, S. & Detmar, M. Mechanisms of lymphatic metastasis. *J Clin Investigation* **124**, 922–8 (2014).

131. Fukumura, D., Duda, D. G., Munn, L. L. & Jain, R. K. Tumor microvasculature and microenvironment: novel insights through intravital imaging in pre-clinical models. *Microcirc New York N Y 1994* **17**, 206–25 (2010).

132. Müller, A. *et al.* Involvement of chemokine receptors in breast cancer metastasis. *Nature* **410**, 50–56 (2001).

133. Shields, J. D., Kourtis, I. C., Tomei, A. A., Roberts, J. M. & Swartz, M. A. Induction of lymphoidlike stroma and immune escape by tumors that express the chemokine CCL21. *Sci New York N Y* **328**, 749–52 (2010).

134. Kim, M. *et al.* CXCR4 signaling regulates metastasis of chemoresistant melanoma cells by a lymphatic metastatic niche. *Cancer Res* **70**, 10411–21 (2010).

135. Beasley, N. J. P. *et al.* Intratumoral lymphangiogenesis and lymph node metastasis in head and neck cancer. *Cancer Res* **62**, 1315–20 (2002).

136. Dadras, S. S. *et al.* Tumor Lymphangiogenesis - A Novel Prognostic Indicator for Cutaneous Melanoma Metastasis and Survival. *Am J Pathology* **162**, 1951–1960 (2003).

137. Boer, M. de, Dijck, J. A. A. M. van, Bult, P., Borm, G. F. & Tjan-Heijnen, V. C. G. Breast Cancer Prognosis and Occult Lymph Node Metastases, Isolated Tumor Cells, and Micrometastases. *Jnci J National Cancer Inst* **102**, 410–425 (2010).

138. Alitalo, K., Tammela, T. & Petrova, T. V. Lymphangiogenesis in development and human disease. *Nature* **438**, 946–953 (2005).

139. Lim, S. S. *et al.* A comparative risk assessment of burden of disease and injury attributable to 67 risk factors and risk factor clusters in 21 regions, 1990-2010: a systematic analysis for the Global Burden of Disease Study 2010. *Lancet Lond Engl* **380**, 2224–60 (2012).

140. Machnik, A. *et al.* Macrophages regulate salt-dependent volume and blood pressure by a vascular endothelial growth factor-C-dependent buffering mechanism. *Nat Med* **15**, 545–52 (2009).

141. Duewell, P. *et al.* NLRP3 inflammasomes are required for atherogenesis and activated by cholesterol crystals. *Nature* **464**, 1357–61 (2010).

142. Small, D. M., Bond, M. G., Waugh, D., Prack, M. & Sawyer, J. K. Physicochemical and histological changes in the arterial wall of nonhuman primates during progression and regression of atherosclerosis. *J Clin Invest* **73**, 1590–1605 (1984).

143. Martel, C. *et al.* Lymphatic vasculature mediates macrophage reverse cholesterol transport in mice. *J Clin Investigation* **123**, 1571–9 (2013).

144. Brakenhielm, E. & Alitalo, K. Cardiac lymphatics in health and disease. *Nature Reviews Cardiology* 1–13 (2018) doi:10.1038/s41569-018-0087-8.

145. Eijkelenboom, A. & Burgering, B. M. T. FOXOs: signalling integrators for homeostasis maintenance. *Nature Reviews Molecular Cell Biology* **14**, 83–97 (2013).

146. Wilhelm, K. *et al.* FOXO1 couples metabolic activity and growth state in the vascular endothelium. *Nature* **529**, 216–220 (2016).

147. Furuyama, T., Nakazawa, T., Nakano, I. & Mori, N. Identification of the differential distribution patterns of mRNAs and consensus binding sequences for mouse DAF-16 homologues. *Biochem J.* 629–634 (2000).

148. Lam, E. W.-F., Brosens, J. J., Gomes, A. R. & Koo, C.-Y. Forkhead box proteins: tuning forks for transcriptional harmony. *Nature Reviews Cancer* **13**, 1–14 (2013).

149. Kaestner, K. H., Knöchel, W. & Martinez, D. E. Unified nomenclature for the winged helix/forkhead transcription factors. *Genes & Development* **14**, 142–146 (2000).

150. Burgering, B. M. T. A brief introduction to FOXOlogy. *Oncogene* **27**, 2258–2262 (2008).

151. Fu, Z. & Tindall, D. J. FOXOs, cancer and regulation of apoptosis. *Oncogene* **27**, 2312–2319 (2008).

152. Furuyama, T. *et al.* Abnormal Angiogenesis inFoxo1(Fkhr)-deficient Mice. *J Biol Chem* **279**, 34741–34749 (2004).

153. Hosaka, T. *et al.* Disruption of forkhead transcription factor (FOXO) family members in mice reveals their functional diversification. *Proc National Acad Sci* **101**, 2975–2980 (2004).

154. Castrillon, D. H., Miao, L., Kollipara, R., Horner, J. W. & DePinho, R. A. Suppression of Ovarian Follicle Activation in Mice by the Transcription Factor Foxo3a. *Science* **301**, 215–218 (2003).

155. Paik, J.-H. *et al.* FoxOs Are Lineage-Restricted Redundant Tumor Suppressors and Regulate Endothelial Cell Homeostasis. *Cell* **128**, 309–323 (2007).

156. Ho, K. K., Myatt, S. S. & Lam, E. W. F. Many forks in the path: cycling with FoxO. *Oncogene* **27**, 2300–2311 (2008).

157. Bracken, A. P., Ciro, M., Cocito, A. & Helin, K. E2F target genes: unraveling the biology. *Trends in Biochemical Sciences* **29**, 409–417 (2004).

158. Alvarez, B., Martínez-A, C., Burgering, B. M. T. & Carrera, A. C. Forkhead transcription factors contribute to execution of the mitotic programme in mammals. *Nature* **413**, 744–747 (2001).

159. Medema, R. H., Kops, G. J. P. L., Bos, J. L. & Burgering, B. M. T. AFX-like Forkhead transcription factors mediate cell-cycle regulation by Ras and PKB through p27kip1. *Nature* **404**, 782–787 (2000).

160. Katayama, K., Nakamura, A., Sugimoto, Y., Tsuruo, T. & Fujita, N. FOXO transcription factor-dependent p15(INK4b) and p19(INK4d) expression. *Oncogene* **27**, 1677–86 (2007).

161. Gomis, R. R. *et al.* A FoxO-Smad synexpression group in human keratinocytes. *Proc National Acad Sci* **103**, 12747–12752 (2006).

162. Seoane, J., Le, H.-V., Shen, L., Anderson, S. A. & Massagué, J. Integration of Smad and Forkhead Pathways in the Control of Neuroepithelial and Glioblastoma Cell Proliferation. *Cell* **117**, 211–223 (2004).

163. Keizer, P. L. J. de *et al.* Activation of forkhead box O transcription factors by oncogenic BRAF promotes p21cip1-dependent senescence. *Cancer Res* **70**, 8526–36 (2010).

164. Mattos, S. F. de *et al.* FoxO3a and BCR-ABL Regulate cyclin D2 Transcription through a STAT5/BCL6-Dependent Mechanism. *Mol Cell Biol* **24**, 10058–10071 (2004).

165. Bandara, L. R. *et al.* DP-1: a cell cycle-regulated and phosphorylated component of transcription factor DRTF1/E2F which is functionally important for recognition by pRb and the adenovirus E4 orf 6/7 protein. *Embo J* **13**, 3104–14 (1994).

166. Löbrich, M. & Jeggo, P. A. The impact of a negligent G2/M checkpoint on genomic instability and cancer induction. *Nat Rev Cancer* **7**, 861–869 (2007).

167. Takano, M. *et al.* Transcriptional Cross Talk between the Forkhead Transcription Factor Forkhead Box O1A and the Progesterone Receptor Coordinates Cell Cycle Regulation and Differentiation in Human Endometrial Stromal Cells. *Mol Endocrinol* **21**, 2334–2349 (2007).

168. Martínez-Gac, L., Marqués, M., García, Z., Campanero, M. R. & Carrera, A. C. Control of Cyclin G2 mRNA Expression by Forkhead Transcription Factors: Novel Mechanism for Cell Cycle Control by Phosphoinositide 3-Kinase and Forkhead. *Mol Cell Biol* **24**, 2181–2189 (2004).

169. Tran, H. *et al.* DNA Repair Pathway Stimulated by the Forkhead Transcription Factor FOXO3a Through the Gadd45 Protein. *Science* **296**, 530–534 (2002).

170. Tang, T. T.-L. *et al.* The Forkhead Transcription Factor AFX Activates Apoptosis by Induction of the BCL-6 Transcriptional Repressor. *J Biol Chem* **277**, 14255–14265 (2002).

171. Wang, X., Kiyokawa, H., Dennewitz, M. B. & Costa, R. H. The Forkhead Box m1b transcription factor is essential for hepatocyte DNA replication and mitosis during mouse liver regeneration. *Proc National Acad Sci* **99**, 16881–16886 (2002).

172. Delpuech, O. *et al.* Induction of Mxi1-SRα by FOXO3a Contributes to Repression of Myc-Dependent Gene Expression. *Mol Cell Biol* **27**, 4917–4930 (2007).

173. Chen, C.-C. *et al.* FoxOs Inhibit mTORC1 and Activate Akt by Inducing the Expression of Sestrin3 and Rictor. *Developmental Cell* **18**, 592–604 (2010).

174. Saxton, R. A. & Sabatini, D. M. mTOR Signaling in Growth, Metabolism, and Disease. *Cell* **168**, 960–976 (2017).

175. Düvel, K. *et al.* Activation of a Metabolic Gene Regulatory Network Downstream of mTOR Complex 1. *Mol Cell* **39**, 171–183 (2010).

176. Bhaskar, P. T. & Hay, N. The Two TORCs and Akt. *Developmental Cell* **12**, 487–502 (2007).

177. Huang, J. & Manning, B. D. The TSC1–TSC2 complex: a molecular switchboard controlling cell growth. *Biochem J* **412**, 179–190 (2008).

178. Hay, N. Interplay between FOXO, TOR, and Akt. *BBA - Molecular Cell Research* **1813**, 1965–1970 (2011).

179. Birkenkamp, K. U. *et al.* FOXO3a Induces Differentiation of Bcr-Abl-transformed Cells through Transcriptional Down-regulation of Id1. *J Biol Chem* **282**, 2211–2220 (2006).

180. Essers, M. A. G. *et al.* FOXO transcription factor activation by oxidative stress mediated by the small GTPase Ral and JNK. *The EMBO Journal* **23**, 4802–4812 (2004).

181. Kops, G. J. P. L. *et al.* Forkhead transcription factor FOXO3a protects quiescent cells from oxidative stress. *Nature* **419**, 316–321 (2002).

182. Marinkovic, D. *et al.* Foxo3 is required for the regulation of oxidative stress in erythropoiesis. *J Clin Invest* **117**, 2133–2144 (2007).

183. Nemoto, S. & Finkel, T. Redox Regulation of Forkhead Proteins Through a p66shc-Dependent Signaling Pathway. *Science* **295**, 2450–2452 (2002).

184. Chiribau, C. B. *et al.* FOXO3A regulates peroxiredoxin III expression in human cardiac fibroblasts. *J Biological Chem* **283**, 8211–7 (2008).

185. Olmos, Y. *et al.* SirT1 regulation of antioxidant genes is dependent on the formation of a FoxO3a/PGC-1α complex. *Antioxid Redox Sign* **19**, 1507–21 (2013).

186. Horst, A. van der & Burgering, B. M. T. Stressing the role of FoxO proteins in lifespan and disease. *Nature Reviews Molecular Cell Biology* **8**, 440–450 (2007).

187. Brunet, A. *et al.* Akt Promotes Cell survival by phosphorylating and Inhibiting a Forkhead Transcription Factor. *Cell* **96**, 857–868 (1999).

188. Brunet, A. *et al.* Stress-Dependent Regulation of FOXO Transcription Factors by the SIRT1 Deacetylase. *Science* **303**, 2011–2015 (2004).

189. Modur, V., Nagarajan, R., Evers, B. M. & Milbrandt, J. FOXO Proteins Regulate Tumor Necrosis Factor-related Apoptosis Inducing Ligand Expression: Implications for PTEN mutation in prostate cancer. *J Biol Chem* **277**, 47928–47937 (2002).

190. Gilley, J., Coffer, P. J. & Ham, J. FOXO transcription factors directly activate bim gene expression and promote apoptosis in sympathetic neurons. *J Cell Biology* **162**, 613–622 (2003).

191. Dijkers, P. F., Medema†, R. H., Lammers, J.-W. J., Koenderman, L. & Coffer, P. J. Expression of the pro-apoptotic Bcl-2 family member Bim is regulated by the forkhead transcription factor FKHR-L1. *Curr Biol* **10**, 1201–1204 (2000).

192. Stahl, M. *et al.* The forkhead transcription factor FoxO regulates transcription of p27Kip1 and Bim in response to IL-2. *J Immunol Baltim Md 1950* **168**, 5024–31 (2002).

193. Sunters, A. *et al.* FoxO3a Transcriptional Regulation of Bim Controls Apoptosis in Paclitaxel-treated Breast Cancer Cell Lines. *J Biol Chem* **278**, 49795–49805 (2003).

194. Cantley, L. C. The Phosphoinositide 3-Kinase Pathway. *Science* **296**, 1655–1657 (2002).

195. Hawkins, P. T., Anderson, K. E., Davidson, K. & Stephens, L. R. Signalling through Class I PI3Ks in mammalian cells. *Biochem Soc T* **34**, 647–662 (2006).

196. Vanhaesebroeck, B., Guillermet-Guibert, J., Graupera, M. & Bilanges, B. The emerging mechanisms of isoform-specific PI3K signalling. *Nat Rev Mol Cell Bio* **11**, 329–341 (2010).

197. Oellerich, M. F. & Potente, M. FOXOs and Sirtuins in Vascular Growth, Maintenance, and Aging. *Circulation Research* **110**, 1238–1251 (2012).

198. Datta, S. R., Brunet, A. & Greenberg, M. E. Cellular survival: a play in three Akts. *Genes & Development* **13**, 2905–2926 (1999).

199. Vivanco, I. & Sawyers, C. L. The phosphatidylinositol 3-Kinase–AKT pathway in human cancer. *Nature reviews. Cancer* **2**, 489–501 (2002).

200. Alessi, D. *et al.* Mechanism of activation of protein kinase B by insulin and IGF-1. *The EMBO Journal* **15**, 6541–6551 (1996).

201. Kops, G. J. P. L. *et al.* Direct control of the Forkhead transcription factor AFX by protein kinase B. *Nature* **398**, 630–634 (1999).

202. Nakae, J., Park, B.-C. & Accili, D. Insulin Stimulates Phosphorylation of the Forkhead Transcription Factor FKHR on Serine 253 through a Wortmannin-sensitive Pathway. *The journal of biological chemistry* **274**, 15982–15985 (1999).

203. Rena, G., Guo, S., Cichy, S. C., Unterman, T. G. & Cohen, P. Phosphorylation of the Transcription Factor Forkhead Family Member FKHR by Protein Kinase B*. *The journal of biological chemistry* **274**, 17179–17183 (1999).

204. Takaishi, H. *et al.* Regulation of nuclear translocation of Forkhead transcription factor AFX by protein kinase B. *Proc. Natl. Acad. Sci.* **96**, 11836–11841 (1999).

205. Muslin, A. J., Tanner, J. W., Allen, P. M. & Shaw, A. S. Interaction of 14-3-3 with signaling Proteins is mediated by the Recognition of Phosphoserine. *Cell* **84**, 889–897 (1996).

206. Fu, H., Subramanian, R. R. & Masters, S. C. 14-3-3 Proteins: Structure, Function, and Regulation. *Annual Review of Pharmacology and Toxology* **40**, 617–647 (2000).

207. Aitken, A. 14-3-3 proteins: A historic overview. *Seminars in Cancer Biology* **16**, 162–172 (2006).

208. Biggs, W. H., Meisenhelder, J., Hunter, T., Cavenne, W. K. & Arden, K. C. Protein kinase B/Akt-mediated phosphorylation promotes nuclear exclusion of the winged helix transcription factor FKHR1. *Proc. Natl. Acad. Sci.* **96**, 7421–7426 (1999).

209. Brunet, A. *et al.* 14-3-3 transits to the nucleus and participates in dynamic nucleocytoplasmic transport. *The Journal of Cell Biology* **156**, 817–828 (2002).

210. Tang, E. D., Nunez, G., Barr, F. G. & Guan, K.-L. Negative Regulation of the Forkhead Transcription Factor FKHR by Akt*. *The journal of biological chemistry* **274**, 16741–16746 (1999).

211. Huang, H. *et al.* Skp2 inhibits FOXO1 in tumor suppression through ubiquitin-mediated degradation. *Proc. Natl. Acad. Sci.* **102**, 1649–1654 (2005).

212. Wang, F. *et al.* Deacetylation of FOXO3 by SIRT1 or SIRT2 leads to Skp2-mediated FOXO3 ubiquitination and degradation. *Oncogene* **31**, 1546–1557 (2012).

213. Wang, Y.-Q. *et al.* SIRT1 Protects Against Oxidative Stress-Induced Endothelial Progenitor Cells Apoptosis by Inhibiting FOXO3a via FOXO3a Ubiquitination and Degradation. *Journal of Cellular Physiology* **230**, 2098–2107 (2015).

214. Clément, S. *et al.* The lipid phosphatase SHIP2 controls insulin sensitivity. *Nature* **409**, 92–97 (2001).

215. Maehama, T. & Dixon, J. E. PTEN: a tumour suppressor that functions as a phospholipid phosphatase. *Trends Cell Biol* **9**, 125–128 (1999).

216. Yuan, T. L. *et al.* Class 1A PI3K regulates vessel integrity during development and tumorigenesis. *P Natl Acad Sci Usa* **105**, 9739–44 (2008).

217. Graupera, M. *et al.* Angiogenesis selectively requires the p110α isoform of PI3K to control endothelial cell migration. *Nature* **453**, 662–666 (2008).

218. Zhou, F. *et al.* Akt/Protein Kinase B Is Required for Lymphatic Network Formation, Remodeling, and Valve Development. *Am J Pathology* **177**, 2124–2133 (2010).

219. Fereydooni, A., Dardik, A. & Nassiri, N. Molecular changes associated with vascular malformations. *J Vasc Surg* **70**, 314-326.e1 (2019).

220. Sunayama, J., Tsuruta, F., Masuyama, N. & Gotoh, Y. JNK antagonizes Akt-mediated survival signals by phosphorylating 14-3-3. *J Cell Biology* **170**, 295–304 (2005).

221. Berg, M. C. W. van den & Burgering, B. M. T. Integrating Opposing Signals Toward Forkhead Box O. *Antioxidants & Redox Signaling* **14**, 607–621 (2011).

222. Mihaylova, M. M. & Shaw, R. J. The AMPK signalling pathway coordinates cell growth, autophagy and metabolism. *Nat Cell Biol* **13**, 1016–23 (2011).

223. Greer, E. L. *et al.* The Energy Sensor AMP-activated Protein Kinase Directly Regulates the Mammalian FOXO3 Transcription Factor. *J Biol Chem* **282**, 30107–30119 (2007).

224. Obsil, T. & Obsilova, V. Structure/function relationships underlying regulation of FOXO transcription factors. *Oncogene* **27**, 2263–2275 (2008).

225. Calnan, D. R. & Brunet, A. The FoxO code. *Oncogene* **27**, 2276–2288 (2008).

226. Sengupta, A., Chakraborty, S., Paik, J., Yutzey, K. E. & Evans-Anderson, H. J. FoxO1 is required in endothelial but not myocardial cell lineages during cardiovascular development. *Dev Dyn Official Publ Am Assoc Anatomists* **241**, 803–13 (2012).

227. Betsholtz, C. Transcriptional control of endothelial energy. *News & Views, Nature* 1–2 (2016).

228. Niimi, K. *et al.* FOXO1 regulates developmental lymphangiogenesis by upregulating CXCR4 in the mouse-tail dermis. *Development* **147**, dev181545 (2020).

229. Scallan, J. P. *et al.* Foxo1 deletion promotes the growth of new lymphatic valves. *J Clin Invest* **131**, e142341 (2021).

230. Niimi, K., Nakae, J., Inagaki, S. & Furuyama, T. FOXO1 represses lymphatic valve formation and maintenance via PRDM1. *Cell Reports* **37**, 110048 (2021).

231. Barr, F. G. Gene fusions involving PAX and FOX family members in alveolar rhabdomyosarcoma. *Oncogene* **20**, 5736–5746 (2001).

232. Xia, S. J. & Barr, F. G. Analysis of the transforming and growth suppressive activities of the PAX3-FKHR oncoprotein. *Oncogene* **23**, 6864–6871 (2004).

233. Lagutina, I., Conway, S. J., Sublett, J. & Grosveld, G. C. Pax3-FKHR Knock-In Mice Show Developmental Aberrations but Do Not Develop Tumors. *Mol Cell Biol* **22**, 7204–7216 (2002).

234. Bois, P. R. J. & Grosveld, G. C. FKHR (FOXO1a) is required for myotube fusion of primary mouse myoblasts. *Embo J* **22**, 1147–1157 (2003).

235. Zhang, L. & Wang, C. PAX3-FKHR Transformation Increases 26 S Proteasome-dependent Degradation of p27Kip1, a Potential Role for Elevated Skp2 Expression. *J Biol Chem* **278**, 27–36 (2002).

236. Nakamura, N. *et al.* Forkhead Transcription Factors Are Critical Effectors of Cell Death and Cell Cycle Arrest Downstream of PTEN. *Mol Cell Biol* **20**, 8969–8982 (2000).

237. Ramaswamy, S., Nakamura, N., Sansal, I., Bergeron, L. & Sellers, W. R. A novel mechanism of gene regulation and tumor suppression by the transcription factor FKHR. *Cancer Cell* **2**, 81–91 (2002).

238. Naka, K. *et al.* TGF-beta-FOXO signalling maintains leukaemia-initiating cells in chronic myeloid leukaemia. *Nature* **463**, 676–80 (2010).

239. Sykes, S. M. *et al.* AKT/FOXO signaling enforces reversible differentiation blockade in myeloid leukemias. *Cell* **146**, 697–708 (2011).

240. Kim, H., Kim, M., Im, S.-K. & Fang, S. Mouse Cre-LoxP system: general principles to determine tissue-specific roles of target genes. *Laboratory Animal Research* **34**, 147–13 (2018).

241. Indra, A. K. *et al.* Temporally-controlled site-specific mutagenesis in the basal layer of the epidermis: comparison of the recombinase activity of the tamoxifen-inducible Cre-ER. *Nucleic Acids Research* 4324–4327 (1999).

242. Bazigou, E. *et al.* Genes regulating lymphangiogenesis control venous valve formation and maintenance in mice. *Journal of Clinical Investigation* **121**, 2984–2992 (2011).

243. Keller, C. *et al.* Alveolar rhabdomyosarcomas in conditional Pax3:Fkhr mice: cooperativity of Ink4a/ARF and Trp53 loss of function. *Genes & Development* **18**, 2614–2626 (2004).

244. Stöhr, O. *et al.* Insulin receptor signaling mediates APP processing and β-amyloid accumulation without altering survival in a transgenic mouse model of Alzheimer's disease. *AGE* **35**, 83–101 (2011).

245. Yamakoshi, H. *et al.* Imaging of EdU, an Alkyne-Tagged Cell Proliferation Probe, by Raman Microscopy. *Journal of the American Chemical Society* **133**, 6102–6105 (2011).

246. Jerome, W. G. J. & Price, R. L. *Basic Confocal Microscopy*. (2018).

247. Holland, P. M., Abramosin, R. D., Watson, R. & Gelfand, D. H. Detection of specific polymerase chain reaction product by utilizing the 5’ 3’ exonuclease activity of Thermus aquaticus DNA polymerase. *Proc. Natl. Acad. Sci.* 7276–7280 (1991).

248. Maher, C. A. *et al.* Transcriptome sequencing to detect gene fusions in cancer. *Nature Publishing Group* **457**, 97–101 (2009).

249. Bolger, A. M., Lohse, M. & Usadel, B. Trimmomatic: a flexible trimmer for Illumina sequence data. *Bioinformatics* 2114–2120 (2014) doi:10.1093/bioinformatics/btu170/-/dc1.

250. Dobin, A. *et al.* STAR: ultrafast universal RNA-seq aligner. *Bioinformatics* **29**, 15–21 (2012).

251. Liao, Y., Smyth, G. K. & Shi, W. featureCounts: an efficient general purpose program for assigning sequence reads to genomic features. *Bioinformatics* **30**, 923–930 (2014).

252. Mäkinen, T. & Wilkinson, george A. PDZ interaction site in ephrinB2 is required for the remodeling of lymphatic vasculature. *Genes & Development* 1–15 (2005).

253. Zhang, Y. *et al.* Heterogeneity in VEGFR3 levels drives lymphatic vessel hyperplasia through cell-autonomous and non-cell-autonomous mechanisms. *Nature Communications* **9**, 1–15 (2018).

254. Niessen, K., Zhang, G., Ridgway, J. B., Chen, H. & Yan, M. ALK1 signaling regulates early postnatal lymphatic vessel development. *Blood* 1–9 (2010) doi:10.1182/blood-2009-07.

255. McDermaid, A., Monier, B., Zhao, J., Liu, B. & Ma, Q. Interpretation of differential gene expression results of RNA-seq data: review and integration. *Brief Bioinform* **20**, 2044–2054 (2018).

256. Subramanian, A. & Mesirov, J. P. Gene set enrichment analysis: A knowledge-based approach for interpreting genome-wide expression profiles. *Proc. Natl. Acad. Sci.* 1–6 (2005).

257. Liberzon, A. *et al.* The Molecular Signatures Database Hallmark Gene Set Collection. *Cell Syst* **1**, 417–425 (2015).

258. Kanehisa, M. & Goto, S. KEGG: Kyoto Encyclopedia of Genes and Genomes. *Nucleic Acids Res* **28**, 27–30 (2000).

259. Zou, Z., Tao, T., Li, H. & Zhu, X. mTOR signaling pathway and mTOR inhibitors in cancer: progress and challenges. *Cell Biosci.* **10**, 31 (2020).

260. Ruijtenberg, S. & Heuvel, S. van den. Coordinating cell proliferation and differentiation: Antagonism between cell cycle regulators and cell type-specific gene expression. *Cell Cycle* **15**, 196–212 (2016).

261. Zhu, L. & Skoultchi, A. I. Coordinating cell proliferation and differentiation. *Curr Opin Genet Dev* **11**, 91–97 (2001).

262. Davis, M. J., Zawieja, S. D. & Yang, Y. Developmental progression of lymphatic valve morphology and function. *Front. Cell Dev. Biol.* **12**, 1331291 (2024).

263. Mendoza, M. C., Er, E. E. & Blenis, J. The Ras-ERK and PI3K-mTOR pathways: cross-talk and compensation. *Trends Biochem Sci* **36**, 320–328 (2011).

264. Schmidt, M. *et al.* Cell cycle inhibition by FoxO forkhead transcription factors involves downregulation of cyclin D. *Molecular and Cellular Biology* **22**, 7842–7852 (2002).

265. WU, P. *et al.* Starvation and diabetes increase the amount of pyruvate dehydrogenase kinase isoenzyme 4 in rat heart. *Biochem J* **329**, 197–201 (1998).

266. Lamming, D. W. & Sabatini, D. M. A Central Role for mTOR in Lipid Homeostasis. *Cell Metab* **18**, 465–469 (2013).

267. Peterson, T. R. *et al.* mTOR Complex 1 Regulates Lipin 1 Localization to Control the SREBP Pathway. *Cell* **146**, 408–420 (2011).

268. Horton, J. D., Goldstein, J. L. & Brown, M. S. SREBPs: activators of the complete program of cholesterol and fatty acid synthesis in the liver. *J Clin Invest* **109**, 1125–1131 (2002).

269. Deng, X. *et al.* FoxO1 Inhibits Sterol Regulatory Element-binding Protein-1c (SREBP-1c) Gene Expression via Transcription Factors Sp1 and SREBP-1c*. *J Biol Chem* **287**, 20132–20143 (2012).

270. Wong, B. W. *et al.* The role of fatty acid β-oxidation in lymphangiogenesis. *Nature Publishing Group* **542**, 49–54 (2017).

271. Wong, B. W., Zecchin, A., García-Caballero, M. & Carmeliet, P. Emerging Concepts in Organ-Specific Lymphatic Vessels and Metabolic Regulation of Lymphatic Development. *Developmental Cell* **45**, 289–301 (2018).

272. Haibe, Y. *et al.* Resistance Mechanisms to Anti-angiogenic Therapies in Cancer. *Frontiers Oncol* **10**, 221 (2020).

273. Mumprecht, V., Roudnicky, F. & Detmar, M. Inflammation-Induced Lymph Node Lymphangiogenesis Is Reversible. *Am J Pathology* **180**, 874–879 (2012).